U.S. Department of Transportation

Federal Railroad Administration

Office of Research, Development and Technology
Washington, DC 20590

Locomotive Crash Energy Management Train-to-Train Collision Test

DOT/FRA/ORD-23/22

Final Report | August 2023

REPORT DOCUMENTATION PAGE	*Form Approved* *OMB No. 0704-0188*

1. REPORT DATE *(DD-MM-YYYY*	**2. REPORT TYPE**	**3. DATES COVERED** *(From - To)*
21/09/2022	Technical Report	August–September 2022

4. TITLE AND SUBTITLE	
Locomotive Crash Energy Management Train-to-Train Collision Test	**5a. CONTRACT NUMBER** DTFR5311D00008L
	5b. GRANT NUMBER
	5c. PROGRAM ELEMENT NUMBER
6. AUTHOR(S) Matthew DeGeorge – https://orcid.org/0000-0003-1466-6607 Travis Gorhum – https://orcid.org/0000-0002-3088-9096	**5d. PROJECT NUMBER**
	5e. TASK NUMBER 693JJ619F000102
	5f. WORK UNIT NUMBER

7. PERFORMING ORGANIZATION NAME(S) AND ADDRESS(ES)	**8. PERFORMING ORGANIZATION REPORT NUMBER**
Transportation Technology Center, Inc. 55500 DOT Road PO BOX 11130 Pueblo, CO 81001-0130	
9. SPONSORING/MONITORING AGENCY NAME(S) AND ADDRESS(ES)	**10. SPONSOR/MONITOR'S ACRONYM(S)**
U.S. Department of Transportation Federal Railroad Administration Office of Research, Development, and Technology Washington, DC 20590	**11. SPONSOR/MONITOR'S REPORT NUMBER(S)** DOT/FRA/ORD-23/22

12. DISTRIBUTION/AVAILABILITY STATEMENT
This document is available to the public through the FRA Web site at http://www.fra.dot.gov

13. SUPPLEMENTARY NOTES
COR: Jeff Gordon

14. ABSTRACT

The Federal Railroad Administration (FRA) sponsored MxV Rail to conduct a collision test using both a moving and a stationary three-car consist. The moving consist included an EMD F40 passenger locomotive equipped with crash energy management (CEM) components backed by two M1-series passenger cars. The M1 passenger cars were also equipped for three occupant protection experiments using wheelchairs and anthropomorphic test devices (ATDs). The stationary consist included a conventional F40 passenger locomotive backed by two empty freight cars. The impact test was performed on August 11, 2022, at the Transportation Technology Center in Pueblo, Colorado. The moving consist impacted the stationary consist at 24.3 mph. The impact initiated deformation of the anti-climber, activated the push-back coupler, and broke all the shear bolts. The occupant experiments were all successful in that the wheelchair securement devices retained their structural integrity, remained attached to the carbody, compartmentalized the ATDs, and resulted in injury values that were likely survivable for an occupant.

15. SUBJECT TERMS
Impact test, crash energy management, CEM, occupant protection systems, transportation safety, passenger car safety

16. SECURITY CLASSIFICATION OF:			**17. LIMITATION OF ABSTRACT**	**18. NUMBER OF PAGES**	**19a. NAME OF RESPONSIBLE PERSON**
a. REPORT	**b. ABSTRACT**	**c. THIS PAGE**			Matt DeGeorge, Sr. Engineer II, MxV Rail
Unclassified	Unclassified	Unclassified		125	**19b. TELEPHONE NUMBER** *(Include area code)* 719-584-0724

Standard Form 298 (Rev. 8/98)
Prescribed by ANSI Std. Z39.18

METRIC/ENGLISH CONVERSION FACTORS

ENGLISH TO METRIC

LENGTH (APPROXIMATE)

1 inch (in)	=	2.5 centimeters (cm)
1 foot (ft)	=	30 centimeters (cm)
1 yard (yd)	=	0.9 meter (m)
1 mile (mi)	=	1.6 kilometers (km)

AREA (APPROXIMATE)

1 square inch (sq in, in^2)	=	6.5 square centimeters (cm^2)
1 square foot (sq ft, ft^2)	=	0.09 square meter (m^2)
1 square yard (sq yd, yd^2)	=	0.8 square meter (m^2)
1 square mile (sq mi, mi^2)	=	2.6 square kilometers (km^2)
1 acre = 0.4 hectare (he)	=	4,000 square meters (m^2)

MASS - WEIGHT (APPROXIMATE)

1 ounce (oz)	=	28 grams (gm)
1 pound (lb)	=	0.45 kilogram (kg)
1 short ton = 2,000 pounds (lb)	=	0.9 tonne (t)

VOLUME (APPROXIMATE)

1 teaspoon (tsp)	=	5 milliliters (ml)
1 tablespoon (tbsp)	=	15 milliliters (ml)
1 fluid ounce (fl oz)	=	30 milliliters (ml)
1 cup (c)	=	0.24 liter (l)
1 pint (pt)	=	0.47 liter (l)
1 quart (qt)	=	0.96 liter (l)
1 gallon (gal)	=	3.8 liters (l)
1 cubic foot (cu ft, ft^3)	=	0.03 cubic meter (m^3)
1 cubic yard (cu yd, yd^3)	=	0.76 cubic meter (m^3)

TEMPERATURE (EXACT)

[(x-32)(5/9)] °F = y °C

METRIC TO ENGLISH

LENGTH (APPROXIMATE)

1 millimeter (mm)	=	0.04 inch (in)
1 centimeter (cm)	=	0.4 inch (in)
1 meter (m)	=	3.3 feet (ft)
1 meter (m)	=	1.1 yards (yd)
1 kilometer (km)	=	0.6 mile (mi)

AREA (APPROXIMATE)

1 square centimeter (cm^2)	=	0.16 square inch (sq in, in^2)
1 square meter (m^2)	=	1.2 square yards (sq yd, yd^2)
1 square kilometer (km^2)	=	0.4 square mile (sq mi, mi^2)
10,000 square meters (m^2)	=	1 hectare (ha) = 2.5 acres

MASS - WEIGHT (APPROXIMATE)

1 gram (gm)	=	0.036 ounce (oz)
1 kilogram (kg)	=	2.2 pounds (lb)
1 tonne (t)	=	1,000 kilograms (kg)
	=	1.1 short tons

VOLUME (APPROXIMATE)

1 milliliter (ml)	=	0.03 fluid ounce (fl oz)
1 liter (l)	=	2.1 pints (pt)
1 liter (l)	=	1.06 quarts (qt)
1 liter (l)	=	0.26 gallon (gal)
1 cubic meter (m^3)	=	36 cubic feet (cu ft, ft^3)
1 cubic meter (m^3)	=	1.3 cubic yards (cu yd, yd^3)

TEMPERATURE (EXACT)

[(9/5) y + 32] °C = x °F

QUICK INCH - CENTIMETER LENGTH CONVERSION

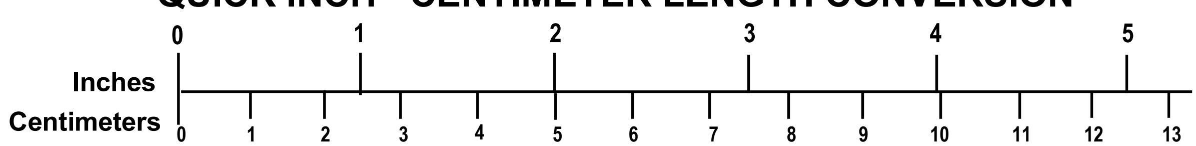

QUICK FAHRENHEIT - CELSIUS TEMPERATURE CONVERSIO

°F	-40°	-22°	-4°	14°	32°	50°	68°	86°	104°	122°	140°	158°	176°	194°	212°
°C	-40°	-30°	-20°	-10°	0°	10°	20°	30°	40°	50°	60°	70°	80°	90°	100°

For more exact and or other conversion factors, see NIST Miscellaneous Publication 286, Units of Weights and Measures. Price $2.50 SD Catalog No. C13 10286

Contents

Illustrations

Tables

Executive Summary

The Federal Railroad Administration (FRA) sponsored MxV Rail to conduct an impact test using a three-car moving consist containing an EMD F40 passenger locomotive equipped with crash energy management (CEM) components backed by two M1-series passenger cars and a stationary consist containing a conventional F40 locomotive backed by two empty freight cars. The Federal Railroad Administration (FRA) sponsored this research to evaluate the performance of the CEM components in a high-energy collision scenario. The retrofitted CEM locomotive was equipped with a push-back coupler (PBC), deformable anti-climber (DAC), and a sliding lug connected to the draft pocket with a set of shear bolts. The M1-series passenger cars were also equipped with three occupant protection devices that included wheelchairs and anthropomorphic test devices (ATDs). The experiments were designed to evaluate the effectiveness of the devices and study the effects of the energy imparted to passengers after the CEM components had been activated on the impacting locomotive. Researchers performed this test on August 11, 2022, at FRA's Transportation Technology Center in Pueblo, Colorado.

The moving consist impacted the stationary consist at 24.3 mph. The CEM locomotive and the conventional locomotive couplers were closed at impact; the impact caused the PBC to crack and the two impacting locomotives to remain engaged. A hydraulic cylinder was required to separate the locomotives after the test. The CEM locomotive sustained structural damage to its front plate, nose, center sill, and draft pocket – in addition to the expected deformation of the CEM components. The impact crushed both sets of anti-climbers, activated the PBC, and sheared the sliding lug bolts. The M1 passenger cars had bent or ejected traction rods, and the plate that held its front yoke into the draft pocket on the first M1 car was ejected as well. The nose of the conventional locomotive experienced significant deformation. The upper DAC contacted the conventional locomotive at the floor structure of its front compartment, causing buckling in both the floor and its support structure where it attached to the locomotive's front plate.

The occupant protection systems held the ATDs and wheelchairs upright during the impact and limited the movement of the equipment and ATDs. A single device was cosmetically damaged due to a point load from the surrogate wheelchair on the chassis' cover plate, but the device was still functional after testing was complete.

Researchers will use test data to validate the computer models and prepare for future crashworthiness testing and occupant protection testing.

1. Introduction

In August 2022, The Federal Railroad Administration (FRA) sponsored MxV Rail to conduct a collision test using a moving three-car consist and a stationary three-car consist. The moving consist included an EMD F40 passenger locomotive equipped with crash energy management (CEM) components backed by two M1-series passenger cars. The M1 passenger cars were also equipped with three occupant protection experiments that included the use of wheelchairs and anthropomorphic test devices (ATDs). The stationary consist included a conventional F40 passenger locomotive backed by two empty freight cars.

Researchers integrated three CEM components onto a locomotive to demonstrate that they could work together to mitigate the effects of a collision and prevent override. The CEM system included a deformable anti-climber (DAC), a push-back coupler (PBC), and a sliding lug connected to the draft pocket with a set of shear bolts. Testing characterized the combined performance of all installed CEM components. The occupant protection experiments included two separate wheelchair restraint systems used in transit buses and a solitary backboard. These experiments were designed to evaluate the effectiveness of the devices during train collision conditions and study the effects of the energy imparted to passengers after the CEM components were activated on the impacting locomotive.

1.1 Background

The Federal Railroad Administration (FRA) and the Volpe National Transportation Systems Center (Volpe) continue to evaluate new technologies designed to increase passenger and operator safety. FRA recognizes the importance of override prevention in train-to-train collisions where one of the vehicles is a locomotive, and has noted the success of crash energy management technologies in passenger trains. Consequently, FRA is interested in evaluating the effectiveness of components that are 1) integrated into the end structure of a locomotive, 2) specifically designed to mitigate the effects of a collision and, in particular, 3) meant to prevent override of one of the lead vehicles onto the other.

On November 18 and 19, 2015, Transportation Technology Center, Inc. (TTCI) conducted impact tests using a conventional passenger locomotive and car. These tests measured and characterized the structural performance of the conventional coupler and the coupling vehicles under a range of dynamic coupling speeds until the car structure sustained damage. The test results established a baseline maximum nondestructive coupling speed for comparison with testing on a locomotive equipped with a CEM system.

On October 3 and 4, 2017, TTCI conducted coupling tests between an F40 locomotive retrofitted with CEM and an M1 passenger car. In these tests, researchers characterized the performance of the PBC by impacting an M1 passenger car with an F40 equipped with a PBC and a DAC at increasing speeds. The team continued these tests until the PBC activated.

On January 23, 2019, TTCI conducted an impact test between an F40 retrofitted with CEM and a conventional F40 locomotive at 19.3 mph. This test was intended to activate the PBC, the DAC, and the shear bolts. However, after activating the PBC and initiating deformation on the top DAC tubes, the remaining energy was insufficient to cause the shear bolts to break.

On November 17, 2021, TTCI conducted an impact test between an F40 passenger locomotive equipped with CEM components and an M1-series passenger car backed by two empty freight cars at 32.8 mph, a speed sufficient to activate the PBC, the DAC, and the shear bolts.

1.2 Objective

The objective of this effort was to demonstrate the combined functionality of the PBC, the shear bolts, and the DAC in a full-scale, train-to-train impact. The team measured and characterized the structural performance of the CEM components, and the impacted vehicles performed at a speed sufficient to activate all the CEM-equipped components.

The secondary objective was to evaluate the functionality of occupant protection equipment in a railroad scenario and to study the effects of the energy imparted to passengers after the CEM components were activated. The team accomplished this objective by installing three occupant protection systems using ATDs, different types of occupant restraint equipment, and manual wheelchairs.

1.3 Overall Approach

The following sections describe the test approach in terms of the equipment used and the general test setup.

1.3.1 CEM Locomotive

The F40PH locomotive is a four-axle, diesel-electric locomotive intended for use in passenger service. The team used F40 Locomotive 234 as the impact vehicle for this test (Figure 1). This locomotive weighed 232,225 lb and was retrofitted with the CEM system.

Figure 1. F40PH Locomotive 234

1.3.2 M1 Passenger Cars

The moving consist contained the CEM locomotive and two M1 passenger cars (Figure 2). The M1 passenger cars were coupled together as a married pair with the cab end of car 8332 coupled to the CEM locomotive and the cab end of car 8221 at the rear of the consist. M1 passenger cars 8332 and 8221 weighed 79,575 lb and 78,000 lb, respectively. Researchers performed asbestos abatement on the M1 passenger cars. The abatement process involved removing the seats, flooring, and interior side paneling from the car. The team replaced the flooring with two layers of 1/2 inch plywood secured to the car frame to simulate the original car floor structure and rigidity. Researchers left empty spaces in the plywood flooring to install three wheeled mobility device restraint systems. The team secured the restraint system components to the frame of the car and filled the area around each experiment with plywood.

Figure 2. M1 Passenger Cars 8332 and 8221

1.3.3 Stationary Consist

The stationary consist included conventional F40 locomotive 4117 backed by two empty hopper cars, BN 531622 and BN 526308 (Figure 3). The team positioned the F40 locomotive with the cab end toward the impact point, and its weight was 255,175 lb. The empty hopper cars weighed 60,075 lb and 59,375 lb, respectively.

Figure 3. Conventional F40 Locomotive 4117 and Empty Hopper Cars

1.3.4 Test Setup

The team performed the impact test on August 11, 2022, at the Transportation Technology Center (TTC) in Pueblo, Colorado. During this test, team members positioned the CEM locomotive and M1 cars uphill from the stationary consist, and another locomotive pushed the moving consist toward a designated location where the team then released it. Researchers allowed the moving consist to roll freely down a slight grade until it impacted the stationary consist. The team determined the release location and speed of the moving consist during speed trials and adjusted these shortly before the test to achieve the desired impact speed. Prior to impact, the team aligned the couplers of the CEM locomotive and the conventional F40 locomotive and closed the knuckles.

To keep the stationary consist in place prior to the impact and to arrest motion after the impact, researchers applied the handbrakes on two empty hopper cars. The team positioned a single loaded hopper car approximately 635 feet behind the stationary locomotive to arrest any remaining momentum if the brakes were not sufficient. They then placed another string of cars approximately 200 feet behind the single loaded hopper car as a backup if the consists continued to move down the track.

Before the test, researchers conducted speed trials using the moving consist to determine the optimum release location and speed needed to achieve the desired impact speed. To achieve a more precise target speed, team members made adjustments immediately before testing to account for current wind speed and direction.

1.4 Scope

This report presents the test results, discusses the execution of the test, and summarizes the overall results of the test.

1.5 Organization of the Report

- Section 2 describes the instrumentation and data collection system used during testing.
- Section 3 describes the results of the test. These results include the test details, the data measured, and a discussion of the post-test damage.
- Section 4 contains the concluding remarks.
- Appendix A describes the target positions.
- Appendix B contains the test data.

2. Test Instrumentation

A Test Implementation Plan described the test configuration and instrumentation. Table 1 lists the instrumentation. Additional instrumentation descriptions are provided in the following subsections.

Table 1. Instrumentation Summary

Type of Instrumentation	Channel Count
Accelerometers	75
String Potentiometers	40
Strain Gages	62
ATD Sensors	51
Total Data Channels	**228**
High-Definition Video	8
High Speed Video	15

2.1 Definition of Coordinate Axes

All local acceleration and displacement coordinate systems were defined relative to the front (i.e., lead) end of each consist. Positive X, Y, and Z directions were defined as forward, left, and up, respectively, relative to the lead end of each consist. The ATD coordinate system was defined in accordance with the SAE J211 requirements (SAE International, 2014).

2.2 CEM Locomotive Instrumentation

The following sections describe the test instrumentation installed on the CEM locomotive.

2.2.1 CEM Locomotive Accelerometers

Researchers placed tri-axial accelerometers at the ends and at the center along the carbody center line. The locomotive had longitudinal and vertical accelerometers placed on the left and right sides of its underframe at its center. Each truck was equipped with a vertical accelerometer and two longitudinal accelerometers, right and left. The locomotive's PBC was fitted with three longitudinal accelerometers, one on each side of the coupler and one on the bottom of the sliding lug. Two percent of full scale is the typical scale factor calibration error for the accelerometers used. Table 2 summarizes all accelerometers on the CEM Locomotive 234. Figure 4 and Figure 5 show the locations of the accelerometers on the locomotive.

Table 2. CEM Locomotive Accelerometer Summary

Name	Range	Location
AM1LE_X	400g	CEM Loco, lead end, center – longitudinal
AM1LE_Y	200g	CEM Loco, lead end, center – lateral
AM1LE_Z	200g	CEM Loco, lead end, center – vertical
AM1UC_X	200g	CEM Loco, underframe center – longitudinal
AM1UC_Y	200g	CEM Loco, underframe center – lateral
AM1UC_Z	200g	CEM Loco, underframe center – vertical
AM1UCR_X	200g	CEM Loco, underframe center right – longitudinal
AM1UCR_Z	200g	CEM Loco, underframe center right – vertical
AM1UCL_X	200g	CEM Loco, underframe center left – longitudinal
AM1UCL_Z	200g	CEM Loco, underframe center left – vertical
AM1TEC_X	200g	CEM Loco, trailing end, center – longitudinal
AM1TEC_Y	200g	CEM Loco, trailing end, center – lateral
AM1TEC_Z	200g	CEM Loco, trailing end, center – vertical
AM1LTL_Z	400g	CEM Loco, lead truck – vertical
AM1LTR_X	400g	CEM Loco, lead truck, right – longitudinal
AM1LTL_X	400g	CEM Loco, lead truck, left – longitudinal
AM1TT_Z	400g	CEM Loco, trailing truck – vertical
AM1TTR_X	400g	CEM Loco, trailing truck, right - longitudinal
AM1TTL_X	400g	CEM Loco, trailing truck, left – longitudinal
AM1CR_X	5000g	CEM Loco, front coupler, right – longitudinal
AM1CL_X	5000g	CEM Loco, front coupler, left – longitudinal
AM1S_X	5000g	CEM Loco, sliding lug – longitudinal

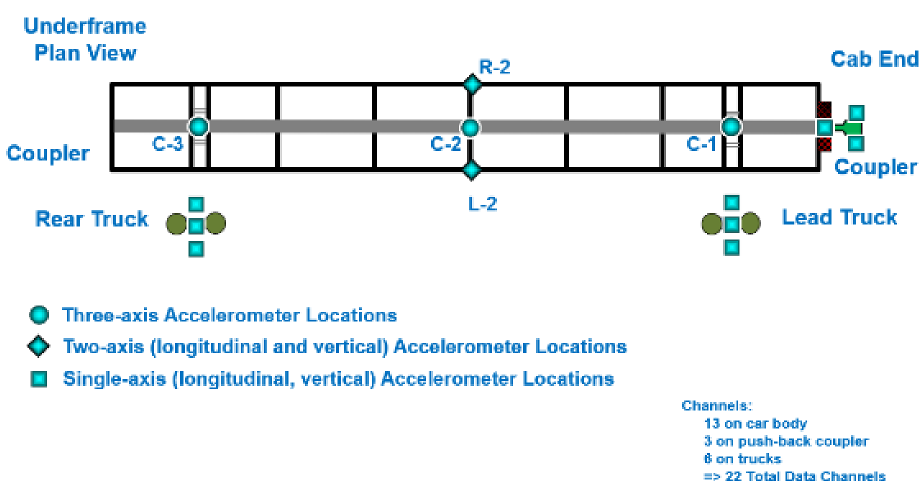

Figure 4. Top View of Accelerometer Locations on CEM Locomotive

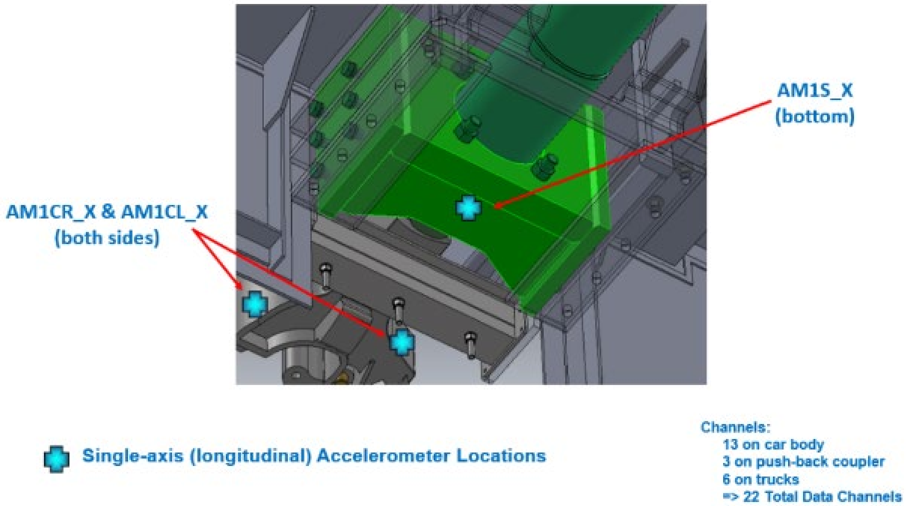

Figure 5. Locations of Accelerometers on CEM Locomotive Sliding Lug and Pushback Coupler

2.2.2 CEM Locomotive String Potentiometers

CEM Locomotive 234 was also instrumented with vertical string potentiometers across each truck's secondary suspension. Two string potentiometers were also fitted to the coupler of the locomotive to measure its longitudinal displacement. Two additional string potentiometers were fitted to the front of the locomotive underframe to measure longitudinal displacements. Each crush tube for the DAC was fitted with a longitudinal string potentiometer to measure the deformation in each portion of the anti-climbers. Table 3 summarizes all string potentiometers on the locomotive. Figure 6 to Figure 12 show the locations of the string potentiometers on the locomotive. Red lines in the figures indicate the measurement, and blue rectangles indicate the mounting location.

Table 3. CEM Locomotive String Potentiometer Summary

Name	Range	Location
DM1LTR_Z	± 5 inch	CEM Loco secondary suspension, lead truck – vertical, right
DM1LTL_Z	± 5 inch	CEM Loco secondary suspension, lead truck – vertical, left
DM1TTR_Z	± 5 inch	CEM Loco secondary suspension, trailing truck – vertical, right
DM1TTL_Z	± 5 inch	CEM Loco secondary suspension, trailing truck – vertical, left
DM1UL_X	+5/-45 inch	CEM Loco underframe, front – longitudinal, left
DM1UR_X	+5/-45 inch	CEM Loco underframe, front – longitudinal, right
DM1CL_X	+20/-30 inch	CEM Loco coupler – longitudinal, left
DM1CR_X	+20/-30 inch	CEM Loco coupler – longitudinal, right
DM1SL_X	+20/-30 inch	CEM Loco sliding lug – longitudinal, left
DM1SR_X	+20/-30 inch	CEM Loco sliding lug – longitudinal, right
DM1ACTL_X	+5/-45 inch	CEM Loco DAC top, left – longitudinal
DM1ACTR_X	+5/-45 inch	CEM Loco DAC top, right – longitudinal
DM1ACL_X	+5/-45 inch	CEM Loco DAC bottom, left – longitudinal
DM1ACR_X	+5/-45 inch	CEM Loco DAC bottom, right – longitudinal

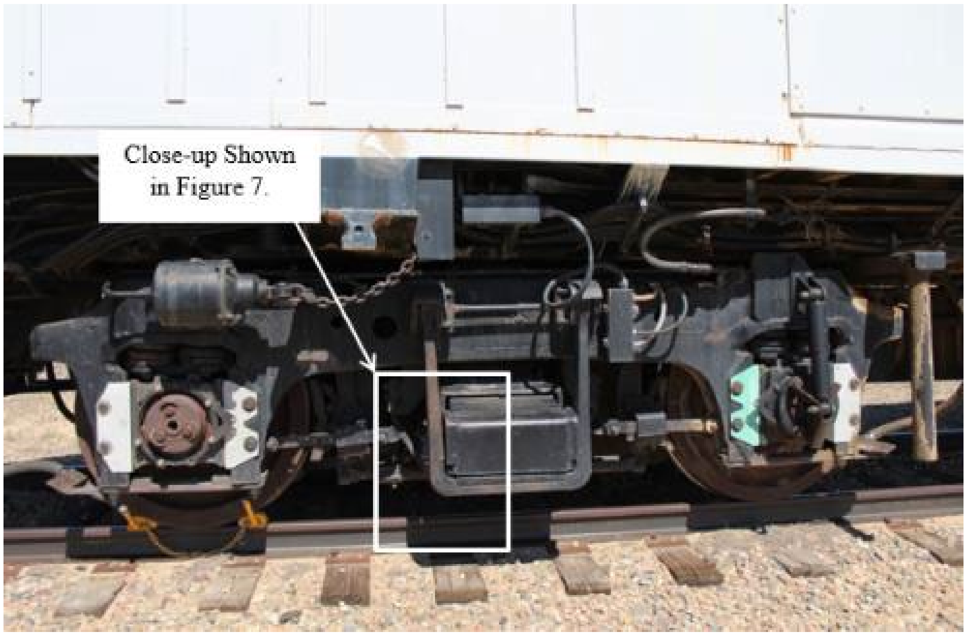

Figure 6. CEM Locomotive Truck

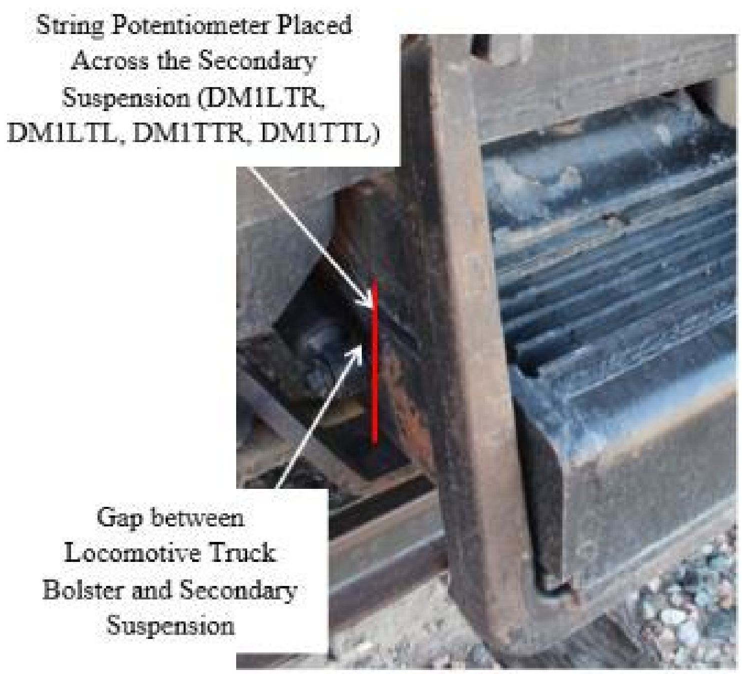

Figure 7. CEM Locomotive Truck Secondary Suspension String Potentiometer Location

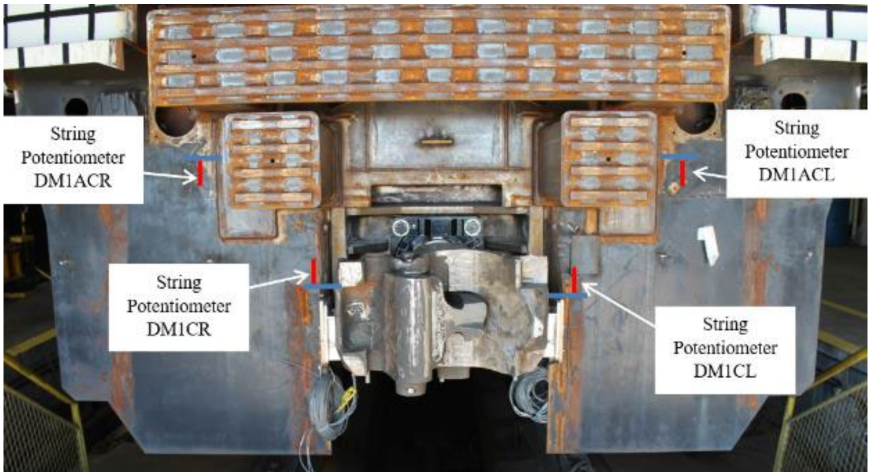

Figure 8. CEM Locomotive Coupler and Anti-Climber String Potentiometers

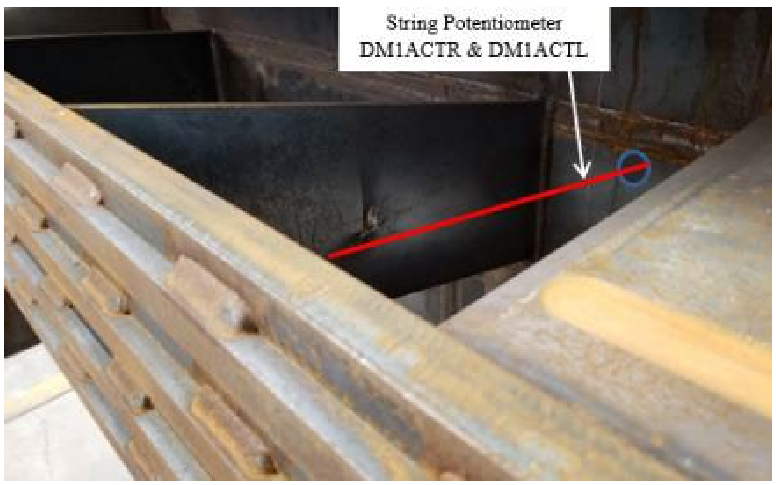

Figure 9. CEM Locomotive Top Anti-climber String Potentiometers

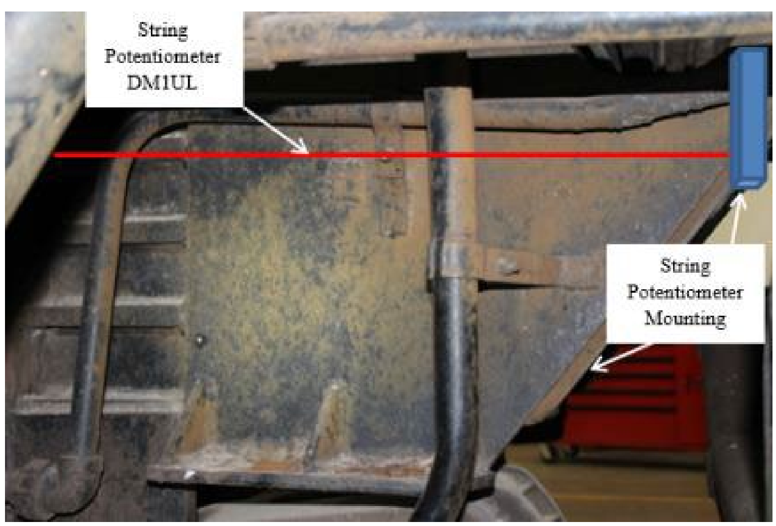

Figure 10. CEM Locomotive Underframe String Potentiometers

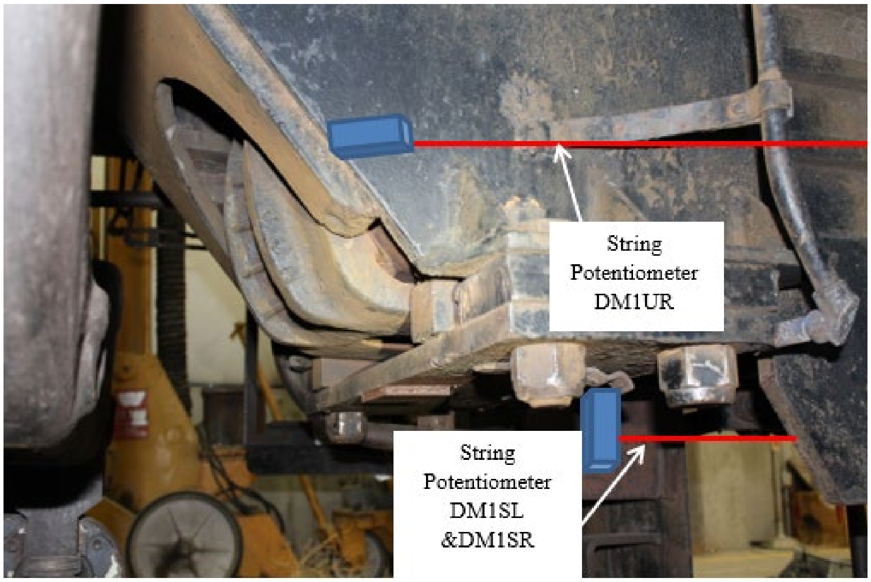

Figure 11. Right Side CEM Locomotive String Potentiometers

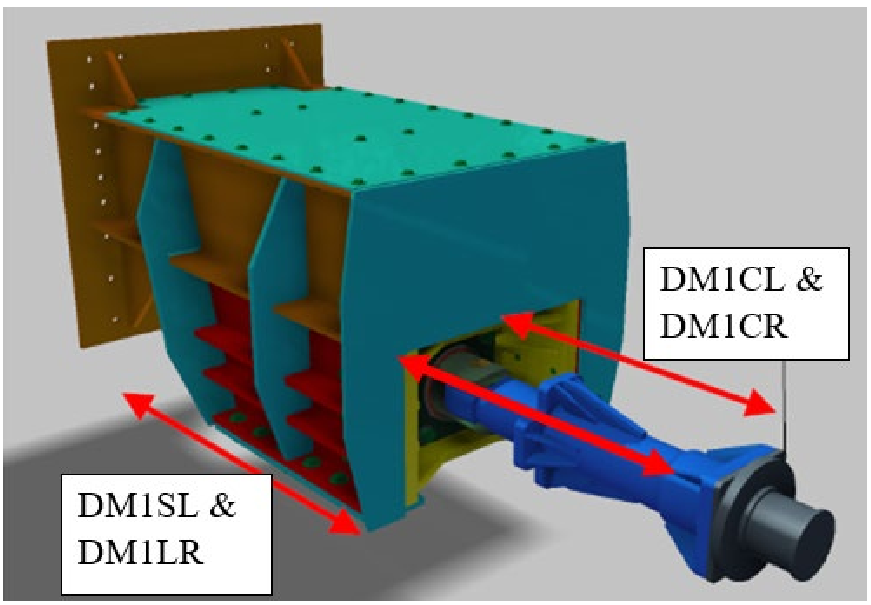

Figure 12. CEM Locomotive Coupler and Sliding Lug String Potentiometers

2.2.3 CEM Locomotive Strain Gages

CEM Locomotive 234 was instrumented with 34 strain gages on the couplers, sliding lug, draft gear pocket, center sill, and cross plate. Table 4 summarizes all the strain gages on the locomotive. Figure 13 through Figure 18 show the locations of the strain gages.

Table 4. CEM Locomotive Strain Gage Summary

Name	Orientation	Location
SM1CST	Longitudinal	CEM Loco, lead coupler shaft, above coupler carrier, top
SM1CSR	Longitudinal	CEM Loco, lead coupler shaft, above coupler carrier, right
SM1CSL	Longitudinal	CEM Loco, lead coupler shaft, above coupler carrier, left
SM1CPR	Longitudinal	CEM Loco, lead coupler shaft at pin, right
SM1CPL	Longitudinal	CEM Loco, lead coupler shaft at pin, left
SM1CRT	Longitudinal	CEM Loco, rear coupler shaft, above coupler carrier, top
SM1SL1	Longitudinal	CEM Loco, sliding lug 1, top right front bolt hole
SM1SL2	Longitudinal	CEM Loco, sliding lug 2, top right rear bolt hole
SM1SL3	Longitudinal	CEM Loco, sliding lug 3, bottom right front bolt hole
SM1SL4	Longitudinal	CEM Loco, sliding lug 4, bottom right rear bolt hole
SM1SL5	Longitudinal	CEM Loco, sliding lug 5, top left front bolt hole
SM1SL6	Longitudinal	CEM Loco, sliding lug 6, top left rear bolt hole
SM1SL7	Longitudinal	CEM Loco, sliding lug 7, bottom left front bolt hole
SM1SL8	Longitudinal	CEM Loco, sliding lug 8, bottom left rear bolt hole
SM1DP1	Longitudinal	CEM Loco, draft pocket 1, top right front bolt hole
SM1DP2	Longitudinal	CEM Loco, draft pocket 2, top right rear bolt hole
SM1DP3	Longitudinal	CEM Loco, draft pocket 3, bottom right front bolt hole
SM1DP4	Longitudinal	CEM Loco, draft pocket 4, bottom right rear bolt hole
SM1DP5	Longitudinal	CEM Loco, draft pocket 5, top left front bolt hole
SM1DP6	Longitudinal	CEM Loco, draft pocket 6, top left rear bolt hole
SM1DP7	Longitudinal	CEM Loco, draft pocket 7, bottom left front bolt hole
SM1DP8	Longitudinal	CEM Loco, draft pocket 8, bottom left rear bolt hole
SM1TDR1	Longitudinal	CEM Loco, top of draft pocket, right front
SM1TDR2	Longitudinal	CEM Loco, top of draft pocket, right rear
SM1TDL1	Longitudinal	CEM Loco, top of draft pocket, left front
SM1TDL2	Longitudinal	CEM Loco, top of draft pocket, left rear
SM1CRF	Longitudinal	CEM Loco, center sill, right front
SM1CRR	Longitudinal	CEM Loco, center sill, right rear
SM1CLF	Longitudinal	CEM Loco, center sill, left front
SM1CLR	Longitudinal	CEM Loco, center sill, left rear
SM1XPR	Longitudinal	CEM Loco, cross plate, right
SM1XPL	Longitudinal	CEM Loco, cross plate, left
SM1DAR	Longitudinal	CEM Loco, draft pocket angled plate, right
SM1DAL	Longitudinal	CEM Loco, draft pocket angled plate, left

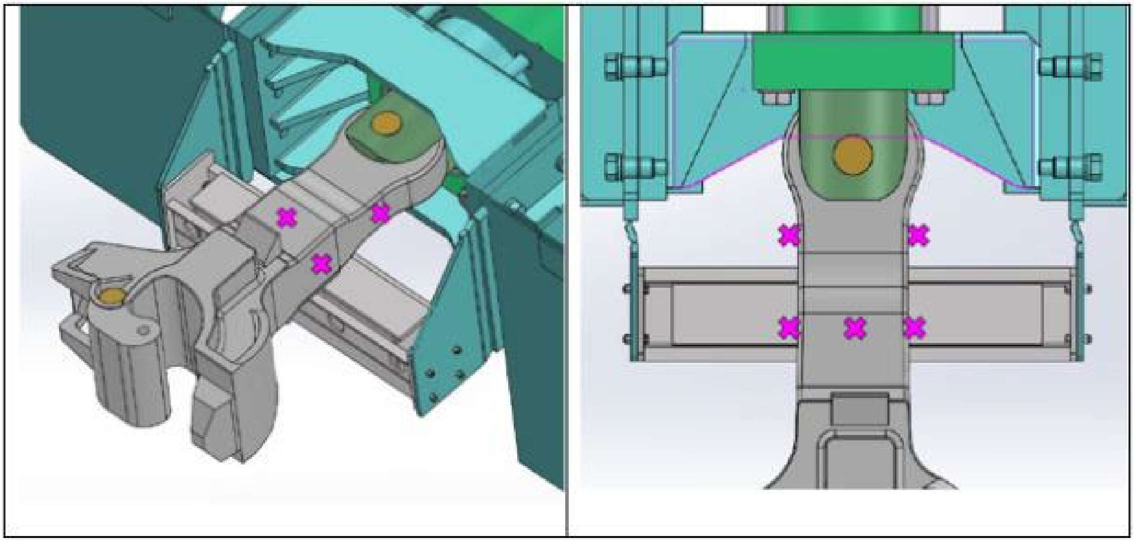

Figure 13. Strain Gage Locations on CEM Locomotive Coupler Shank

Researchers installed strain gages inside of the lug facing the coupler (Figure 14), 1.5 inches outboard (i.e., in front) of each top and bottom hole on each side.

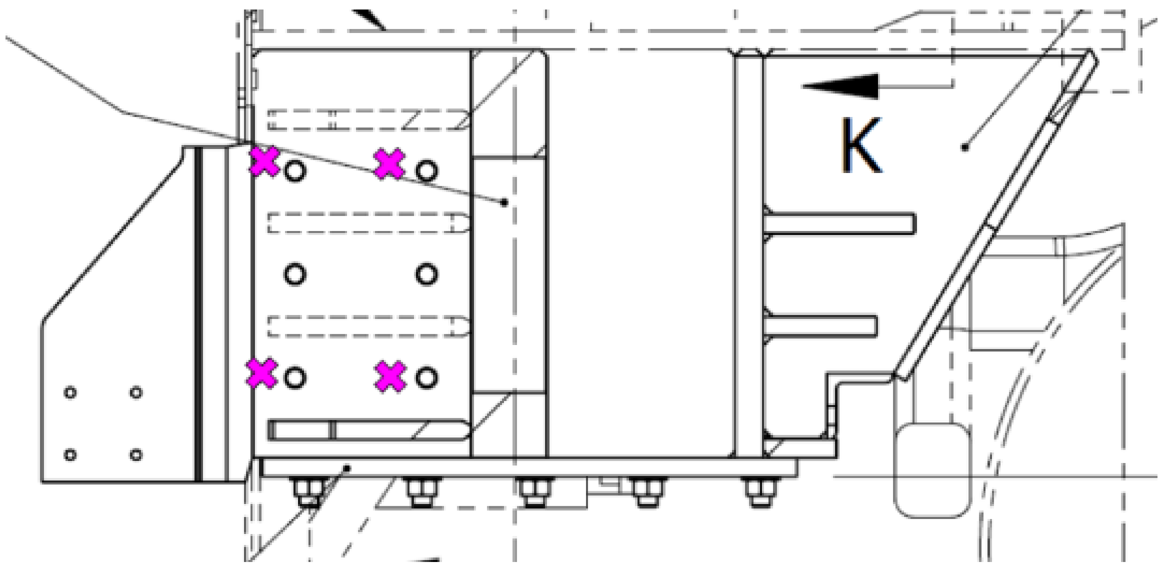

Figure 14. Strain Gage Locations on CEM Locomotive Sliding Lug

Strain gages were installed outside of the pocket facing outside (Figure 15), 1.5 inches inboard (behind) of each top and bottom hole on both sides.

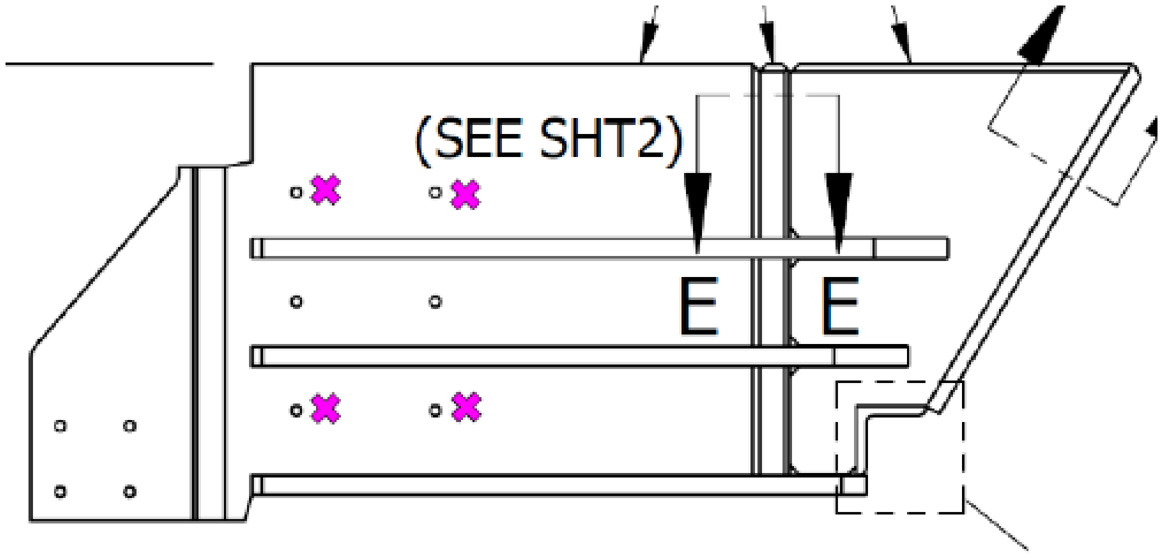

Figure 15. Strain Gage Locations on CEM Locomotive Draft Pocket

Strain gages were installed on the outside of the draft pocket, 2 inches below the connection to the underframe on the left and right sides. Strain gages were installed on the center sill above the draft pocket, 2 inches below the top edge of the center sill on the left and right side. One set of strain gages located on the center sill was placed directly above the back of the draft pocket and the second set of center sill strain gages was placed 82 inches from the front end plate. Figure 16 and Figure 17 show the approximate locations of these strain gages.

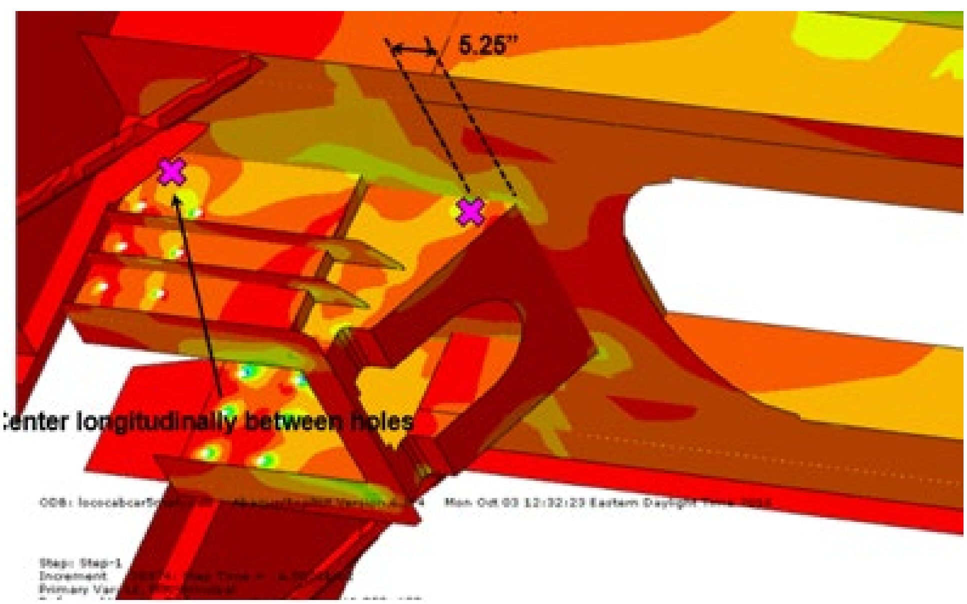

Figure 16. Strain Gage Locations on CEM Locomotive Draft Pocket

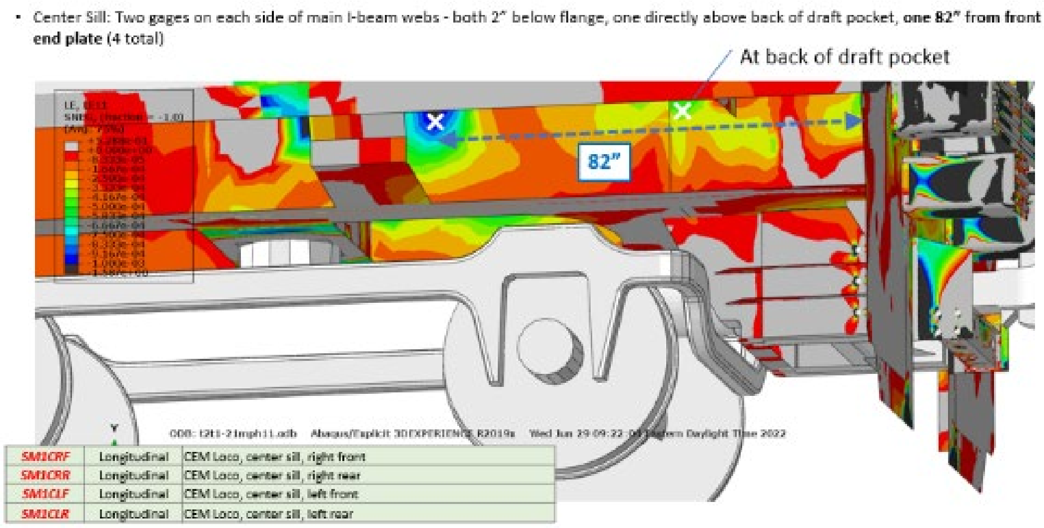

Figure 17. Strain Gage Locations on CEM Locomotive Center Sill

Two additional strain gages (i.e., SM1XPR, SM1XPL) were installed on the cross-plate, and two strain gages (i.e., SM1DAR, SM1DAL) were placed at the draft pocket back plate. The strain gages on the draft pocket back plate were positioned vertically on each near side of the pocket, near the intersection with the cross plate. The strain gages on the cross plate were in line with the side of the pocket corners and positioned longitudinally. Figure 18 shows the approximate locations of these strain gages.

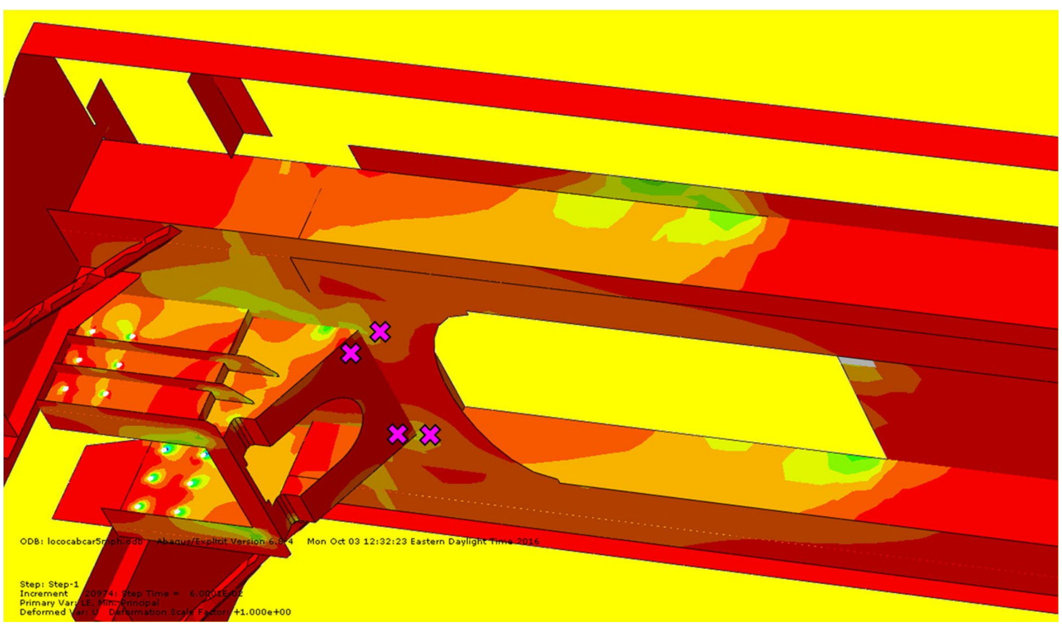

Figure 18. Strain Gage Locations on Cross-Plate and Draft Gear Pocket Back Plate

2.2.4 CEM Locomotive Speed Sensors

Multiple speed sensors accurately measured the impact speed of the CEM locomotive when it was within 20 inches of the impact point. The speed sensor was reflector-based, and it used both ground-based reflectors separated by a known distance and a vehicle-based light sensor that triggers as the locomotive passes over the reflectors. The last reflector was within 10 inches of the impact point. The time interval between reflector passing was recorded, and the speed was calculated from reflector spacing (distance) and time. Backup speed measurements were taken with a handheld radar gun. A second speed trap installed approximately 5 feet after the impact point was used to calculate the speed of the CEM locomotive directly after the collision with the stationary consist.

2.3 First M1 Passenger Car (8332) Instrumentation

The following sections describe the test instrumentation installed on M1 car 8332.

2.3.1 M1 Car 8332 Accelerometers

Tri-axial accelerometers were placed at the two ends of the car and approximately at the center along the car's center line. The center tri-axial accelerometer was located 36 feet 11 inches from the front-end plate due to obstructions under the car. The team placed longitudinal and vertical accelerometers on the left and right sides of its underframe at its center. Two percent of full scale is the typical scale factor calibration error for the accelerometers used. Table 5 summarizes all accelerometers on the M1 passenger car. Figure 19 shows the locations of the accelerometers.

Table 5. M1 Passenger Car Accelerometer Summary

Name	Range	Location
AM2LE_X	400g	First M1, lead end, center – longitudinal
AM2LE_Y	200g	First M1, lead end, center – lateral
AM2LE_Z	200g	First M1, lead end, center – vertical
AM2UC_X	200g	First M1, underframe center – longitudinal
AM2UC_Y	200g	First M1, underframe center – lateral
AM2UC_Z	200g	First M1, underframe center – vertical
AM2UCR_X	200g	First M1, underframe center right – longitudinal
AM2UCR_Z	200g	First M1, underframe center right – vertical
AM2UCL_X	200g	First M1, underframe center left – longitudinal
AM2UCL_Z	200g	First M1, underframe center left – vertical
AM2TEC_X	200g	First M1, trailing end, center – longitudinal
AM2TEC_Y	200g	First M1, trailing end, center – lateral
AM2TEC_Z	200g	First M1, trailing end, center – vertical
AM2LE_X	400g	First M1, lead end, center – longitudinal
AM2LE_Y	200g	First M1, lead end, center – lateral
AM2LE_Z	200g	First M1, lead end, center – vertical
AM2UC_X	200g	First M1, underframe center – longitudinal
AM2UC_Y	200g	First M1, underframe center – lateral
AM2UC_Z	200g	First M1, underframe center – vertical
AM2UCR_X	200g	First M1, underframe center right – longitudinal
AM2UCR_Z	200g	First M1, underframe center right – vertical

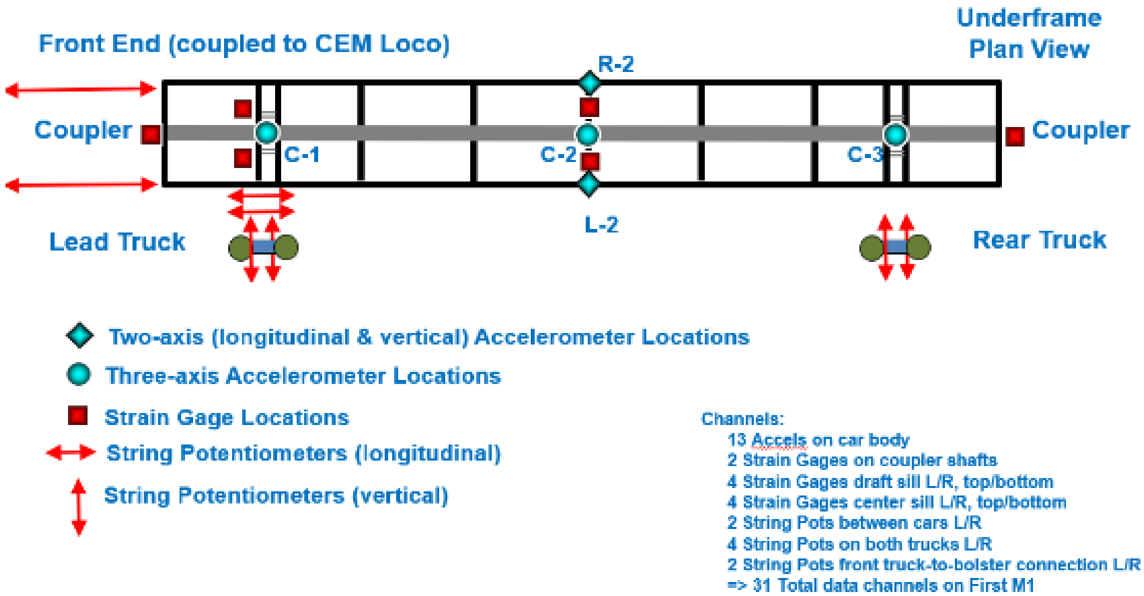

Figure 19. First M1 Passenger Car Instrumentation

2.3.2 M1 Car 8332 String Potentiometers

The first M1 passenger car was equipped with vertical string potentiometers across each truck's secondary suspension. Two string potentiometers were installed between the lead truck and the bolster longitudinally on the left and right sides. Two additional string potentiometers were placed between the rear end of the CEM locomotive and the lead end of the first M1 car on the left and right side, respectively. Table 6 summarizes all string potentiometers on the first M1 passenger car. Figure 20 through Figure 22 show the locations of the string potentiometers.

Table 6. M1 Passenger Car String Potentiometer Summary

Name	Range	Location
DM2L_X	+20/-30 inch	Displacement b/t CEM Loco & 1st M1, left – longitudinal
DM2R_X	+20/-30 inch	Displacement b/t CEM Loco & 1st M1, right – longitudinal
DM2LTBL_X	+20/-30 inch	Displacement at lead truck-to-bolster, left – longitudinal
DM2LTBR_X	+20/-30 inch	Displacement at lead truck-to-bolster, right – longitudinal
DM2LTL_Z	+/- 5 inch	First M1 secondary suspension, lead truck, left
DM2LTR_Z	+/- 5 inch	First M1 secondary suspension, lead truck, right
DM2TTL_Z	+/- 5 inch	First M1 secondary suspension, trailing truck, left
DM2TTR_Z	+/- 5 inch	First M1 secondary suspension, trailing truck, right

Figure 20. First M1 Passenger Car Truck Secondary Suspension String Potentiometers

Figure 21. First M1 Passenger Car Front Coupler String Potentiometers

Figure 22. First M1 Passenger Car Lead Truck to Bolster String Potentiometers

2.3.3 M1 Car 8332 Strain Gages

The first M1 passenger car was fitted with 10 strain gages. Four strain gages were placed on the draft sill, and four were placed on the center sill. The strain gages on the front and rear coupler were placed on top of the coupler shank above the coupler carrier. Table 7 summarizes all strain gages on the first M1 passenger car. Figure 23 through Figure 25 show approximate locations of the strain gages.

Table 7. M1 Passenger Car Strain Gage Summary

Name	Orientation	Location
SM2CL	Longitudinal	First M1, lead coupler shaft, above coupler carrier, top
SM2CT	Longitudinal	First M1, rear coupler shaft, above coupler carrier, top
SM2DLT	Longitudinal	First M1, draft sill, left side, top
SM2DLB	Longitudinal	First M1, draft sill, left side, bottom
SM2DRT	Longitudinal	First M1, draft sill, right side, top
SM2DRB	Longitudinal	First M1, draft sill, right side, bottom
SM2CLT	Longitudinal	First M1, center sill, left side, top
SM2CLB	Longitudinal	First M1, center sill, left side, bottom
SM2CRT	Longitudinal	First M1, center sill, right side, top
SM2CRB	Longitudinal	First M1, center sill, right side, bottom

Researchers installed strain gages on the draft sill on the left and right side, approximately 54 inches from the front-end plate, and 1 inch away from the top and bottom of the sill.

- Draft Sill: Two gages on each side of draft sill, 54" from front end plate, 1" away from top & bottom (4 total)
- Center Sill: Two gages on each side of center sill, as close as possible to the longitudinal center of the car that can be accessed (but at least two away from structural cross members if possible), 1" away from top & bottom

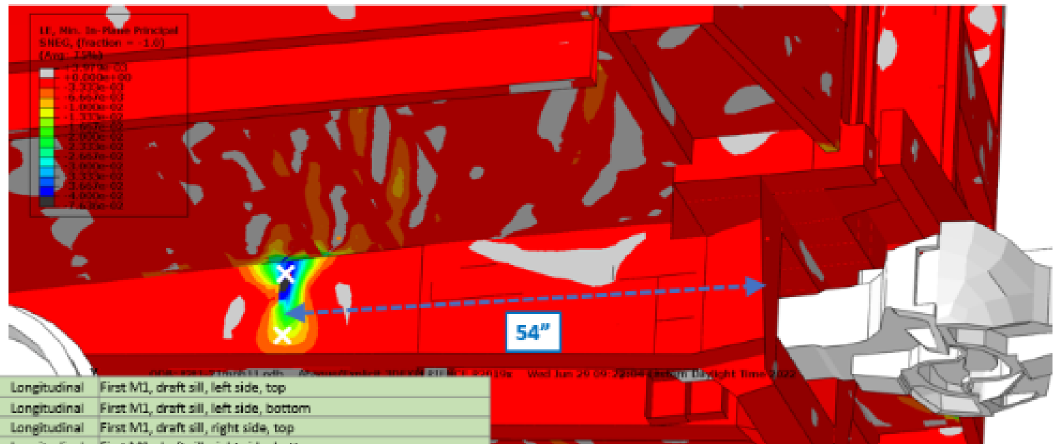

SM2DLT	Longitudinal	First M1, draft sill, left side, top
SM2DLB	Longitudinal	First M1, draft sill, left side, bottom
SM2DRT	Longitudinal	First M1, draft sill, right side, top
SM2DRB	Longitudinal	First M1, draft sill, right side, bottom
SM2CLT	Longitudinal	First M1, center sill, left side, top
SM2CLB	Longitudinal	First M1, center sill, left side, bottom
SM2CRT	Longitudinal	First M1, center sill, right side, top
SM2CRB	Longitudinal	First M1, center sill, right side, bottom

Figure 23. Strain Gage Locations on the First M1 Passenger Car Draft Sill

Strain gages on the center sill were installed on the left and right sides as close as possible to the longitudinal center of the car and centered vertically due to accessibility and curvature. The right-side gages were located 17 feet 3 inches from the front-end plate. The left side gages were located 35 feet 8 inches from the front-end plate. The gages on each side were spaced 12 inches apart.

Figure 24. Strain Gage Locations on the First M1 Passenger Car Center Sill

Figure 25. Strain Gage Location on the First M1 Passenger Car Lead Coupler

2.4 Second M1 Passenger Car (8221) Instrumentation

The following sections describe the test instrumentation installed on M1 car 8221.

2.4.1 M1 Car 8221 Accelerometers

Tri-axial accelerometers were placed at the two ends and at the center along the car's center line. Longitudinal and vertical accelerometers were placed to the left and right sides of the underframe center. Two percent of full scale is the typical scale factor calibration error for these accelerometers. Table 8 summarizes all accelerometers on the second M1 passenger car. Figure 26 shows the locations of the accelerometers.

Table 8. Second M1 Passenger Car Accelerometer Summary

Name	Range	Location
AM3LE_X	400g	Second M1, lead end, center – longitudinal
AM3LE_Y	200g	Second M1, lead end, center – lateral
AM3LE_Z	200g	Second M1, lead end, center – vertical
AM3UC_X	200g	Second M1, underframe center – longitudinal
AM3UC_Y	200g	Second M1, underframe center – lateral
AM3UC_Z	200g	Second M1, underframe center – vertical
AM3UCR_X	200g	Second M1, underframe center right – longitudinal
AM3UCR_Z	200g	Second M1, underframe center right – vertical
AM3UCL_X	200g	Second M1, underframe center left – longitudinal
AM3UCL_Z	200g	Second M1, underframe center left – vertical
AM3TEC_X	200g	Second M1, trailing end, center – longitudinal
AM3TEC_Y	200g	Second M1, trailing end, center – lateral
AM3TEC_Z	200g	Second M1, trailing end, center – vertical

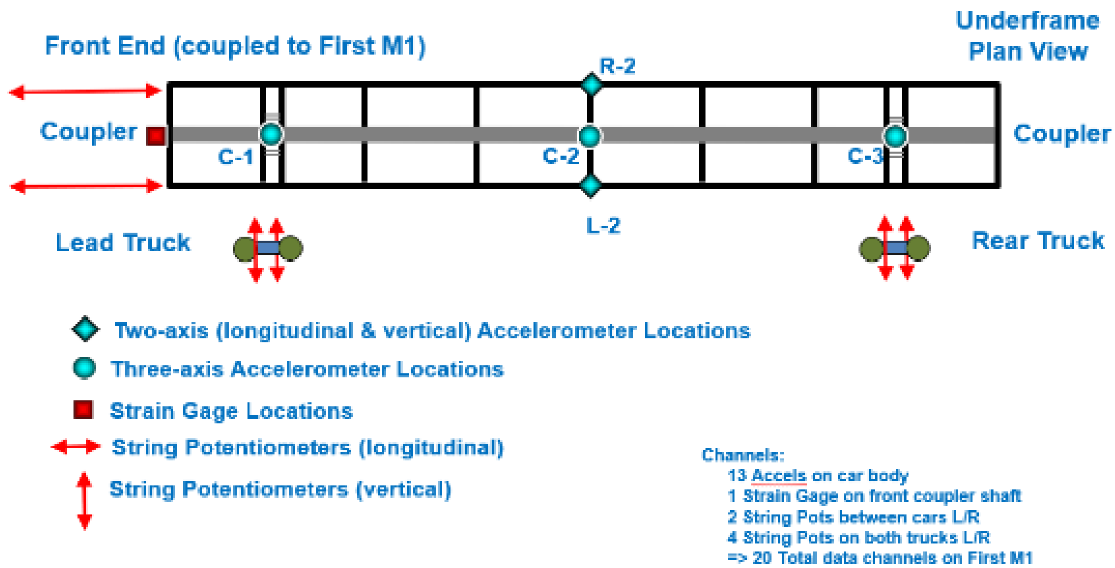

Figure 26. Second M1 Car Instrumentation

2.4.2 M1 Car 8221 String Potentiometers

The second M1 car was fitted with string potentiometers across each truck's secondary suspension. Two additional string potentiometers were placed between the rear end of the first M1 car and the lead end of the second M1 car. Table 9 summarizes all string potentiometers on the M1 passenger car. Figure 27 and Figure 28 show the locations of the string potentiometers.

Table 9. M1 Passenger Car String Potentiometer Summary

Name	Range	Location
DM3L_X	+20/-30 inch	Displacement between 1st M1 & 2nd M1, left – longitudinal
DM3R_X	+20/-30 inch	Displacement between 1st M1 & 2nd M1, right – longitudinal
DM3LTL_Z	+/-5 inch	Second M1 secondary suspension, lead truck, left
DM3LTR_Z	+/- 5 inch	Second M1 secondary suspension, lead truck, right
DM3TTL_Z	+/- 5 inch	Second M1 secondary suspension, trailing truck, left
DM3TTR_Z	+/- 5 inch	Second M1 secondary suspension, trailing truck, right

Figure 27. Second M1 Passenger Car Truck Secondary Suspension String Potentiometer

Figure 28. Second M1 Passenger Car Coupler String Potentiometers

2.4.3 M1 Car 8221 Strain Gages

The second M1 car was fitted with one strain gage on the front coupler shaft. Table 10 summarizes all strain gages on the M1 passenger car. Figure 29 shows the approximate location of the strain gage.

Table 10. M1 Passenger Car Strain Gage Summary

Name	Orientation	Location
SM3CL	Longitudinal	Second M1, lead coupler shaft, above coupler carrier, top

Figure 29. Strain Gage Location on the Second M1 Passenger Car Lead Coupler

2.5 Conventional F40 Locomotive (4117) Instrumentation

The following sections describe the test instrumentation installed on F40 Locomotive 4117.

2.5.1 Conventional F40 Locomotive Accelerometers

Tri-axial accelerometers were placed at the two ends and at the center along the car's center line. Longitudinal and vertical accelerometers were placed on the left and right sides of the underframe center. Each truck was fitted with a vertical accelerometer and one longitudinal accelerometer on the right and left. The front coupler was fitted with two longitudinal accelerometers, right and left. Two percent of full scale is the typical scale factor calibration error for the accelerometers used. Table 11 summarizes all accelerometers on the conventional F40 locomotive. Figure 30 shows the locations of the accelerometers.

Table 11. Conventional F40 Locomotive Accelerometers Summary

Name	Range	Location
AS1LE_X	400g	Conv Loco, lead end, center – longitudinal
AS1LE_Y	200g	Conv Loco, lead end, center – lateral
AS1LE_Z	200g	Conv Loco, lead end, center – vertical
AS1UC_X	200g	Conv Loco, underframe center – longitudinal
AS1UC_Y	200g	Conv Loco, underframe center – lateral
AS1UC_Z	200g	Conv Loco, underframe center – vertical
AS1UCR_X	200g	Conv Loco, underframe center right – longitudinal
AS1UCR_Z	200g	Conv Loco, underframe center right – vertical
AS1UCL_X	200g	Conv Loco, underframe center left – longitudinal
AS1UCL_Z	200g	Conv Loco, underframe center left – vertical
AS1TEC_X	200g	Conv Loco, trailing end, center – longitudinal
AS1TEC_Y	200g	Conv Loco, trailing end, center – lateral
AS1TEC_Z	200g	Conv Loco, trailing end, center – vertical
AS1LTL_Z	400g	Conv Loco, lead truck – vertical
AS1LTR_X	400g	Conv Loco, lead truck, right – longitudinal
AS1LTL_X	400g	Conv Loco, lead truck, left – longitudinal
AS1TTL_Z	400g	Conv Loco, trailing truck – vertical
AS1TTR_X	400g	Conv Loco, trailing truck, right – longitudinal
AS1TTL_X	400g	Conv Loco, trailing truck, left – longitudinal
AS1CR_X	5,000g	Conv Loco, front coupler, right – longitudinal
AS1CL_X	5,000g	Conv Loco, front coupler, left – longitudinal

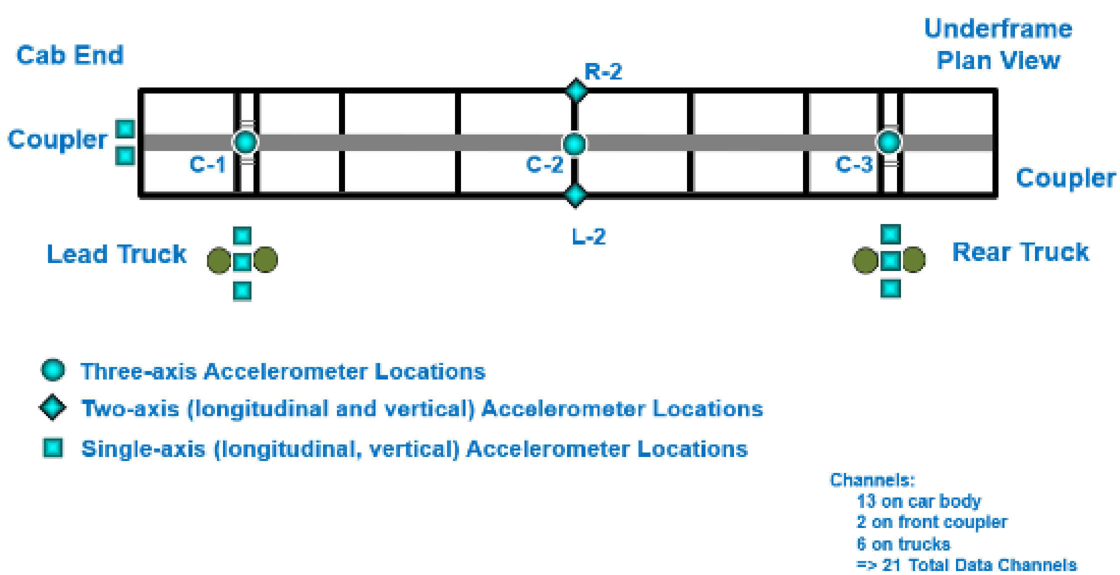

Figure 30. Accelerometer Locations on Conventional F40 Locomotive

2.5.2 Conventional F40 Locomotive String Potentiometers

The conventional locomotive was fitted with string potentiometers across each truck's secondary suspension. The front coupler of the locomotive was fitted with two string potentiometers to measure longitudinal displacement. Two additional string potentiometers were placed on the front of the locomotive on the left and right sides of the underframe. Table 12 summarizes all string potentiometers on the conventional locomotive. Figure 31 shows the locations of the string potentiometers.

Table 12. Conventional F40 Locomotive String Potentiometers Summary

Name	Range	Location
DS1LTR_Z	+/- 5 inch	Conv Loco secondary suspension, lead truck – vertical, right
DS1LTL_Z	+/- 5 inch	Conv Loco secondary suspension, lead truck – vertical, left
DS1TTR_Z	+/- 5 inch	Conv Loco secondary suspension, trailing truck – vertical, right
DS1TTL_Z	+/- 5 inch	Conv Loco secondary suspension, trailing truck – vertical, left
DS1UL_X	+5/-45 inch	Conv Loco underframe, front – longitudinal, left
DS1UR_X	+5/-45 inch	Conv Loco underframe, front – longitudinal, right
DS1CL_X	+20/-30 inch	Conv Loco coupler – longitudinal, left
DS1CR_X	+20/-30 inch	Conv Loco coupler – longitudinal, right

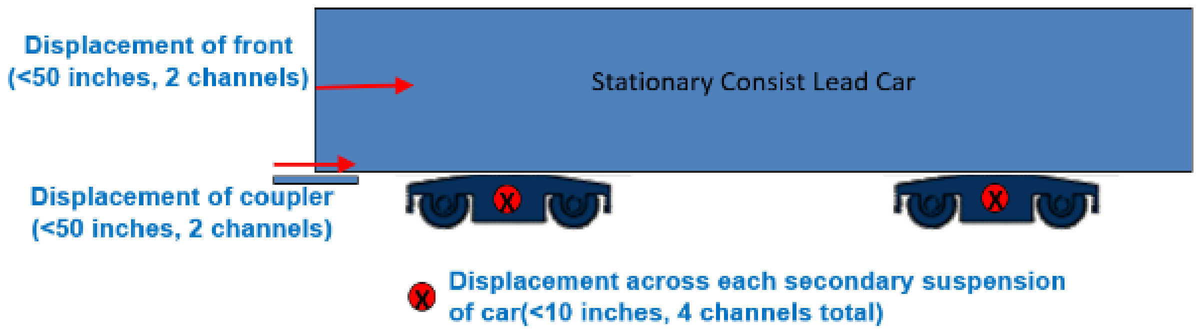

Figure 31. Conventional F40 Locomotive String Potentiometer Locations

2.5.3 Conventional F40 Locomotive Strain Gages

The conventional F40 locomotive was fitted with 14 strain gages on the couplers, draft pocket, center sill, and cross plate. Table 13 summarizes all strain gages on the conventional F40 locomotive. Figure 32 and Figure 33 show the locations of the strain gages. The strain gage on the rear coupler was placed on top of the coupler shank above the coupler carrier.

Table 13. Conventional F40 Locomotive Strain Gages Summary

Name	Orientation	Location
SS1CST	Longitudinal	Conv Loco, coupler shaft, above coupler carrier, top
SS1CSR	Longitudinal	Conv Loco, coupler shaft, above coupler carrier, right
SS1CSL	Longitudinal	Conv Loco, coupler shaft, above coupler carrier, left
SS1CPR	Longitudinal	Conv Loco, coupler shaft at pin, right
SS1CPL	Longitudinal	Conv Loco, coupler shaft at pin, left
SS1CRT	Longitudinal	Conv Loco, rear coupler shaft, above coupler carrier, top
SS1CRF	Longitudinal	Conv Loco, center sill, right front
SS1CRR	Longitudinal	Conv Loco, center sill, right rear
SS1CLF	Longitudinal	Conv Loco, center sill, left front
SS1CLR	Longitudinal	Conv Loco, center sill, left rear
SS1XPR	Longitudinal	Conv Loco, cross plate, right
SS1XPL	Longitudinal	Conv Loco, cross plate, left
SS1DAR	Longitudinal	Conv Loco, draft pocket angled plate, right
SS1DAL	Longitudinal	Conv Loco, draft pocket angled plate, left

Strain gages on the draft pocket were installed on the outside, 2 inches below the connection to the underframe, on the left and right sides. Strain gages on the center sill above the draft pocket were installed 2 inches below the top edge of the center sill, on the left and right sides (Figure 33). One set of strain gages located on the left side of the center sill were positioned 49 inches back from the front-end plate. The second set of center sill strain gages were positioned on the right side and the bottom gage was located 49 inches from the front-end plate, while the top gage was located 82 inches from the front-end plate.

Two additional strain gages (i.e., SS1XPR, SS1XPL) were installed on the cross-plate, and two more strain gages (i.e., SS1DAR, SS1DAL) were installed at the draft pocket back plate. The strain gages on the draft pocket back plate were positioned longitudinally on each side of the pocket and near the intersection with the cross plate . The strain gages on the cross plate were in line with the side of the pocket corners and positioned longitudinally. Figure 32 shows the approximate locations of these strain gages.

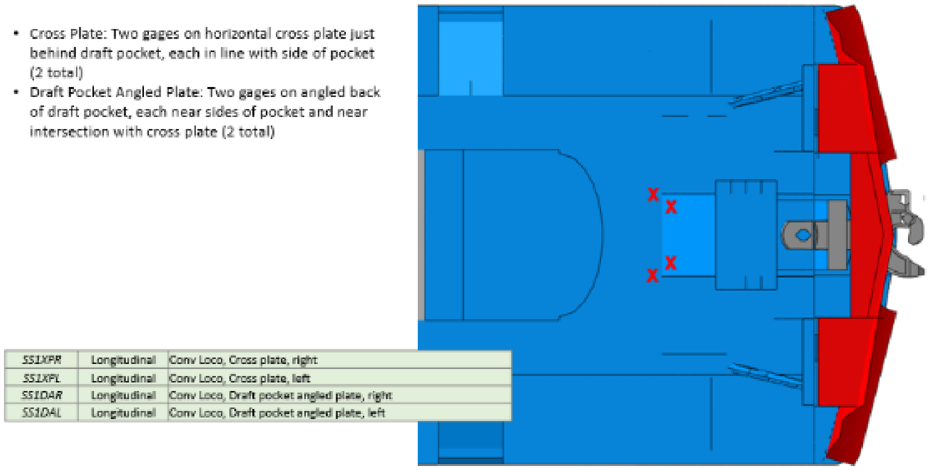

Figure 32. Strain Gages on the Cross-plate and the Draft Gear Pocket Back Plate

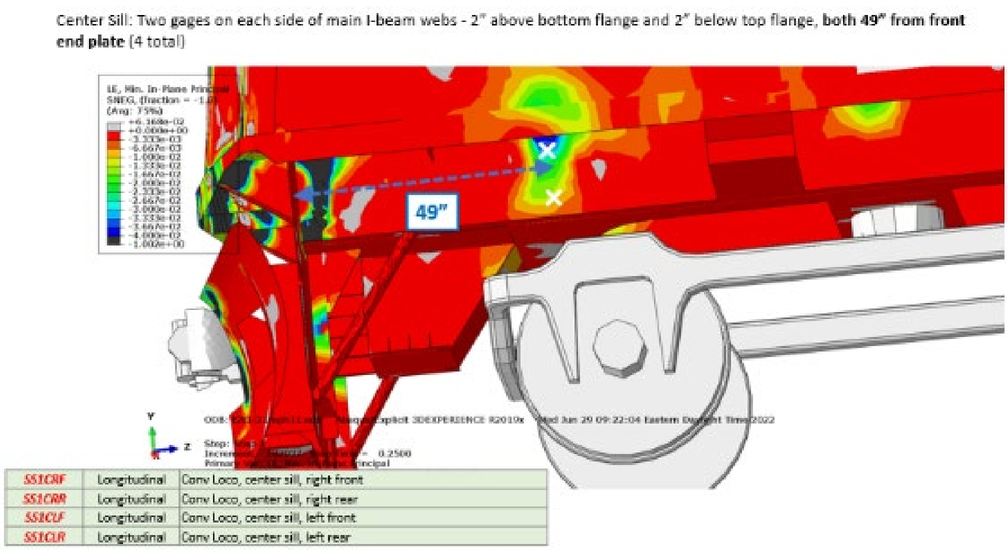

Figure 33. Strain Gage Locations on the Center Sill

2.6 First Hopper Car (BN 531622) Instrumentation

The following sections describe the test instrumentation installed on hopper car BN 531622.

2.6.1 BN 531622 Accelerometers

A tri-axial accelerometer was placed at the center of the first hopper car along the car's center line. Table 14 summarizes the accelerometers on the first hopper car. Figure 34 displays the location of the accelerometer.

Table 14. First Hopper Car Accelerometers Summary

Name	Range	Location
AS2UC_X	200g	First Hopper, underframe center – longitudinal
AS2UC_Y	200g	First Hopper, underframe center – lateral
AS2UC_Z	200g	First Hopper, underframe center – vertical

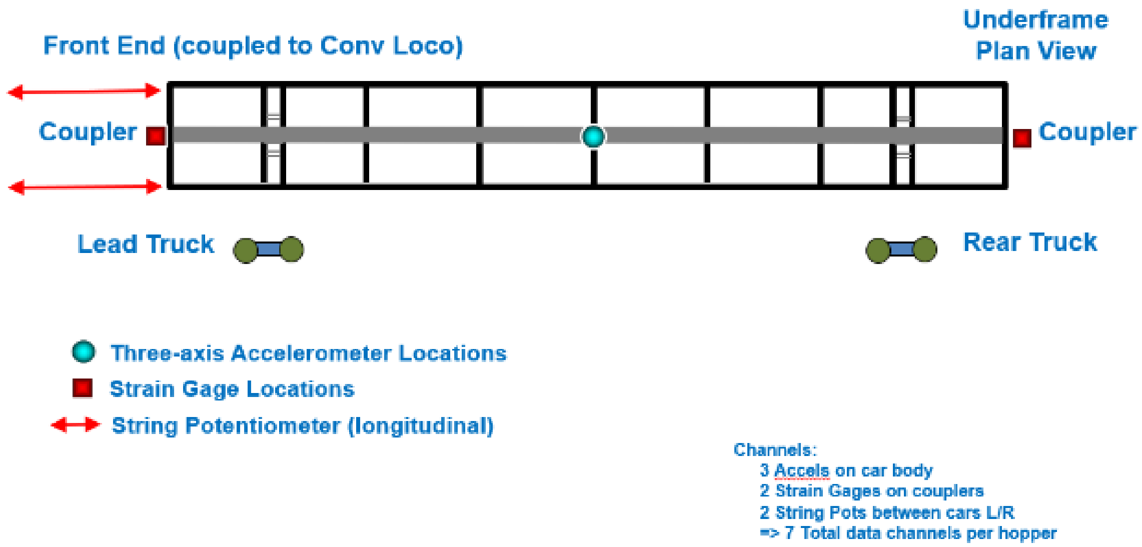

Figure 34. First Hopper Car Instrumentation

2.6.2 BN 531622 String Potentiometers

The first hopper car was fitted with string potentiometers between the rear end of the conventional locomotive and on the left and right sides of the front end of the first hopper car. Table 15 summarizes the string potentiometers on the first hopper car. Figure 34 displays the locations of the string potentiometers.

Table 15. First Hopper Car String Potentiometers Summary

Name	Range	Location
DS2L_X	+20/-30 inch	Displacement b/t Conv Loco & First Hopper, left – longitudinal
DS2R_X	+20/-30 inch	Displacement b/t Conv Loco & First Hopper, right – longitudinal

2.6.3 BN 531622 Strain Gages

The first hopper car was fitted with two uniaxial strain gages, one each on its front and rear coupler. The gages were installed on top of the coupler shank above the coupler carrier. Table 16 summarizes all strain gages on the first hopper car. Figure 34 displays the locations of the strain gages.

Table 16. First Hopper Car Strain Gage Summary

Name	Orientation	Location
SS2CL	Longitudinal	First Hopper, lead coupler shaft, above coupler carrier, top
SS2CT	Longitudinal	First Hopper, trailing coupler shaft, above coupler carrier, top

2.7 Second Hopper Car (BN 526308) Instrumentation

The following sections describe the test instrumentation installed on hopper car BN 526308.

2.7.1 BN 526308 Accelerometers

A tri-axial accelerometer was placed at the center of the second hopper car along the car's center line. Table 17 summarizes the accelerometers on the second hopper car. Figure 35 displays the location of the accelerometer.

Table 17. Second Hopper Car Accelerometers Summary

Name	Range	Location
AS3UC_X	200g	Second Hopper, underframe center – longitudinal
AS3UC_Y	200g	Second Hopper, underframe center – lateral
AS3UC_Z	200g	Second Hopper, underframe center – vertical

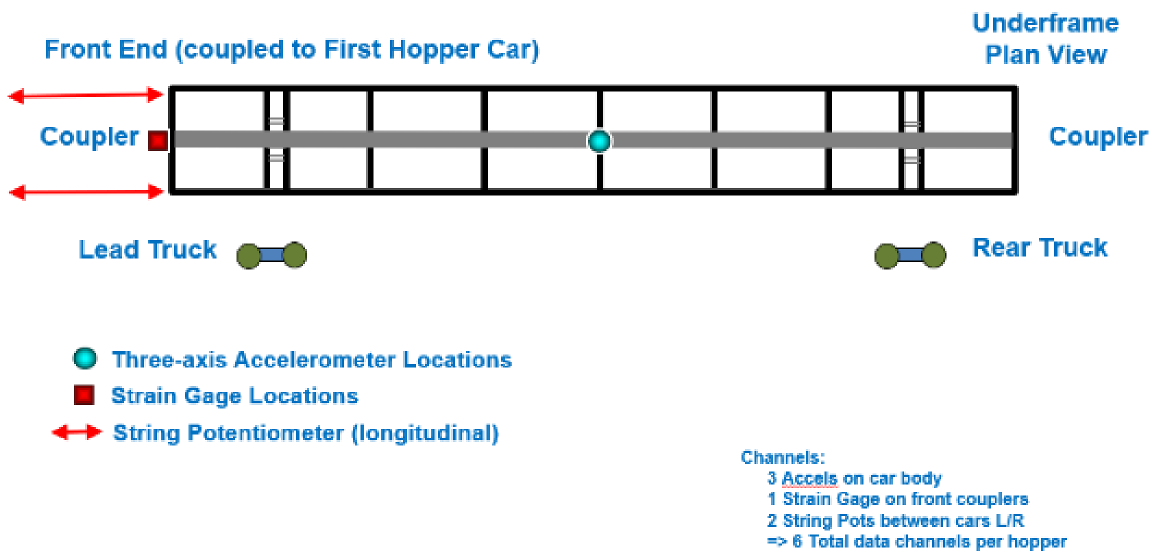

Figure 35. Second Hopper Car Instrumentation

2.7.2 BN 526308 String Potentiometers

The second hopper car was fitted with string potentiometers between the rear end of the first hopper car and on the left and right sides of the front end of the second hopper car. Table 18 summarizes the string potentiometers on the second hopper car. Figure 35 displays the locations of the string potentiometers.

Table 18. Second Hopper Car String Potentiometers Summary

Name	Range	Location
DS3L_X	+20/-30 inch	Displacement b/t First Hopper & Second Hopper, left – longitudinal
DS3R_X	+20/-30 inch	Displacement b/t First Hopper & Second Hopper, right – longitudinal

2.7.3 BN 526308 Strain Gages

The second hopper car was fitted with one uniaxial strain gage on its front coupler. The gage was installed on top of the coupler shank above the coupler carrier. Table 19 summarizes the strain gage on the second hopper car. Figure 35 displays the locations of the strain gage.

Table 19. Second Hopper Car Strain Gage Summary

Name	Orientation	Location
SS3CL	Longitudinal	Second Hopper, lead coupler shaft, above coupler carrier, top

2.8 Occupant Protection Experiments

Researchers installed three occupant protection experiments in the M1 passenger cars behind the CEM locomotive in the moving consist. These experiments included different types of wheelchairs and restraint systems. Each experiment had a 50th percentile male (i.e., H3-50M) ATD equipped with instrumentation that collected data that included forces, accelerations, and displacements, which were used to compute injury levels.

2.8.1 Experiment 1.1

This experiment was located in the first M1 passenger car (i.e., 8332) of the moving consist. It was installed at the rear of the vehicle and included an unrestrained, rear-facing H3-50M ATD seated in a standard unrestrained manual wheelchair with brakes applied. The ATD was compartmentalized with a Quantum® backboard (fore) and a commuter seat (aft). There were 59 inches of maneuverable space, longitudinally, between the backboard and the commuter seat. Table 20 describes the ATD channel list for this experiment. Figure 36 shows the Quantum backboard and Figure 37 displays the final experiment setup that consisted of the backboard, wheelchair, ATD, and commuter seat. Targets were added on the floor, wall, and experiment components to aid in the analysis of the footage from two interior high-speed (HS) cameras. The ATD and wheelchair were tethered to the car to prevent excessive damage to the equipment as it traveled within the 59 inches of maneuverable space.

Table 20. Experiment 1.1 ATD Instrumentation List

Name	Description
AM11HD_X	Head X Accelerometer, Ax
AM11HD_Y	Head Y Accelerometer, Ay
AM11HD_Z	Head Z Accelerometer, Az
FM11NK_X	Upper Neck Load Cell, Fx
FM11NK_Z	Upper Neck Load Cell, Fz
MM11NK_Y	Upper Neck Load Cell, My
AM11CH_X	Chest X Accelerometer, Ax
AM11CH_Y	Chest Y Accelerometer, Ay
AM11CH_Z	Chest Z Accelerometer, Az
DM11CH_X	Chest X Displacement Potentiometer, Delta x
AM11PL_X	Pelvis X Accelerometer, Ax
AM11PL_Y	Pelvis Y Accelerometer, Ay
AM11PL_Z	Pelvis Z Accelerometer, Az
FM11FMRL	Left Femur Load Cell, Fz
FM11FMRR	Right Femur Load Cell, Fz

Figure 36. Quantum Backboard Restraint Device

Figure 37. Experiment 1.1 Final Setup

2.8.2 Experiment 2.1

This experiment was located in the second M1 car (8221) of the moving consist. It was installed on the right side of the vehicle at the front end (i.e., the end closest to the impact point, or the leading end with respect to the travel direction) and included a restrained, forward-facing H3-50M ATD seated in a surrogate wheelchair designed for testing. The wheelchair was restrained to the floor at four locations, and the ATD was restrained to the wheelchair with a three-point harness, the upper point of which was attached to the sidewall of the car using the Q'Straint One™ restraint system. Table 21 describes the ATD channel list for this experiment. Figure 38 displays the final experiment setup consisting of the Q'Straint One system, the surrogate wheelchair, and the ATD. Targets were added on the floor, wall, and the experiment components to aid in the analysis of the footage from two interior HS cameras. The ATD and surrogate wheelchair were tethered to prevent excessive damage to the equipment in case the restraint system failed, with allowable travel of approximately 5 feet.

Table 21. Experiment 2.1 ATD Instrumentation List

Name	Description
AM21HD_X	Head X Accelerometer, Ax
AM21HD_Y	Head Y Accelerometer, Ay
AM21HD_Z	Head Z Accelerometer, Az
RM21HD_X	Head X Angular Rate Sensor, ωx
RM21HD_Y	Head Y Angular Rate Sensor, ωy
RM21HD_Z	Head Z Angular Rate Sensor, ωz
FM21NK_X	Upper Neck Load Cell, Fx
FM21NK_Z	Upper Neck Load Cell, Fz
MM21NK_Y	Upper Neck Load Cell, My
AM21CH_X	Chest X Accelerometer, Ax
AM21CH_Y	Chest Y Accelerometer, Ay
AM21CH_Z	Chest Z Accelerometer, Az
DM21CH_X	Chest X Displacement Potentiometer, Delta x
AM21PL_X	Pelvis X Accelerometer, Ax
AM21PL_Y	Pelvis Y Accelerometer, Ay
AM21PL_Z	Pelvis Z Accelerometer, Az
FM21FMRL	Left Femur Load Cell, Fz
FM21FMRR	Right Femur Load Cell, Fz

Figure 38. Experiment 2.1 Final Setup

2.8.3 Experiment 2.2

This experiment was located in the second M1 car (8221) of the moving consist. It was installed on the left side of the vehicle at the cab end (i.e., the end furthest from the impact point, or the trailing end with respect to the travel direction) and included a restrained, rear-facing H3-50M ATD seated in a surrogate wheelchair. The Quantum system restrained the surrogate wheelchair.

The ATD and wheelchair were restrained to the backboard using a three-point harness, the upper point of which was attached to the sidewall of the car. The ATD was compartmentalized with a backboard (fore) and a commuter seat (aft) in case any of the restraints failed. Table 22 describes the ATD channel list for this experiment. Figure 39 shows the Q'Straint® Quantum System. Figure 40 displays the final experiment setup consisting of the Quantum system, surrogate wheelchair, ATD, and commuter seat. Targets were added on the floor, wall, and experiment components to aid in the analysis of the footage from two interior HS cameras. The ATD and surrogate wheelchair were tethered to prevent excessive damage to the equipment in case the restraint system failed, with allowable travel of approximately 5 feet.

Table 22. Experiment 2.1 ATD Instrumentation List

Name	Description
AM22HD_X	Head X Accelerometer, Ax
AM22HD_Y	Head Y Accelerometer, Ay
AM22HD_Z	Head Z Accelerometer, Az
RM22HD_X	Head X Angular Rate Sensor, ωx
RM22HD_Y	Head Y Angular Rate Sensor, ωy
RM22HD_Z	Head Z Angular Rate Sensor, ωz
FM22NK_X	Upper Neck Load Cell, Fx
FM22NK_Z	Upper Neck Load Cell, Fz
MM22NK_Y	Upper Neck Load Cell, My
AM22CH_X	Chest X Accelerometer, Ax
AM22CH_Y	Chest Y Accelerometer, Ay
AM22CH_Z	Chest Z Accelerometer, Az
DM22CH_X	Chest X Displacement Potentiometer, Delta x
AM22PL_X	Pelvis X Accelerometer, Ax
AM22PL_Y	Pelvis Y Accelerometer, Ay
AM22PL_Z	Pelvis Z Accelerometer, Az
FM22FMRL	Left Femur Load Cell, Fz
FM22FMRR	Right Femur Load Cell, Fz

Figure 39. Q'Straint Quantum System

Figure 40. Experiment 2.2 Final Setup

2.9 High-Speed and Real-Time Photography

Researchers used 15 HS and 8 real-time, high definition (HD) video cameras to document the impact event. Figure 41 through Figure 44 show a schematic of the camera position setup. All onboard HS cameras were crashworthy and rated for peak accelerations of 100 G. The team performed the final alignment and sighting of the cameras when the locomotives were positioned at the impact point prior to the start of the test. In addition, lights were installed to provide illumination to the interior of the M1 cars for the occupant protection experiments.

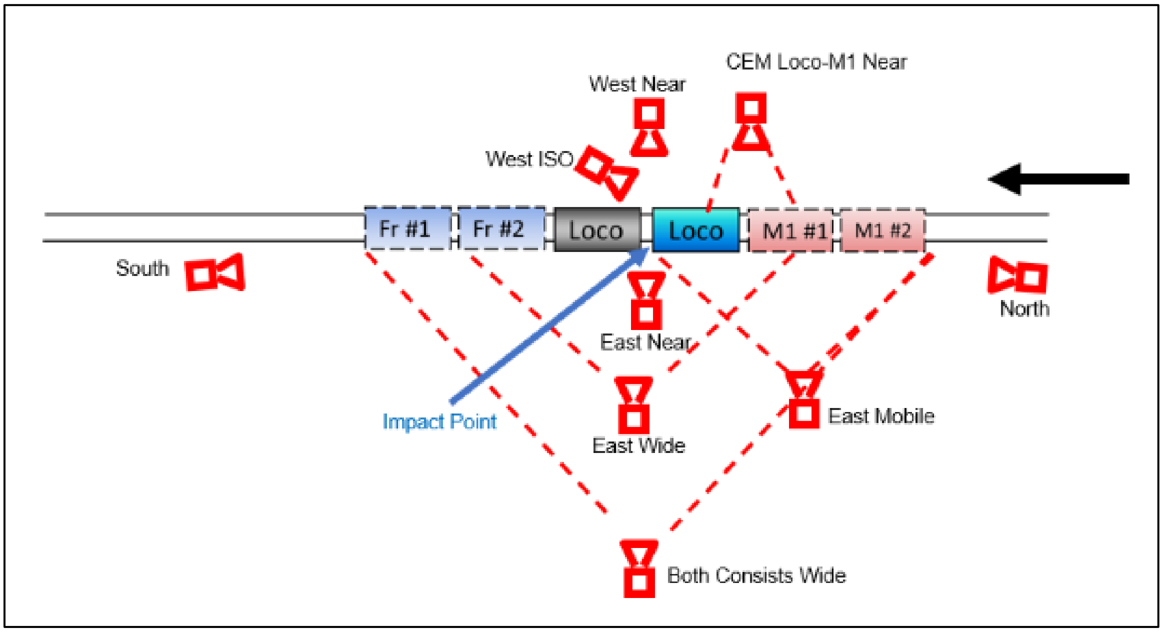

Figure 41. Exterior HS Camera Locations

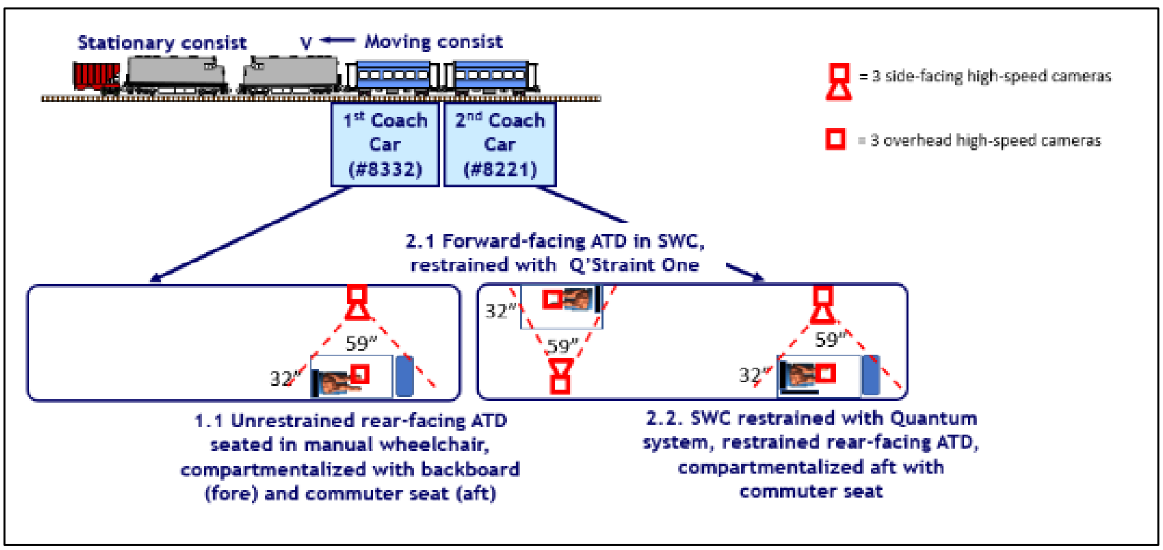

Figure 42. Interior HS Camera Locations

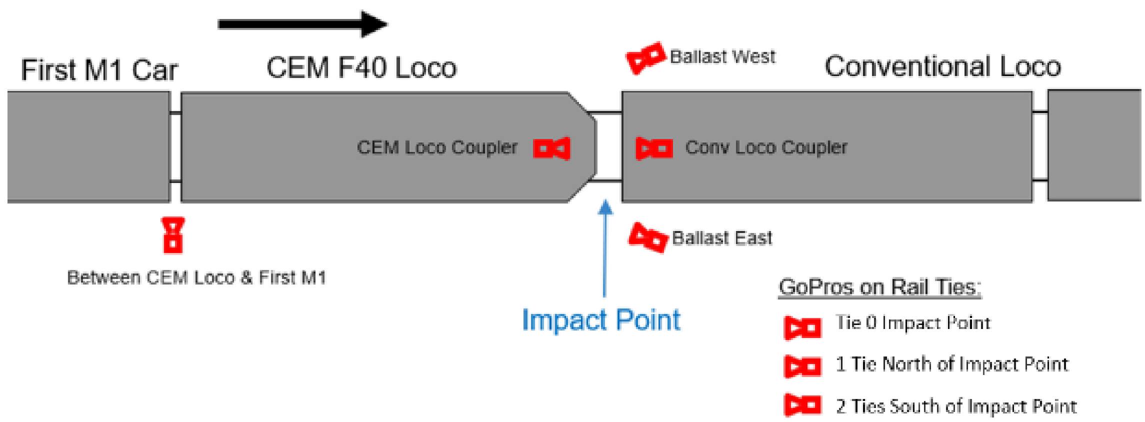

Figure 43. High-Definition Camera Locations

Two camera flashes were installed on both the CEM locomotive and the conventional locomotive and were triggered at the same time as the data acquisition systems. The flashes were visible from the HS cameras and were used to confirm the trigger time and evaluate any trigger time discrepancies between both vehicles.

Targets were placed on the wall and floor of the occupant protection experiments as well as on the ATDs, wheelchairs, and equipment to track relative movement over the course of the test.

2.10 Data Acquisition

The 8-channel, battery-powered, on-board data acquisition systems recorded data from instrumentation mounted on both the moving consist and the stationary consists. These systems provided 1) excitation to the instrumentation, 2) analog anti-aliasing filtering of the signals, 3) analog-to-digital conversion, and 4) recording of each data stream.

The data acquisition systems consisted of GMH Engineering Data BRICK Model II and Model III units. Data acquisition complied with the appropriate sections of SAE J211 [1]. Data from each channel was anti-alias filtered at 1735 Hz then sampled and recorded at 12,800 Hz. Data recorded on the Data BRICKS was synchronized to time zero at initial impact. The time reference was derived from closure of the tape switches on the front of the test vehicle. Each Data BRICK was ruggedized for shock loading up to at least 100 G. On-board battery power was provided by GMH Engineering 1.7 Amp-hour 14.4 Volt NiCad Packs. Tape Switches Inc. Model 1201-131-A tape switches were used to establish event initial contact.

Software in the Data BRICK was used to determine zero levels and calibration factors rather than relying on set gains and expecting no zero drift. The Data BRICKS were set to record 1 second of data before initial impact and 5 seconds of data after initial impact.

3. Results

As described in Section 1, on August 11, 2022, researchers performed an impact test between a F40 locomotive equipped with CEM components coupled to two M1 passenger cars and a stationary conventional F40 locomotive backed by two empty hopper cars. The target impact speed was 21±2 mph. Handbrakes were applied on the empty hopper cars. Ambient conditions are summarized in Table 23.

Table 23. Summary of Ambient Conditions

Wind Speed	Gust Speed	Wind Direction	Temperature
11 mph	19 mph	NE	83°F

3.1 Test Details

Table 24 shows the actual impact speed for the test and the approximate impact forces and energy levels based on accelerometer data.

Table 24. Summary of Test Results

Target Impact Speed	Actual Impact Speed	Approximate Peak Impact Force	Approximate Impact Energy
21 mph	24.3 mph	6,000,000 lbs.	7,700,000 ft.-lbs.

The force of the impact lodged the CEM locomotive's front end into the front end of the conventional locomotive. A hydraulic cylinder was required to pull the vehicles apart after the completion of the test. The second empty hopper car uncoupled from the stationary consist at the initial impact. Eventually, the combined consists caught up to the second hopper car and the vehicle recoupled in a secondary impact. Both consists also came in contact with the single loaded catch car that was positioned approximately 635 feet from the end of the stationary consist. This caused a tertiary impact, and the vehicles came to a complete stop approximately 50 feet after contact was made with the catch car.

3.2 Measured Data

The collected data was processed for zero offset corrections and filtering. An offset adjustment procedure was developed to ensure that the data plotted and analyzed contained only impact-related information and excluded electronic offsets or steady biases. The offset was determined by averaging the data collected before the impact. The offset was then subtracted from the entire dataset for each channel. This post-test offset adjustment is independent of the pre-test offset adjustment made by the data acquisition system.

The post-test filtering of the data was accomplished using a phaseless four-pole digital filter algorithm consistent with SAE J211 requirements [1]. A 60 Hz channel frequency class filter was applied to obtain the filtered acceleration data for the vehicles. Different frequency class filters were applied to the ATD data depending on the measurement and its corresponding filter requirements. A summary of the measured data is provided here. Appendix B contains plots of the time histories of the filtered transducer data for the test.

3.2.1 Accelerations

The team used multiple accelerometers on the vehicles to capture longitudinal acceleration of the moving consist, one of the primary measurements. The CEM locomotive acceleration was used to derive the impact energy and contact force between the moving consist and the stationary consist. The average longitudinal acceleration was obtained by averaging the accelerations measured by the longitudinal accelerometers on the CEM locomotive and the conventional locomotive.

Figure 44 provides the average longitudinal acceleration time history derived from the locomotive accelerometer data. Impact accelerations are shown as positive in these graphs; however, during the impact, the CEM locomotive accelerated in the negative X direction based on the established coordinate system.

All acceleration data are reported in Appendix B.

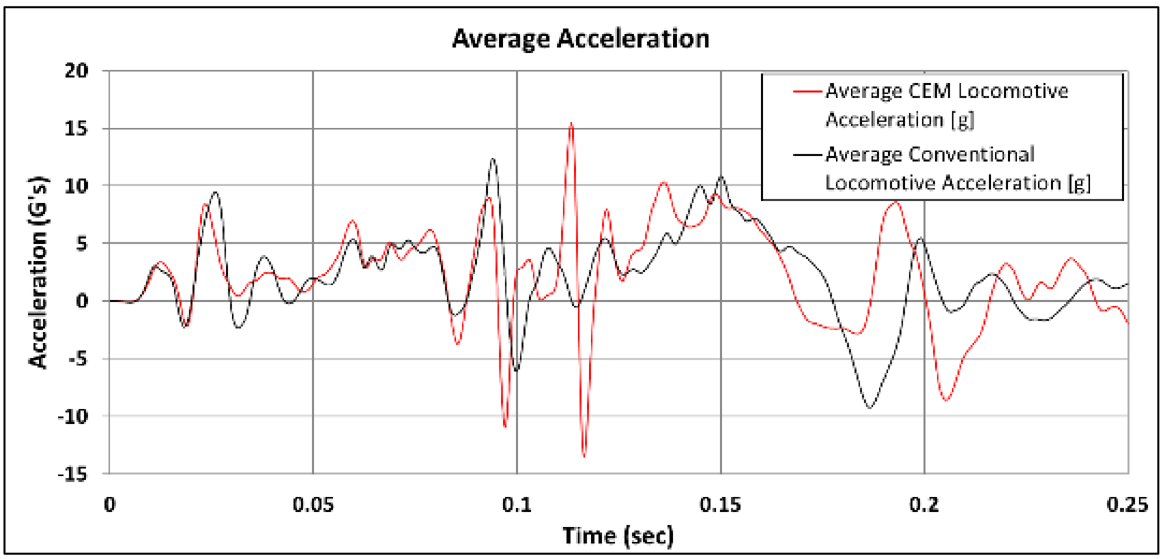

Figure 44. Longitudinal Average Acceleration

3.2.2 Displacements

Figure 46 shows the displacement of the CEM locomotive and the conventional locomotive impacting couplers. DM1CL_X and DM1CR_X represent the left- and right-side displacements on the CEM locomotive's coupler, respectively. DS1CL_X and DS1CR_X represent the left and right-side displacements of the conventional locomotive's coupler, respectively. Eventually, these two string potentiometers were struck during impact and provided inaccurate data after 0.10 seconds. According to the established coordinate system, the coupler moving into the draft pocket was reported as a negative displacement for both the CEM locomotive and the conventional locomotive. The severity of the impact caused the head of the casting on the CEM locomotive coupler to crack and split open vertically.

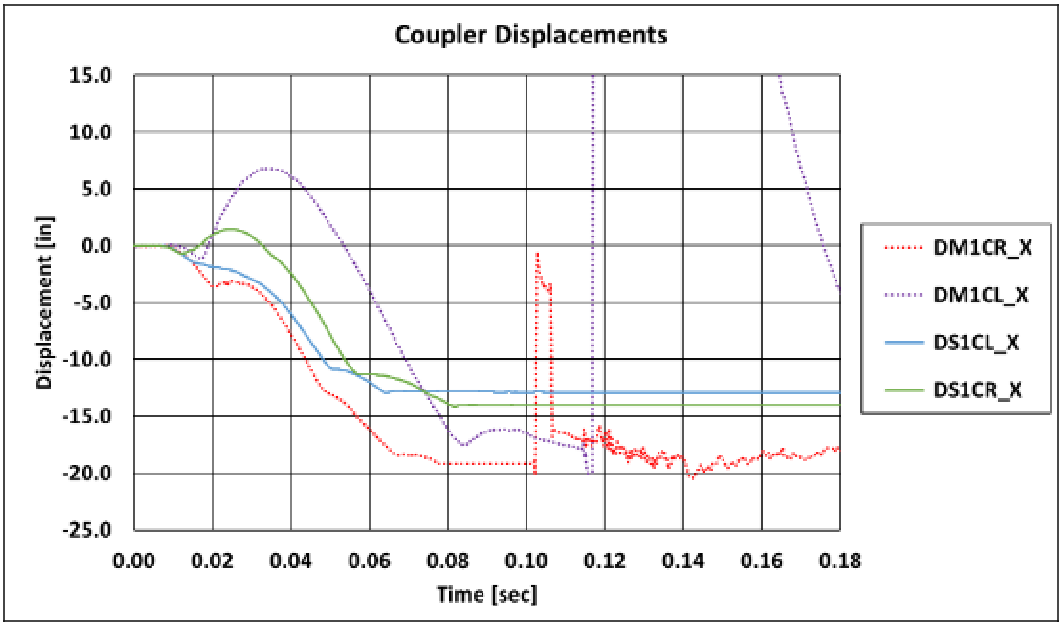

Figure 45. Impacting Coupler Displacements

Figure 47 shows measured longitudinal displacements of all DAC tubes. The bottom tubes were engaged at the impact and deformed approximately 1 inch. The measured displacements (DM1ACR and DM1ACL) included crush displacements of the tubes. The deformation on both sides was fairly symmetrical. The DM1ACL string potentiometer appeared to have disconnected and completely retracted during impact. This accounts for the measurement of approximately 13 inches in the data when the visual inspection produced a value closer to 1 inch. The upper crush tubes of the DAC were fully deformed after contacting the nose of the conventional locomotive (as measured by DM1ACTL and DM1ACTR). The deformation on both sides was fairly symmetrical.

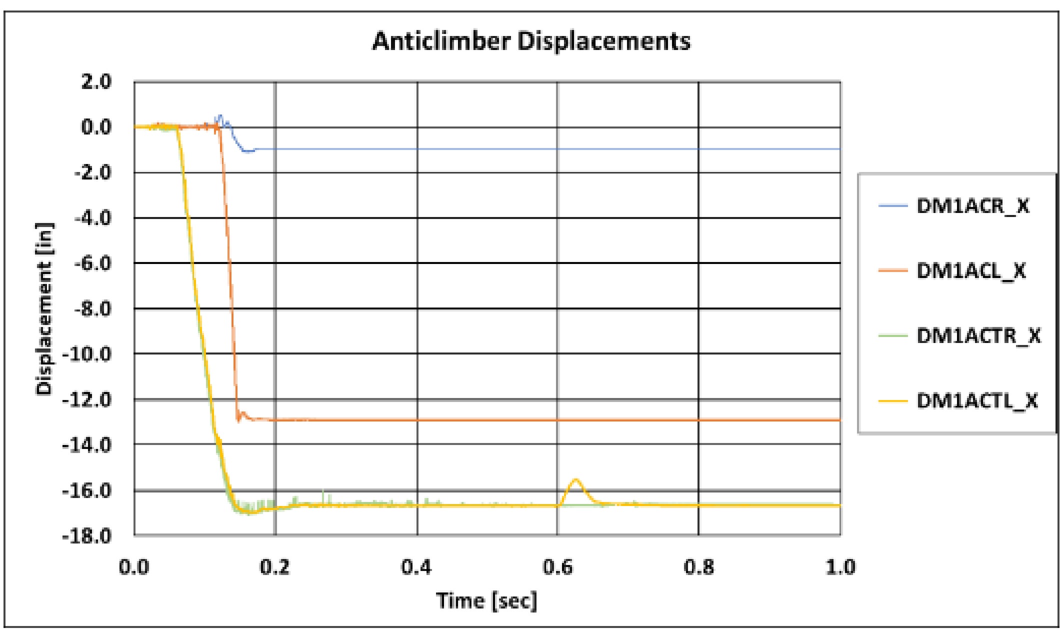

Figure 46. Anti-climber Displacements

The sliding lug bolts were sheared during the impact. The measured displacements of the sliding lug are displayed in Figure 48. Deformation during impact most likely interfered with the DM1SR_X string potentiometer and caused the erratic data between 0.12 and 0.14 seconds.

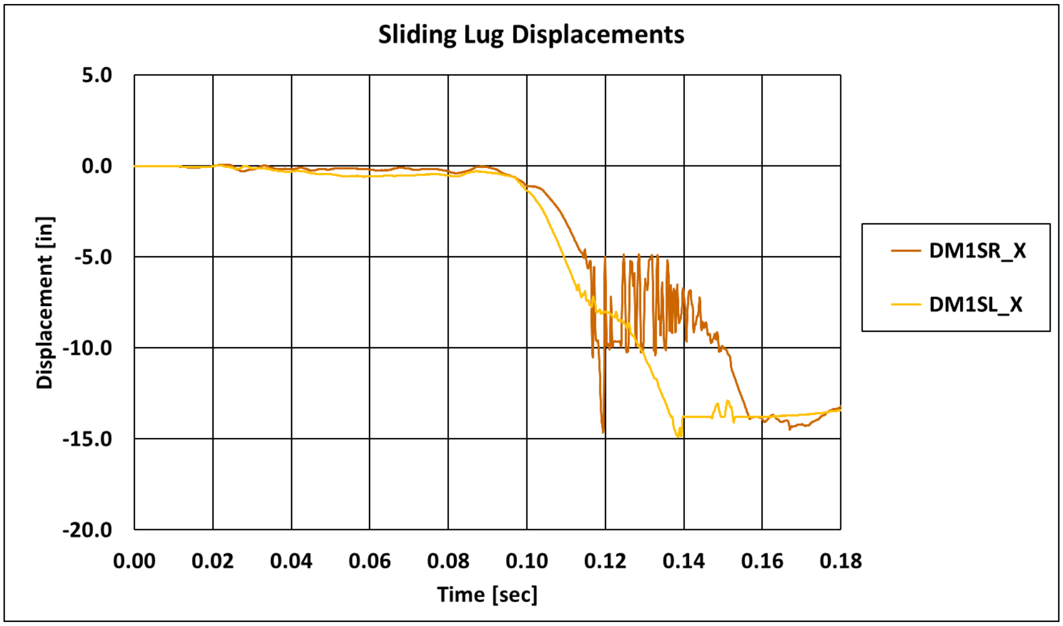

Figure 47. Sliding Lug Displacements

Appendix B includes all measured displacements.

3.2.3 Strains

The CEM locomotive was equipped with 34 strain gages. The first M1 passenger car had 10 strain gages, and the second M1 passenger car had one single strain gage. The conventional locomotive was equipped with 14 strain gages, the first hopper car had two strain gages, and the second hopper car had one strain gage. Data from both the moving consist and the stationary consist are grouped according to their strain gage positions in the vehicles. Figure 49 to Figure 67 show the strain gage data for all instrumented vehicles. During the impact, the cables connected to several strain gages were hit by debris or severed, resulting in a loss of useful data after variable amounts of time. This effect was particularly noticeable on the CEM locomotive's sliding lug and front coupler. Additionally, the first hopper car's rear coupler strain gage appeared to have been damaged during the initial impact that caused the first hopper car to uncouple from the second hopper car. Figure 49 to Figure 67 show data from the first 250 milliseconds of impact, covering the duration of the initial impact. The data acquisition setup resulted in positive strains representing compression and negative strains representing tension.

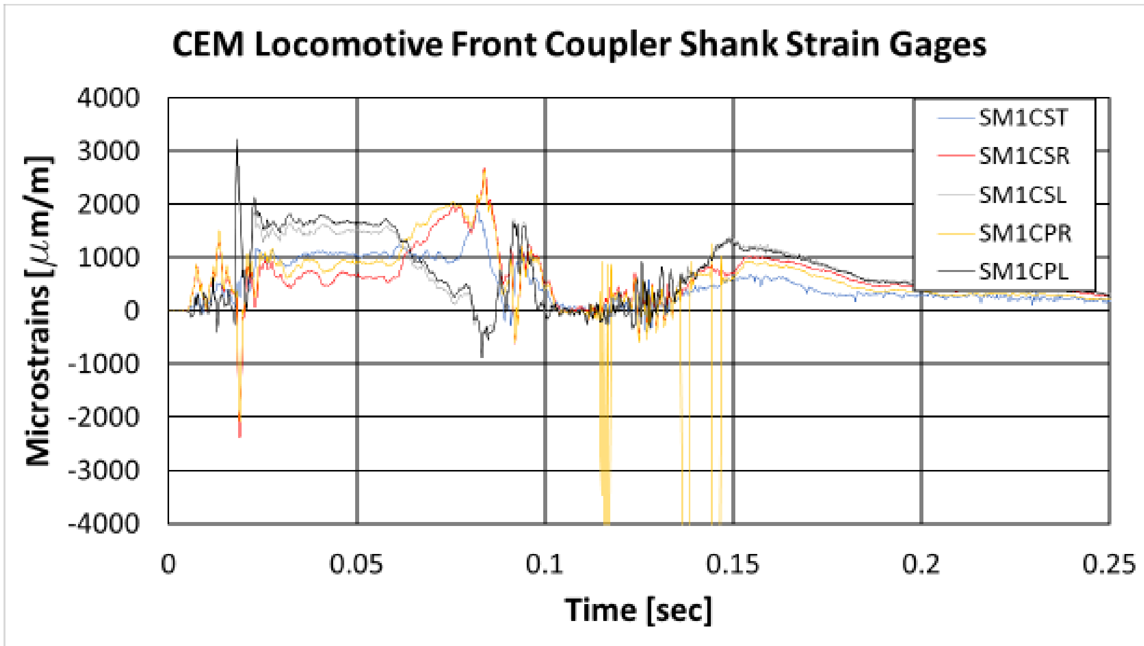

Figure 48. CEM Locomotive Front Coupler Shank Strain Results

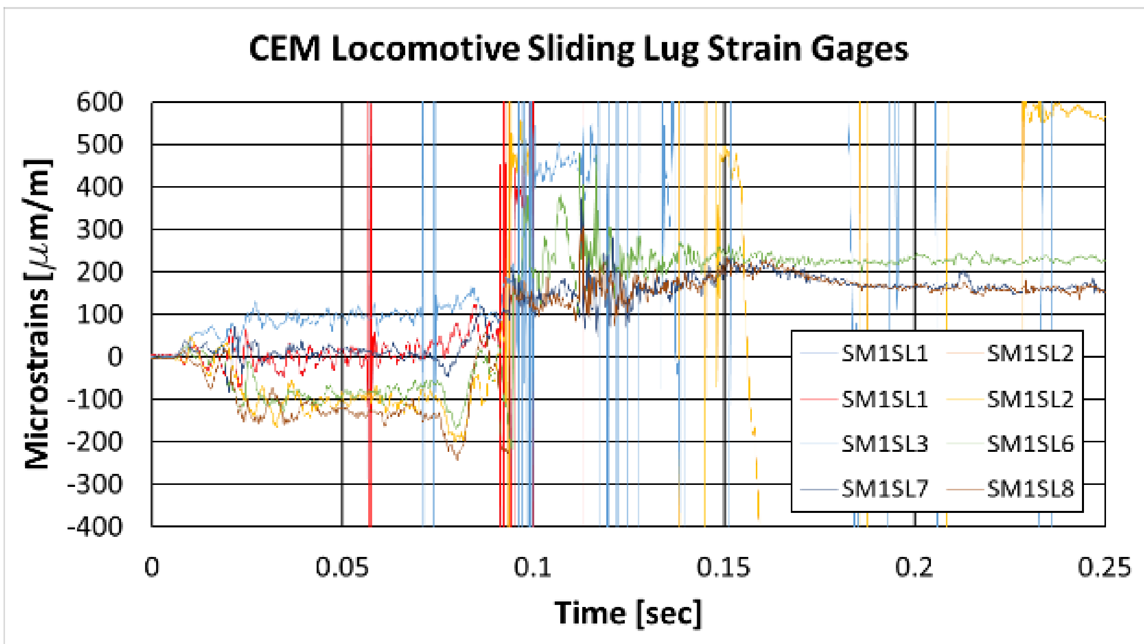

Figure 49. CEM Locomotive Sliding Lug Strain Results

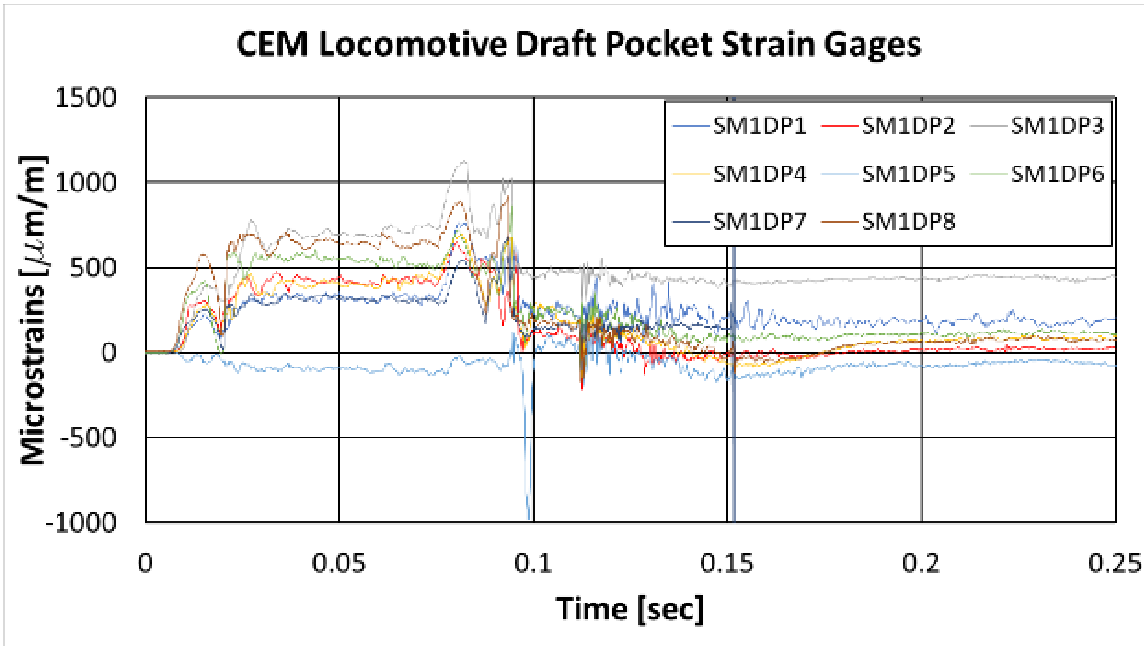

Figure 50. CEM Locomotive Draft Pocket Strain Results

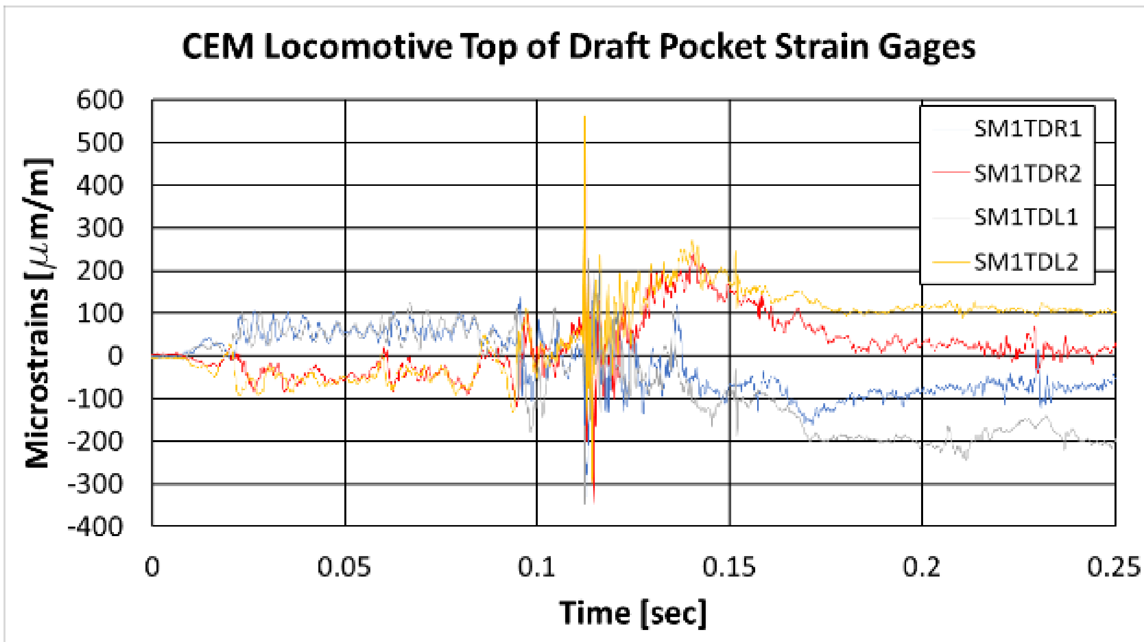

Figure 51. CEM Locomotive Top of Draft Pocket Strain Results

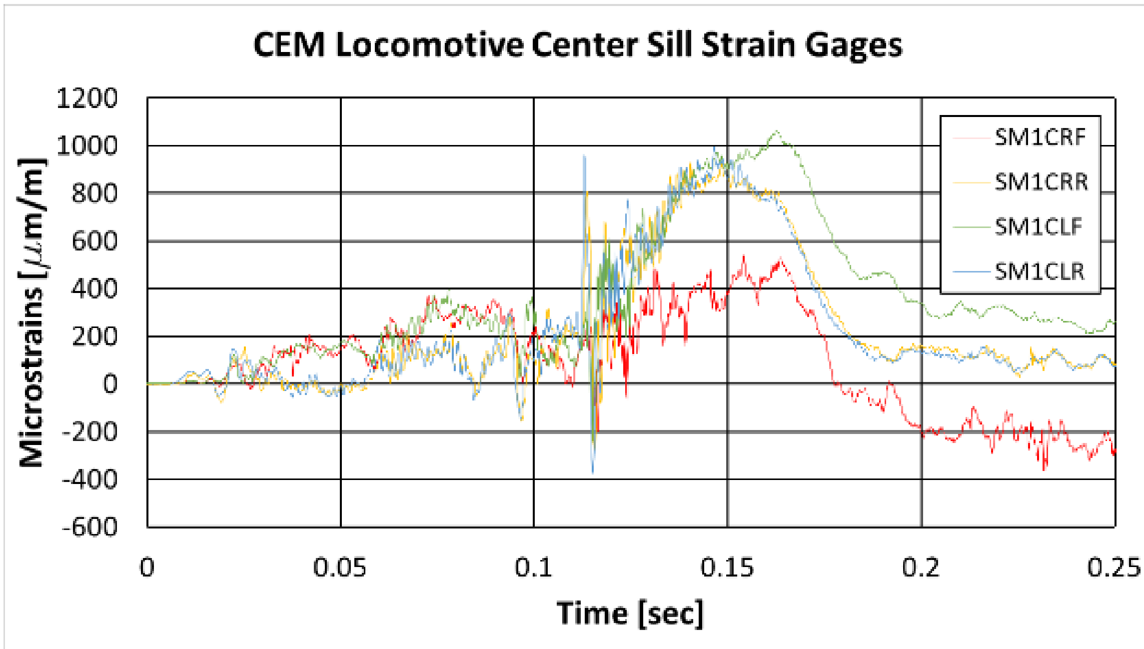

Figure 52. CEM Locomotive Center Sill Strain Results

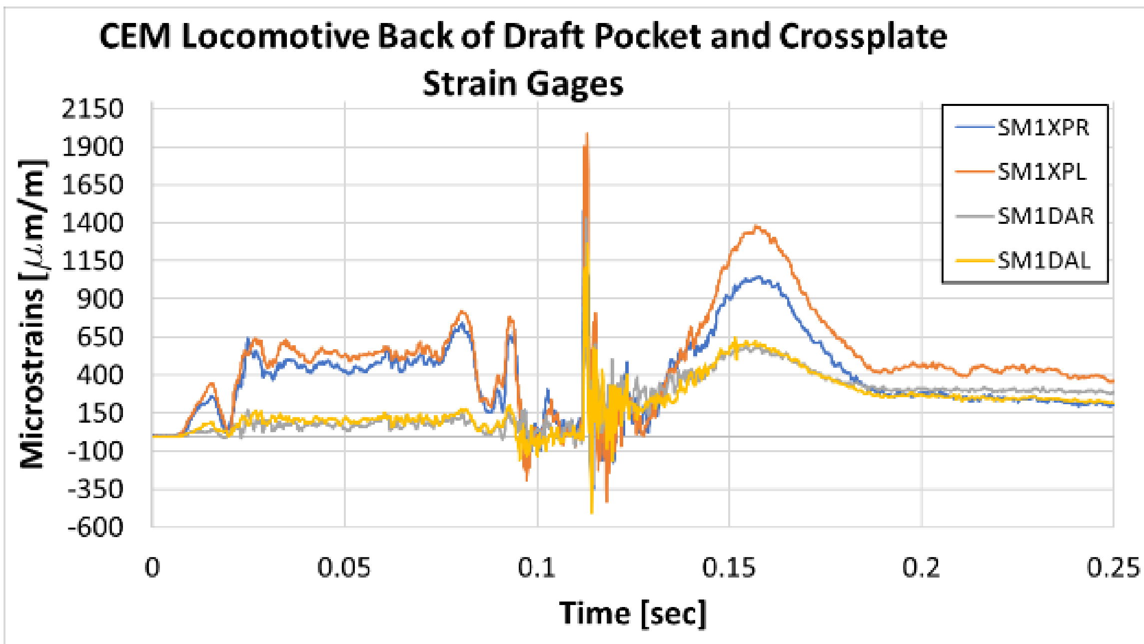

Figure 53. CEM Locomotive Back of Draft Pocket and Cross Plate Strain Results

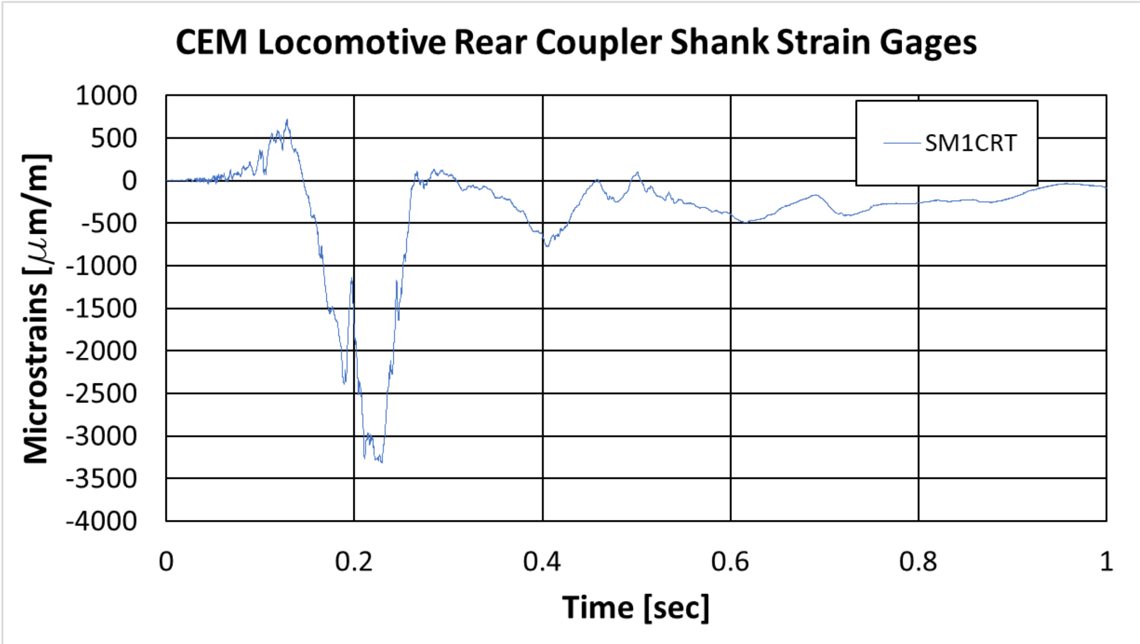

Figure 54. CEM Locomotive Rear Coupler Shank Strain Results

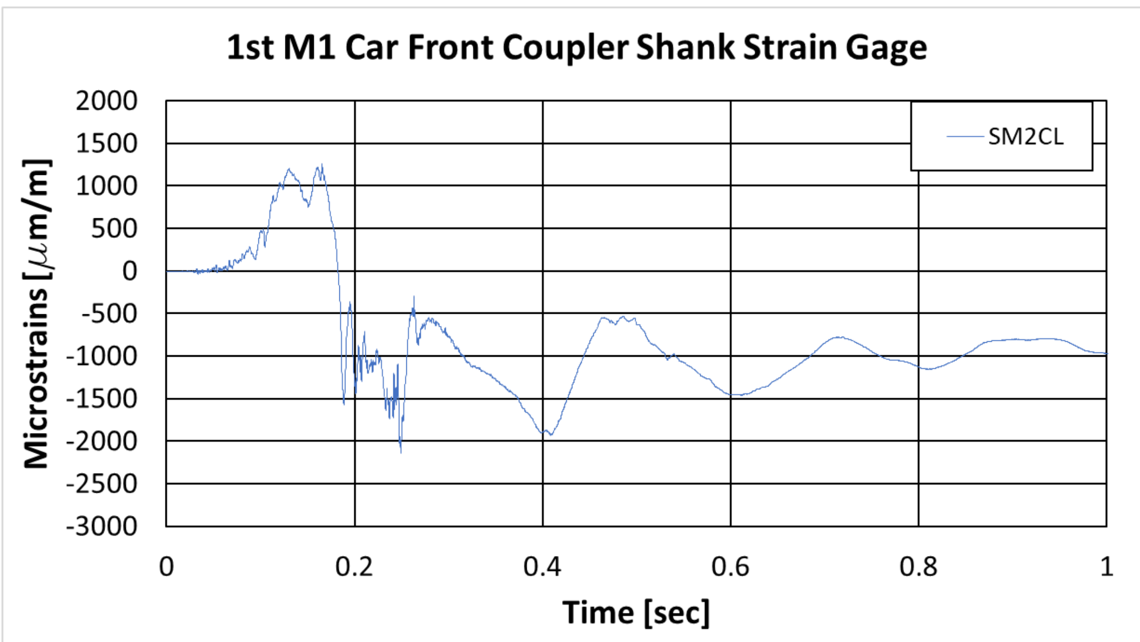

Figure 55. First M1 Passenger Car Front Coupler Shank Strain Results

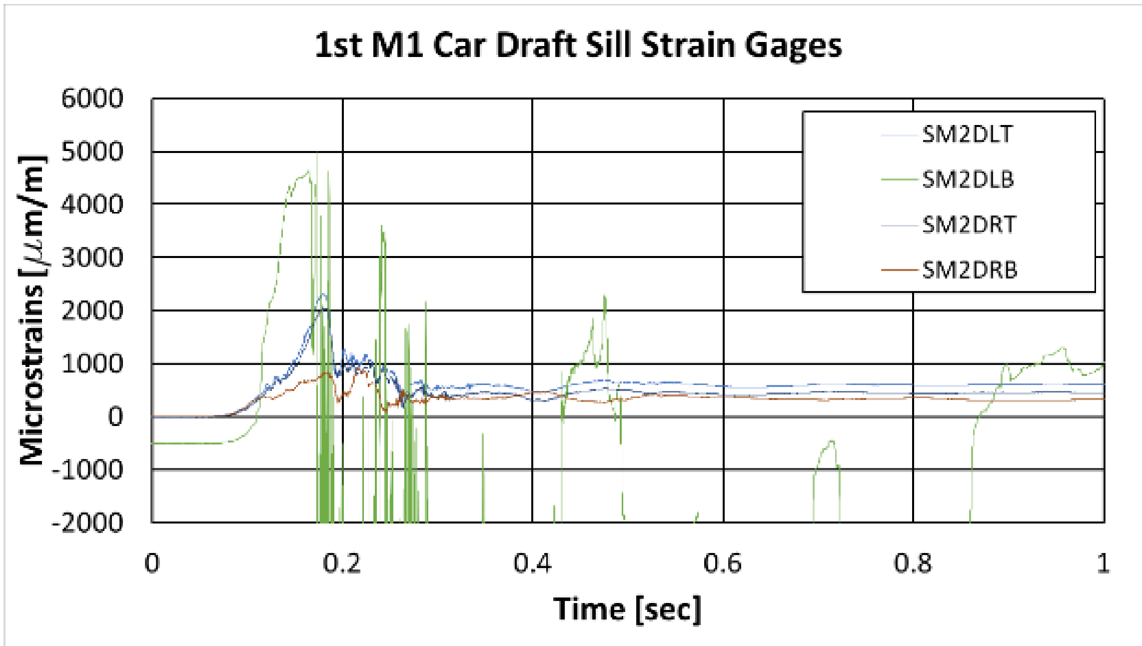

Figure 56. First M1 Passenger Car Draft Sill Strain Results

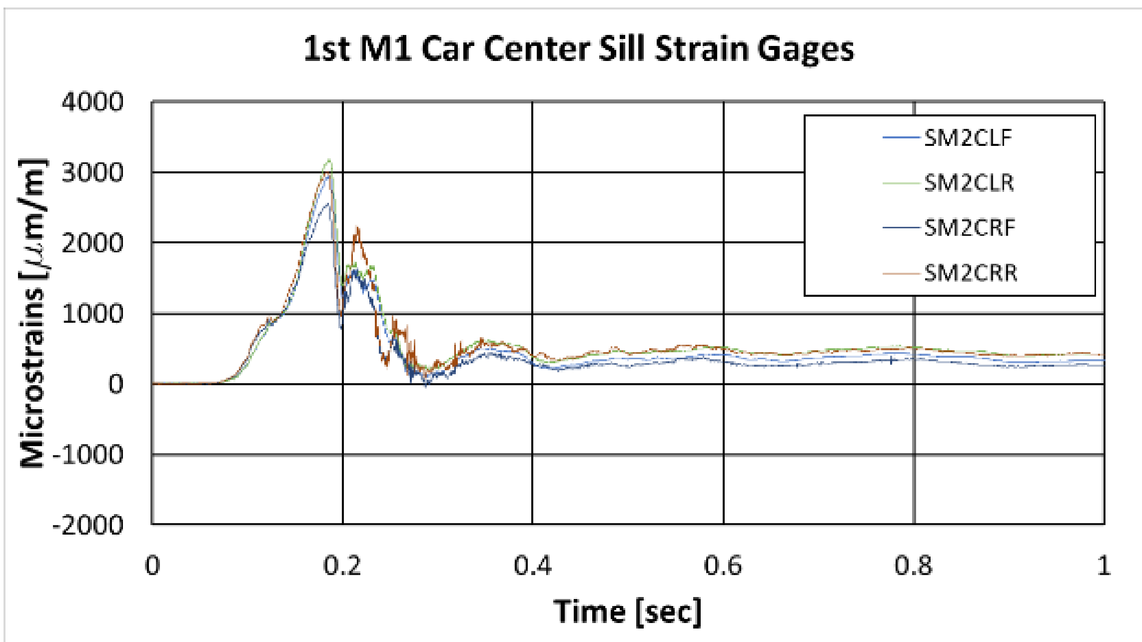

Figure 57. First M1 Passenger Car Center Sill Strain Results

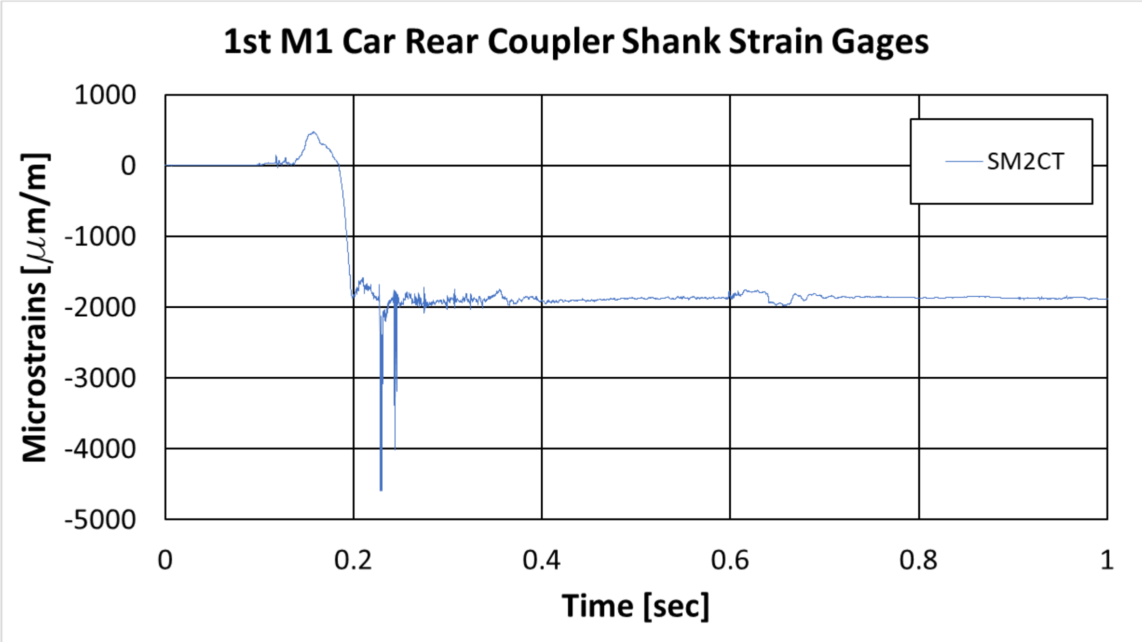

Figure 58. First M1 Passenger Car Rear Coupler Shank Strain Results

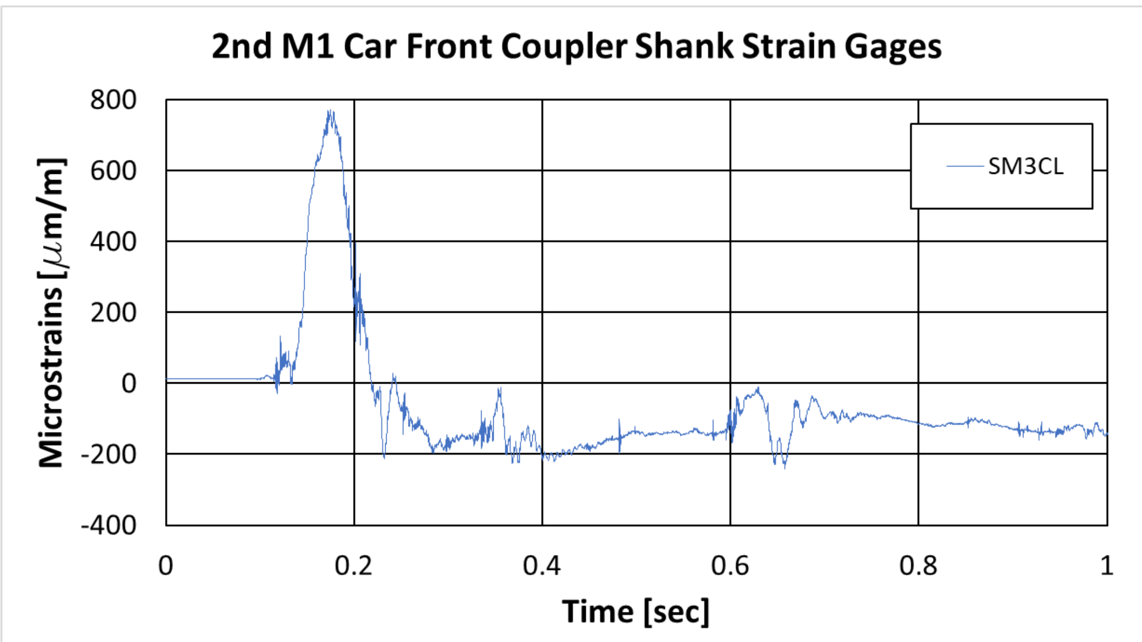

Figure 59. 2nd M1 Passenger Car Front Coupler Shank Strain Results

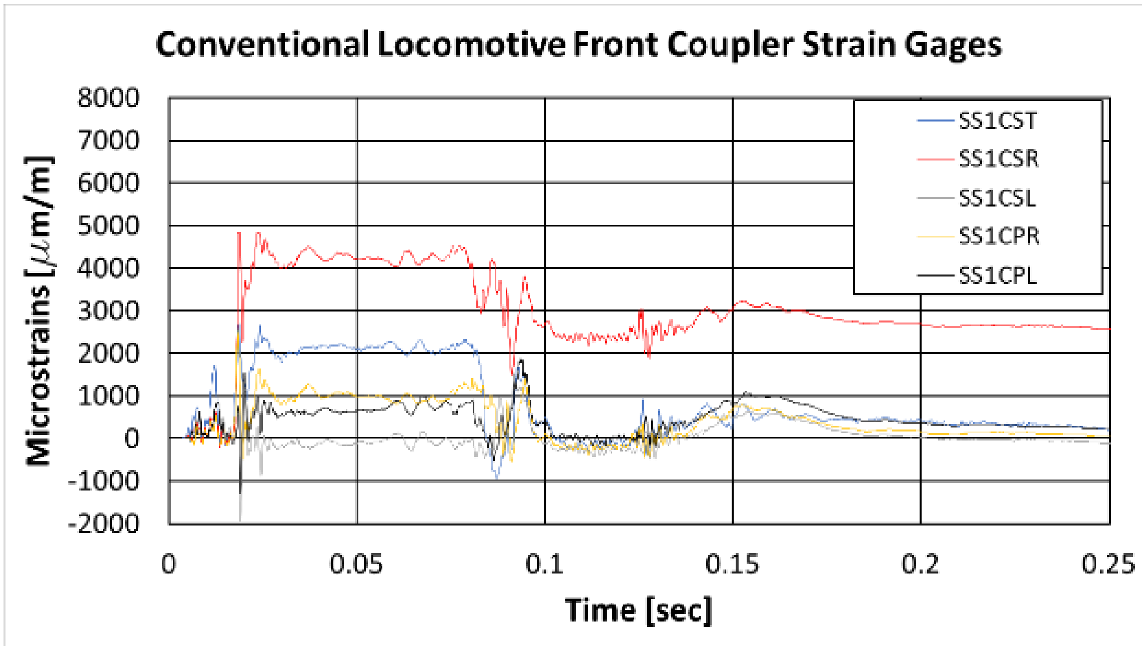

Figure 60. Conventional Locomotive Front Coupler Shank Strain Results

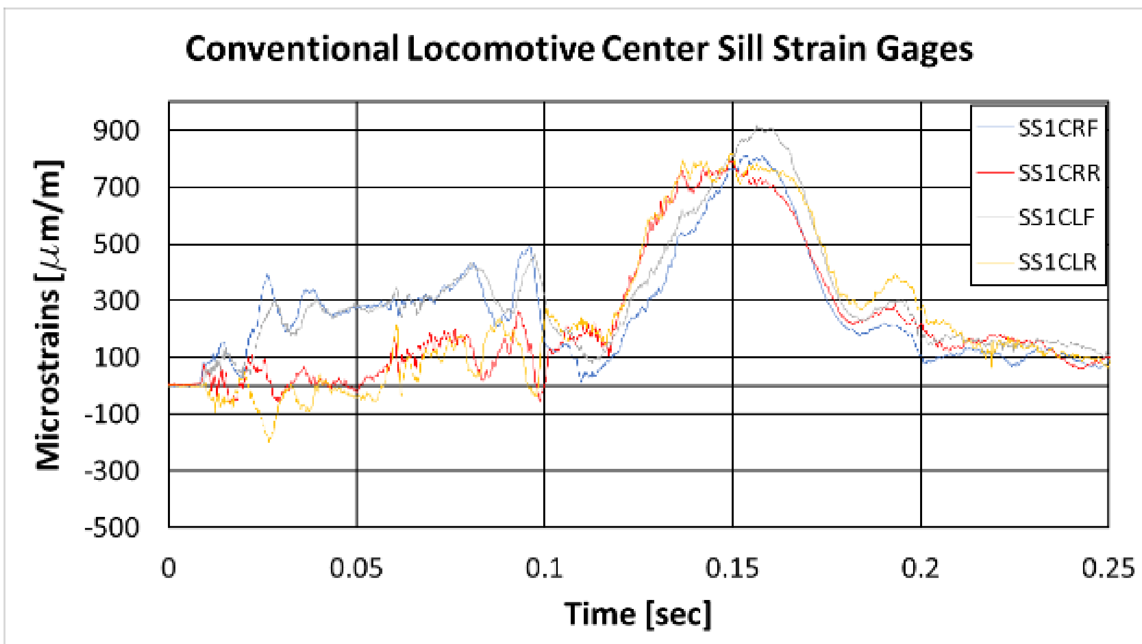

Figure 61. Conventional Locomotive Center Sill Strain Results

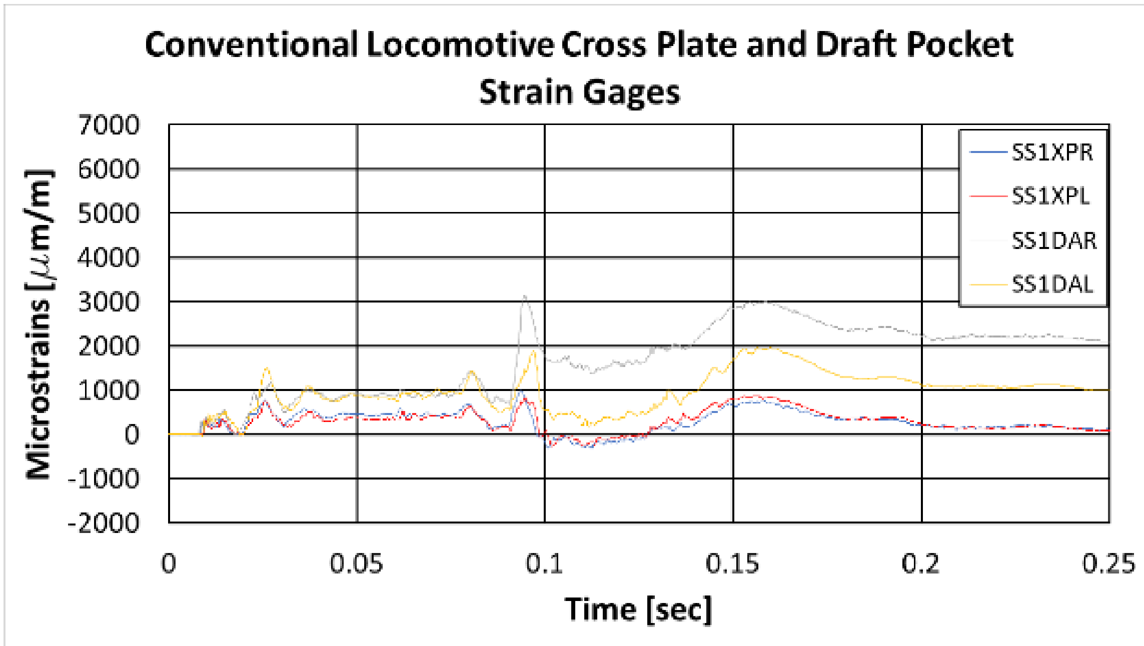

Figure 62. Conventional Locomotive Cross Plate and Draft Pocket Strain Results

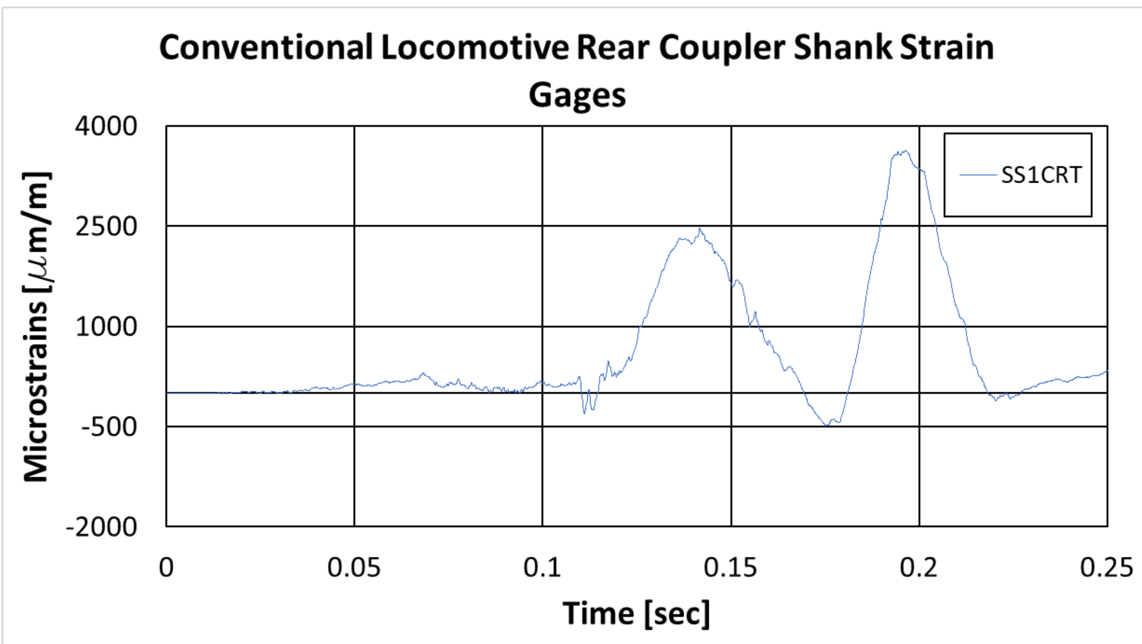

Figure 63. Conventional Locomotive Rear Coupler Shank Strain Results

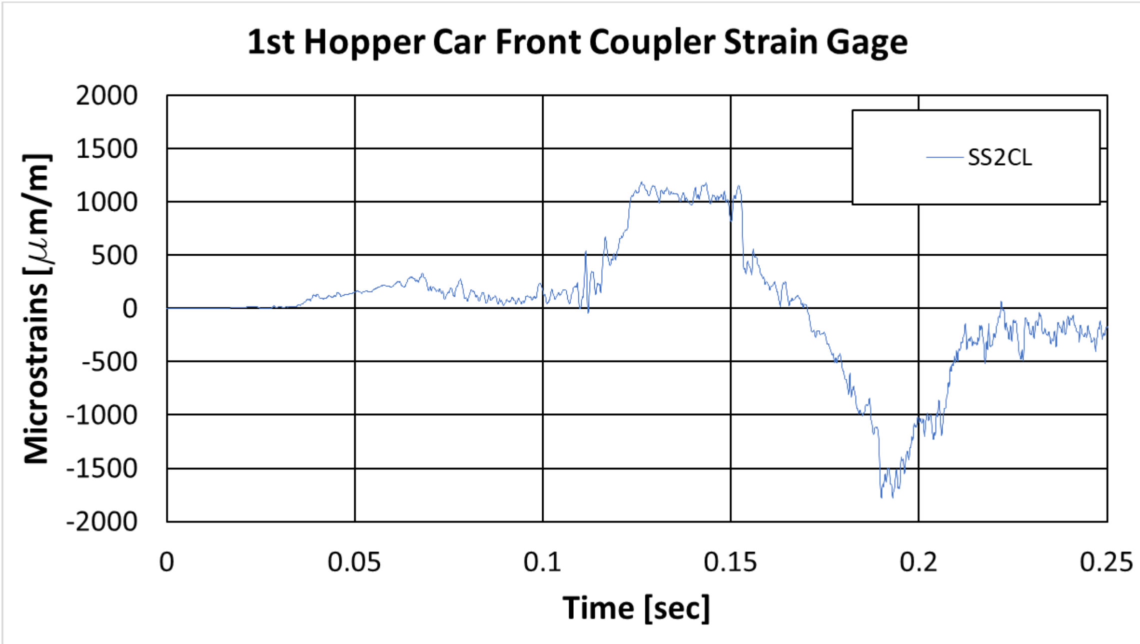

Figure 64. First Hopper Car Front Coupler Shank Strain Results

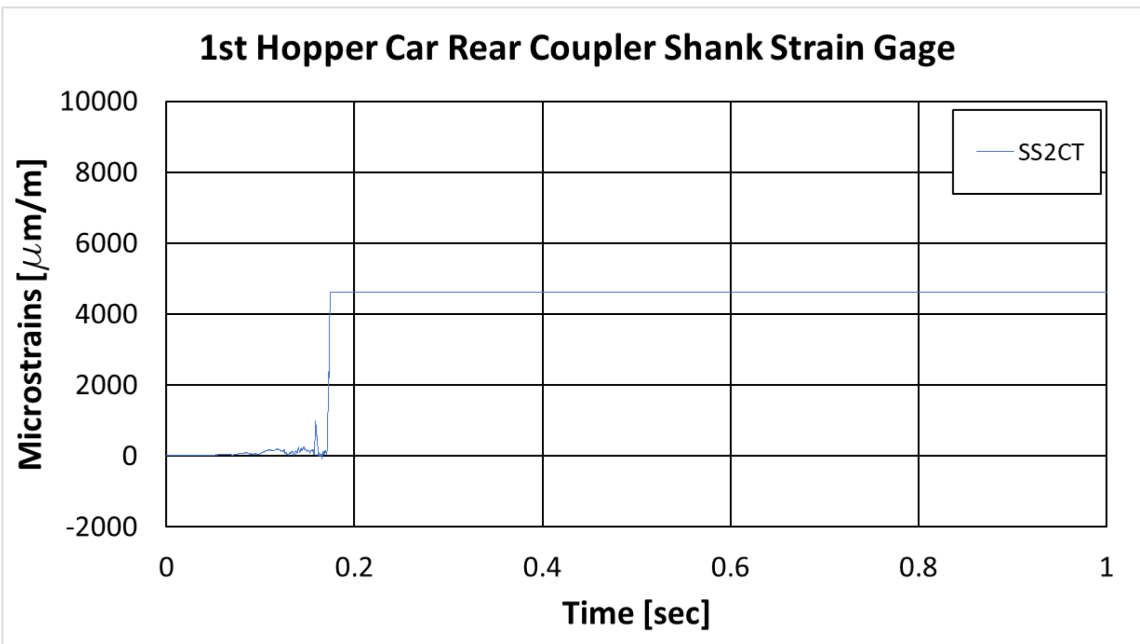

Figure 65. First Hopper Car Rear Coupler Shank Strain Results

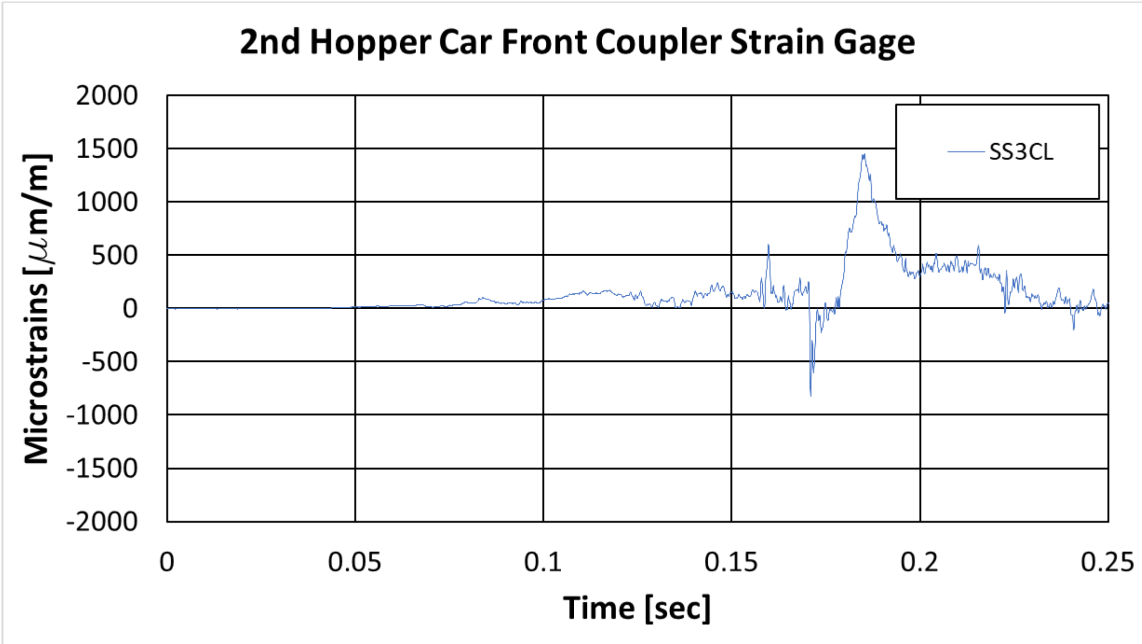

Figure 66. 2nd Hopper Car Front Coupler Shank Strain Results

3.2.4 Forces

Impact forces between the moving consist and the stationary consist are calculated as a product of the average acceleration and mass of the corresponding vehicles. Figure 68 shows the time history of the consist impact forces.

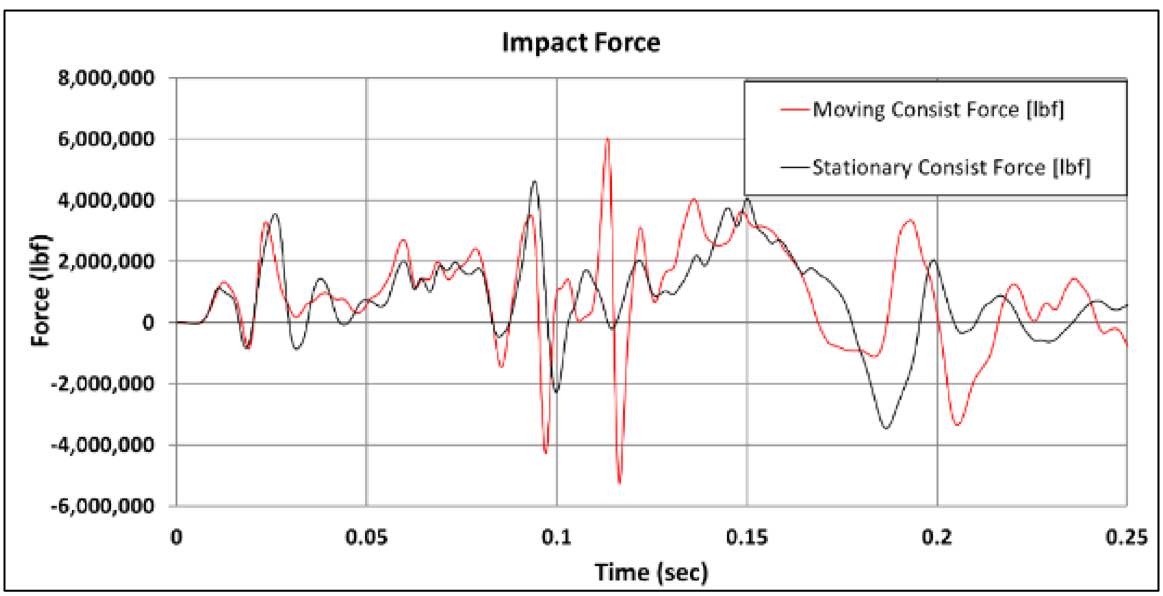

Figure 67. Impact Force

The force-time history was calculated by multiplying consist weight and average carbody acceleration. The average acceleration was taken from longitudinal accelerometers mounted on the underframe of each locomotive as described in Section 3.2.1. The peak impact force was approximately 4,500,000 pound force (lbf) for the stationary consist and 6,000,000 lbf for the moving consist.

3.2.5 Energies

Energy balance is the summary of the energy transfer during the impact. The total energy at the beginning of the impact is equal to the kinetic energy of the moving consist. After the first impact, all vehicles moved forward on the track until they stopped. The dissipated energy accounted for CEM component deformation, braking, structural deformation, and other energy losses. Because the energies should balance, the dissipated energy was obtained by subtracting the kinetic energies from the total energy. Figure 69 shows the energy balance for the initial impact.

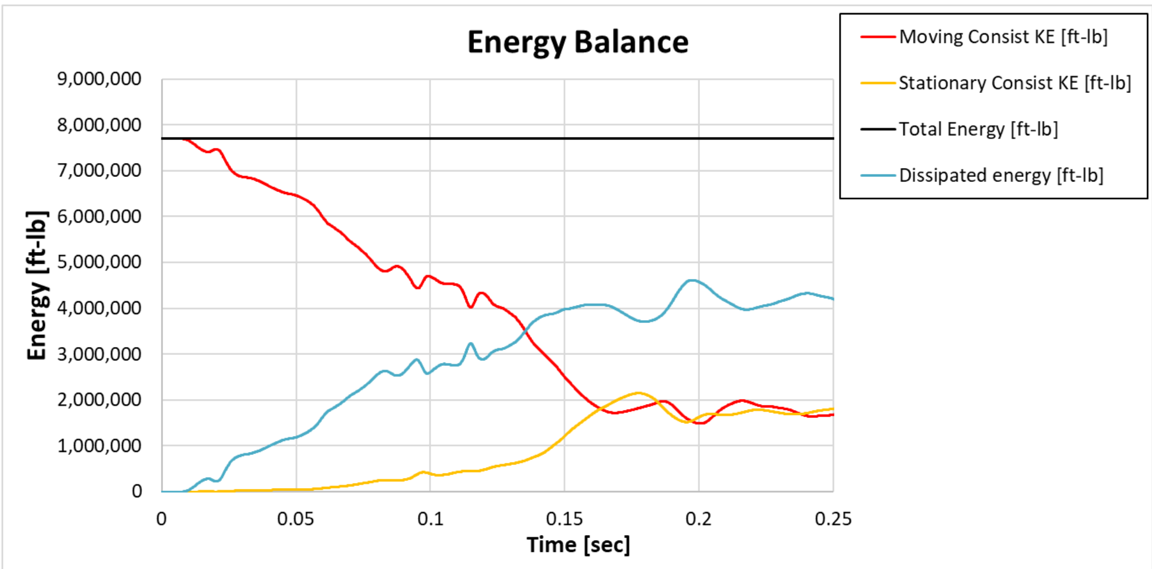

Figure 68. Energy Balance

3.3 ATD Data

The following sections describe the outcomes of the three occupant protection experiments, the ATD measurements, and the calculated injury criteria.

3.3.1 Occupant Protection Experiment 1.1

During the impact, the unrestrained wheelchair and ATD pushed back into the Quantum backboard. The neck of the ATD extended and the back of the head contacted the backboard padding. The chair and the ATD's head rebounded off the backboard and shifted slightly away from the original direction of travel during impact. The ATD and wheelchair became airborne during the rebound and eventually returned to the ground. The ATD landed back in the wheelchair and was upright at the completion of the test. Figure 70 displays the movement experienced by the ATD and the wheelchair during impact.

Figure 69. Occupant Protection Experiment 1.1 Impact Movement

3.3.2 Occupant Protection Experiment 2.1

During the impact, the restrained surrogate wheelchair and ATD slid forward. The surrogate wheelchair's movement was restricted before the ATD began to move. The ATD's head, upper body, and lower body continued to move forward until the seat belt harness halted further movement. The ATD then rebounded, causing its head and upper body to snap backward. The ATD became airborne during the rebound and eventually returned to the seat. The ATD remained seated in the surrogate wheelchair, and both were upright at the completion of the test. Figure 71 displays the different movements experienced by the ATD and the surrogate wheelchair during impact.

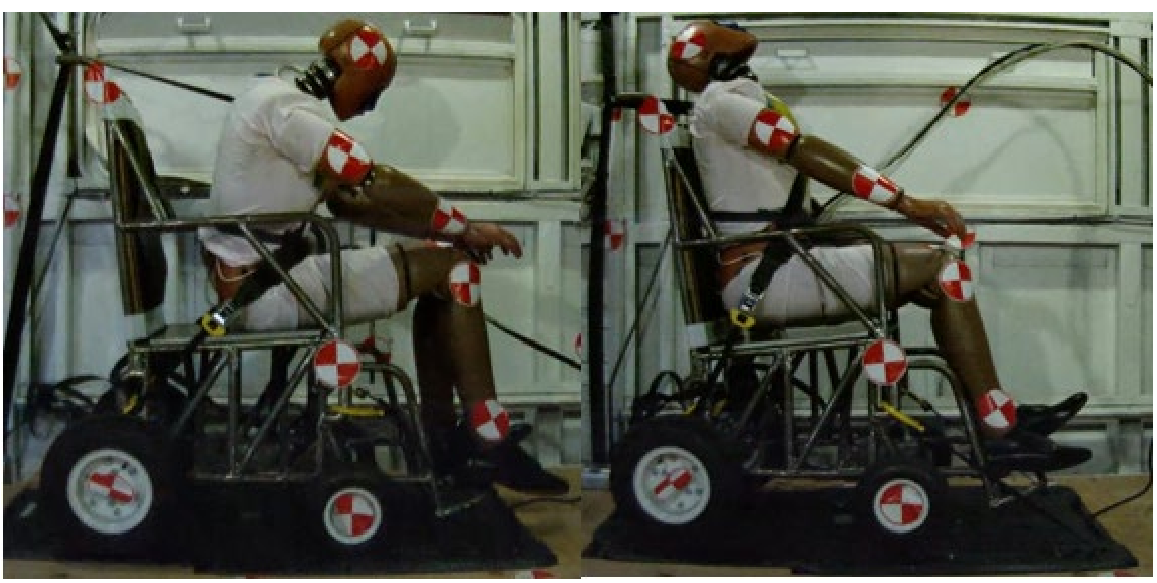

Figure 70. Occupant Protection Experiment 2.1 Impact Movement

3.3.3 Occupant Protection Experiment 2.2

During the impact, the restrained surrogate wheelchair and ATD pushed back into the backboard. Due to the presence of a plate on the bottom of the surrogate wheelchair, the wheelchair contacted the chassis of the Quantum system before the back of the wheelchair could rest against the backboard padding. This contact caused the wheelchair to pivot on its restrained back wheels. As a result of the pivoting motion, the front wheels lifted off the floor and the ATD's head snapped back and contacted the backboard padding. The ATD's head bounced off the backboard and shifted slightly away from the original direction of travel during impact. The ATD became airborne during the rebound and eventually returned to the seat of the surrogate wheelchair. The seatbelt harness helped to prevent the ATD from traveling higher off the seat and possibly falling out of the wheelchair away from the direction of travel on the rebound. The ATD landed back in the wheelchair and was upright at the completion of the test. Figure 72 displays the different movements experienced by the ATD and the surrogate wheelchair during impact.

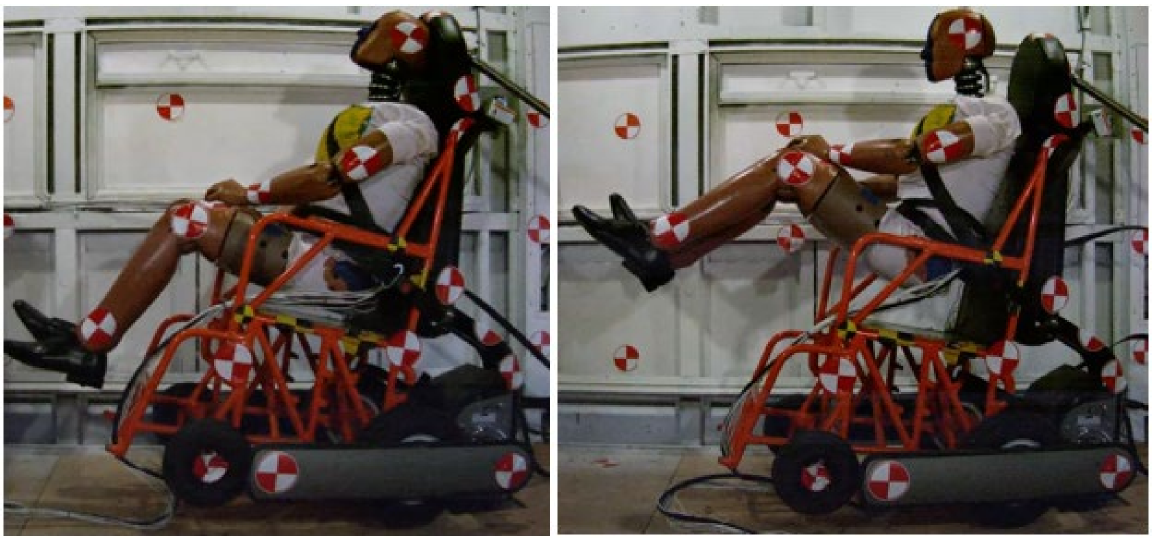

Figure 71. Occupant Protection Experiment 2.2 Impact Movement

3.3.4 Head Accelerations

Tri-axial acceleration data was collected for the ATD heads during the impact test. Figure 73 through Figure 78 display the head acceleration data. The data used a frequency class filter of 1000 Hz. The raw and filtered data are displayed in Appendix B.

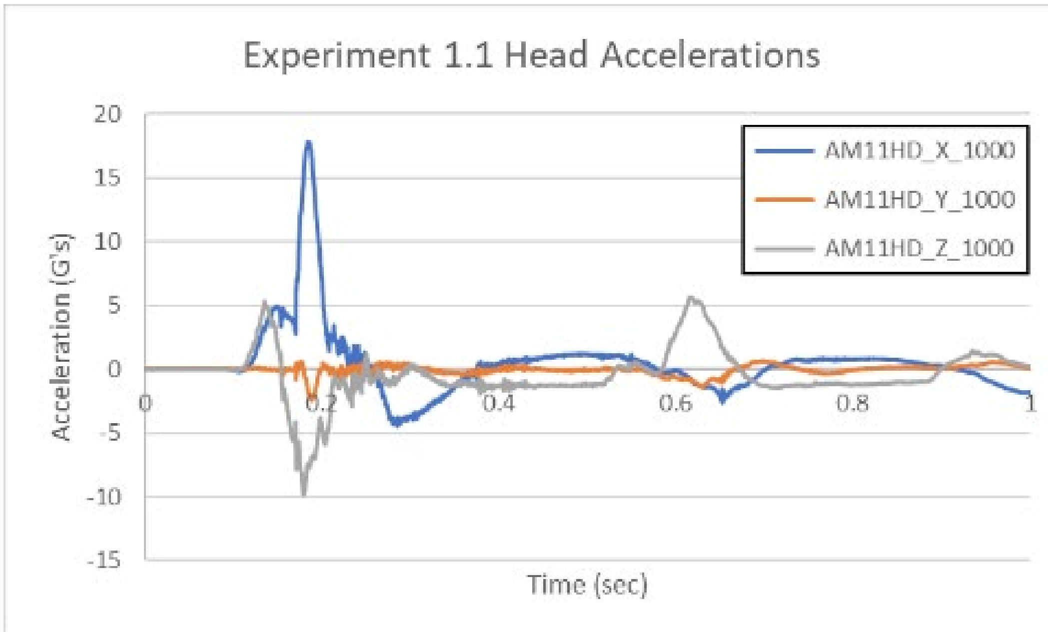

Figure 72. Occupant Protection Experiment 1.1 Head Acceleration Data

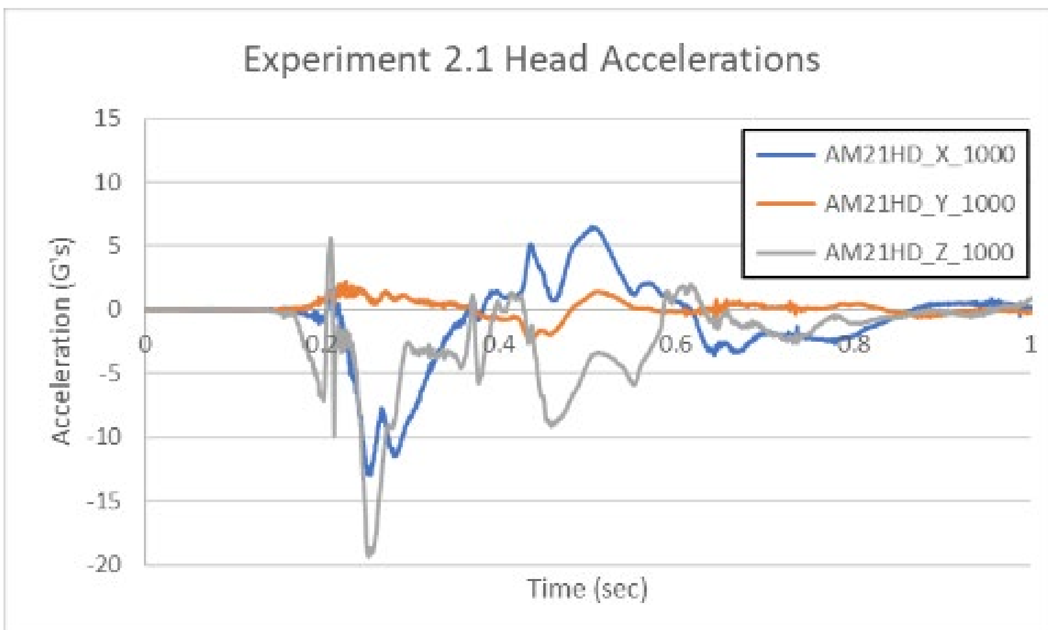

Figure 73. Occupant Protection Experiment 2.1 Head Acceleration Data

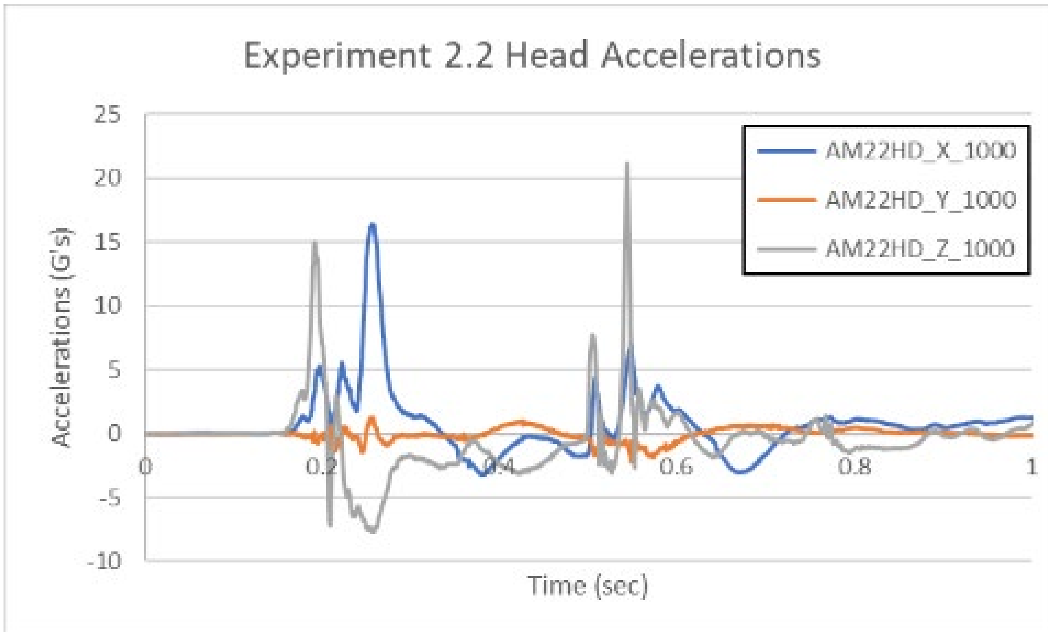

Figure 74. Occupant Protection Experiment 2.2 Head Acceleration Data

3.3.5 Chest Accelerations

Tri-axial acceleration data was collected for the ATD chests during the impact test. Figure 76 through Figure 81 display the chest acceleration data. The data used a frequency class filter of 1000 Hz. The raw and filtered data are displayed in Appendix B.

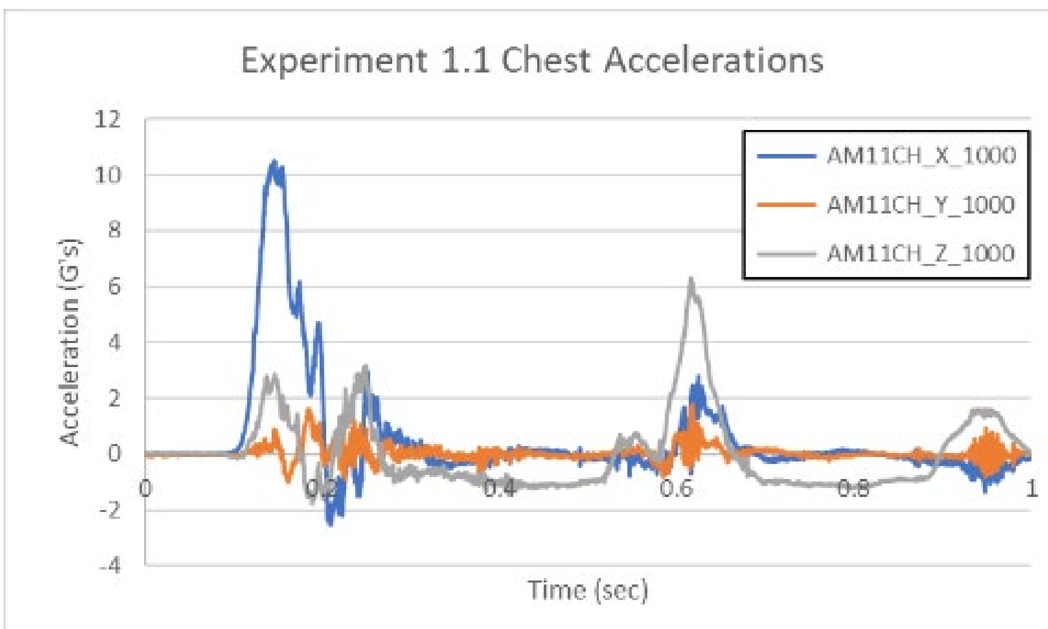

Figure 75. Occupant Protection Experiment 1.1 Chest Acceleration Data

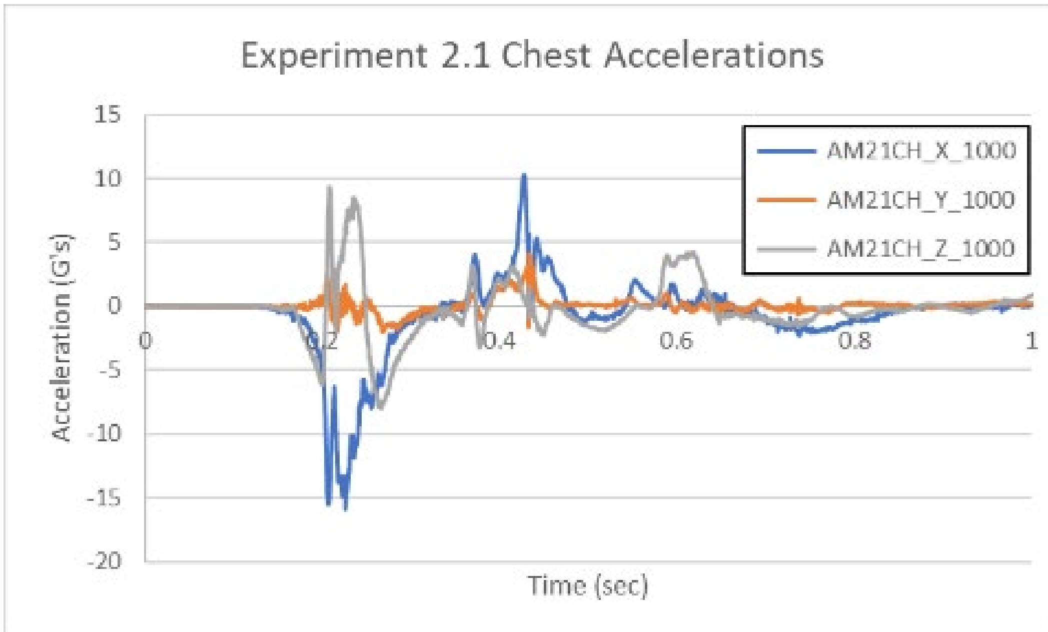

Figure 76. Occupant Protection Experiment 2.1 Chest Acceleration Data

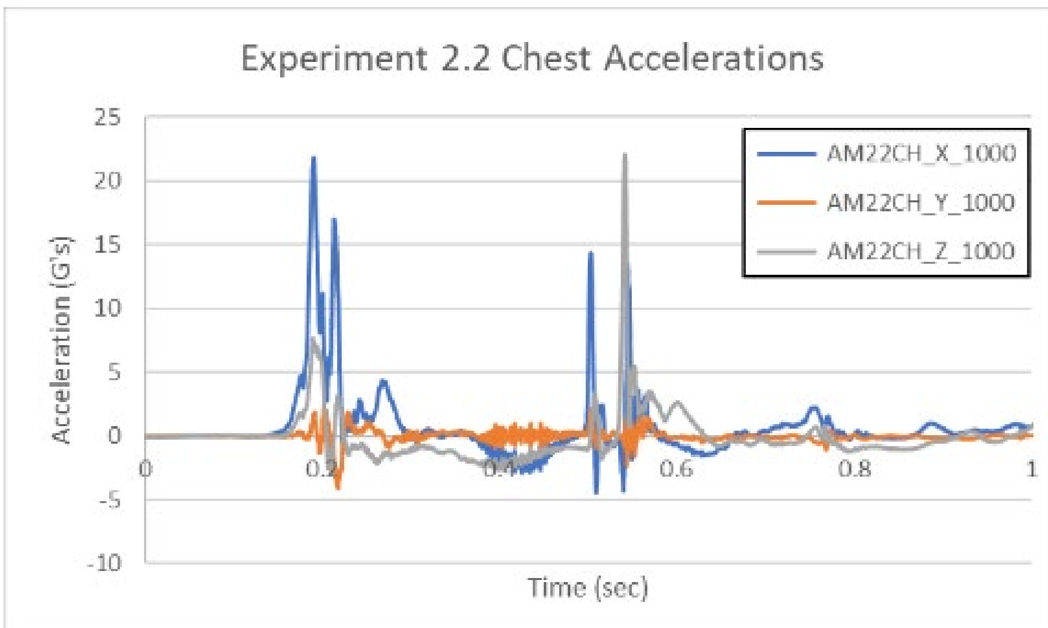

Figure 77. Occupant Protection Experiment 2.2 Chest Acceleration Data

3.3.6 Pelvis Accelerations

Tri-axial acceleration data was collected for the ATD pelvises during the impact test. Figure 79 through Figure 81 display the pelvis acceleration data. The data used a frequency class filter of 1000 Hz. Channel AM22PL_Z did not record usable data even though it performed correctly during pretest checkouts. The raw and filtered data are displayed in Appendix B.

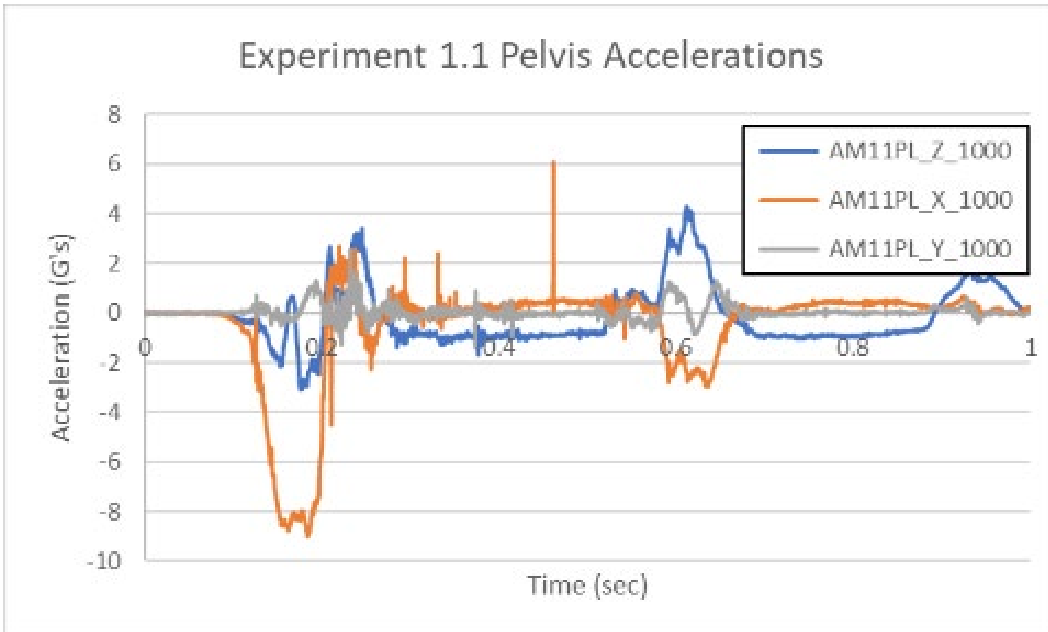

Figure 78. Occupant Protection Experiment 1.1 Pelvis Acceleration Data

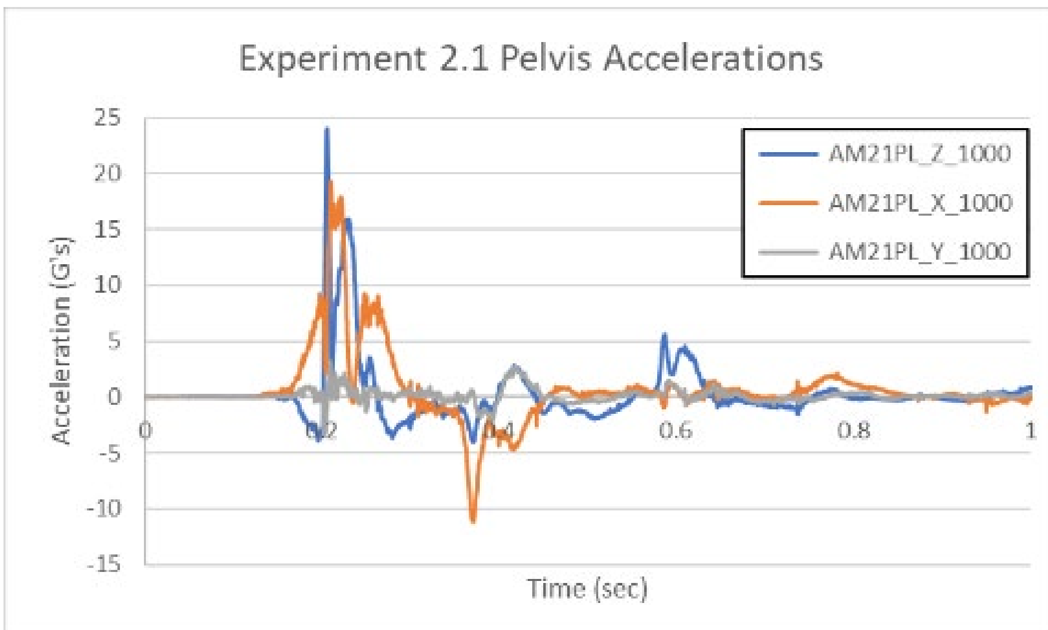

Figure 79. Occupant Protection Experiment 2.1 Pelvis Acceleration Data

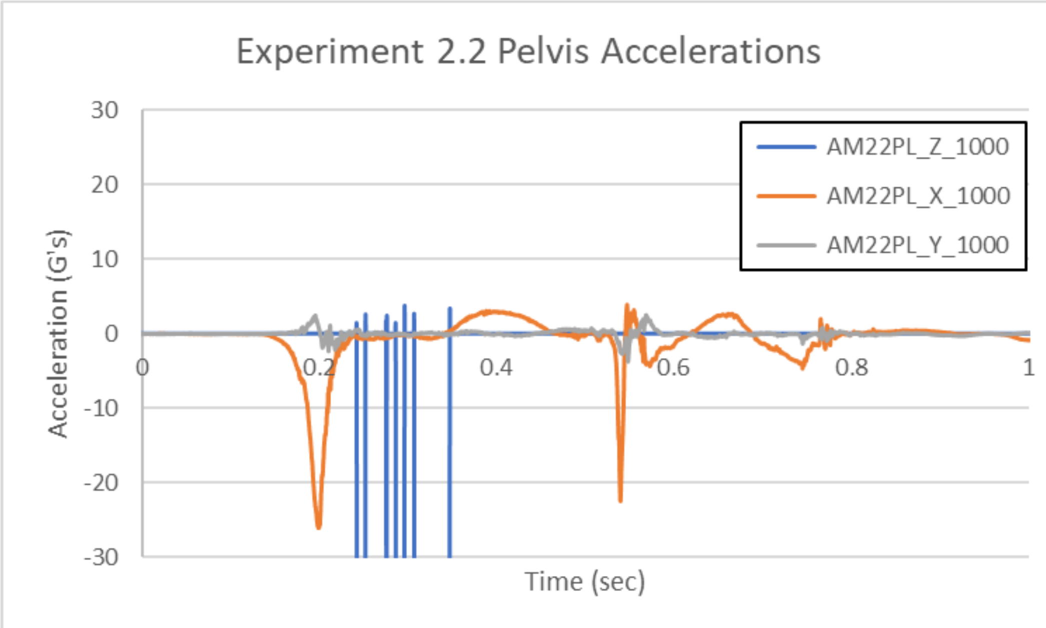

Figure 80. Occupant Protection Experiment 2.2 Pelvis Acceleration Data

3.3.7 Head Rotation

Tri-axial head rotation data was collected for the ATDs in Experiments 2.1 and 2.2 during the impact test. Figure 82 and Figure 83 display the head rotation data. The data used a frequency class filter of 180 Hz. Data clipping occurred at the peaks of channels RM21HD_X, RM21HD_Y, RM21HD_Z, and RM22HD_Y. The raw and filtered data are displayed in Appendix B.

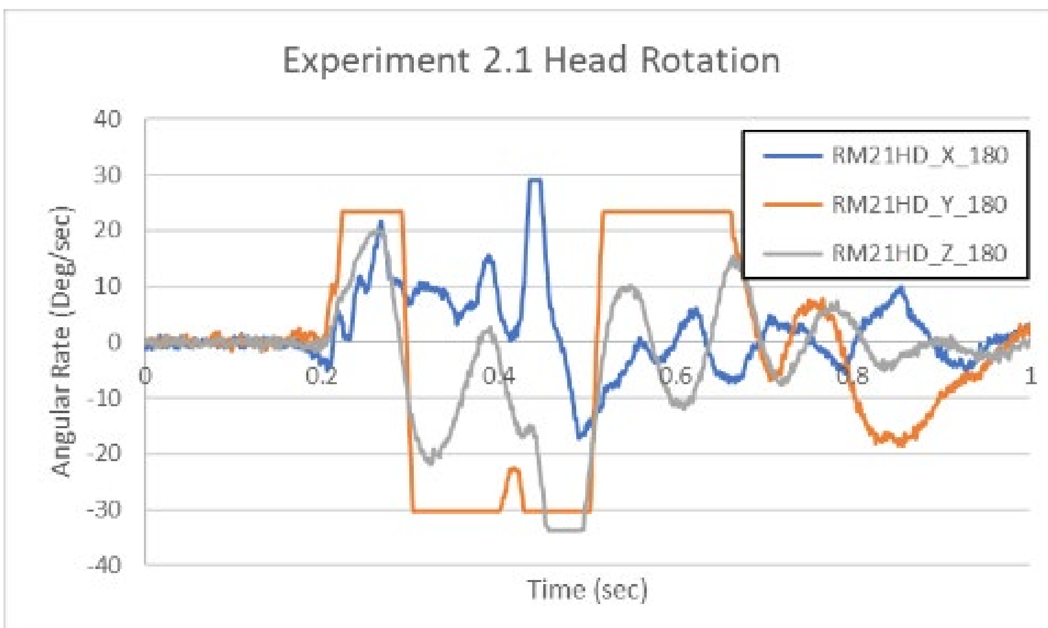

Figure 81. Occupant Protection Experiment 2.1 Head Rotation Data

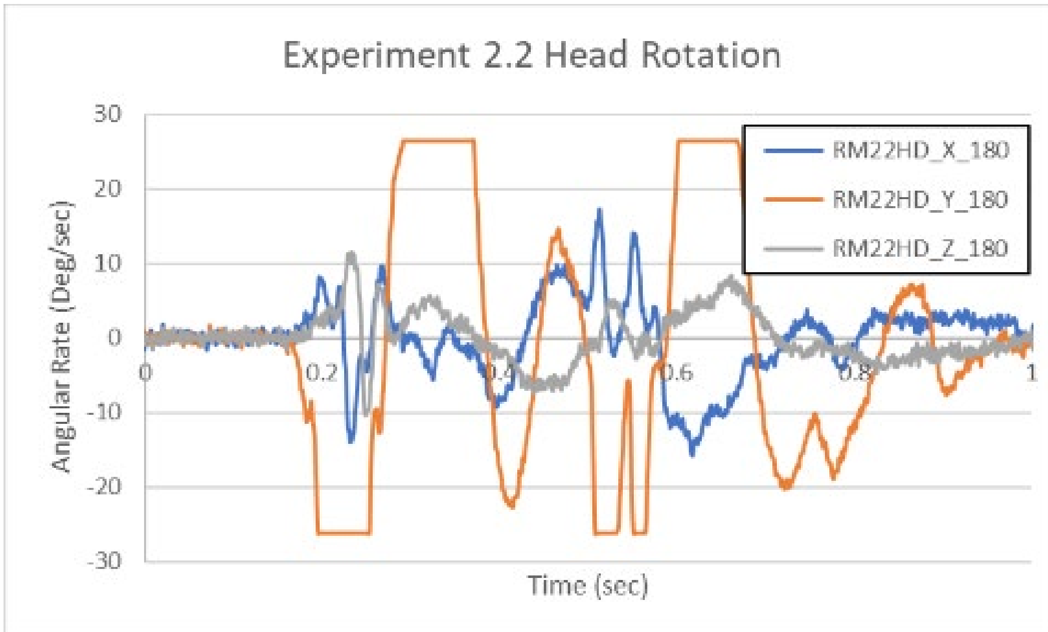

Figure 82. Occupant Protection Experiment 2.2 Head Rotation Data

3.3.8 Femur Force

Left and right femur force data was collected for the ATDs during the impact test. Figure 84 through Figure 86 display the femur force data. The data used a frequency class filter of 600 Hz. The raw and filtered data are displayed in Appendix B.

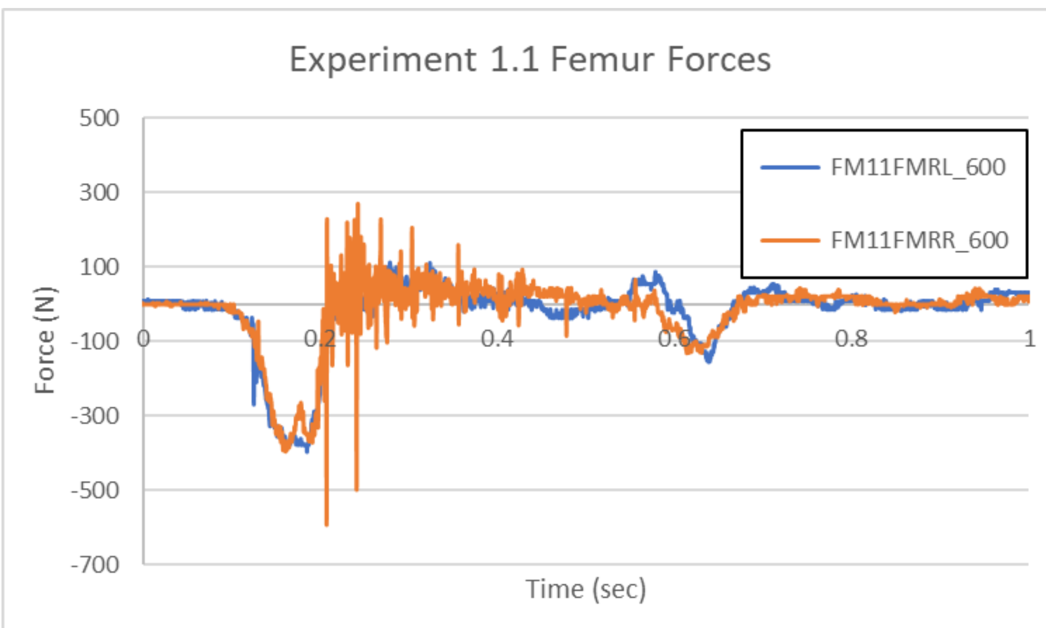

Figure 83. Occupant Protection Experiment 1.1 Femur Force Data

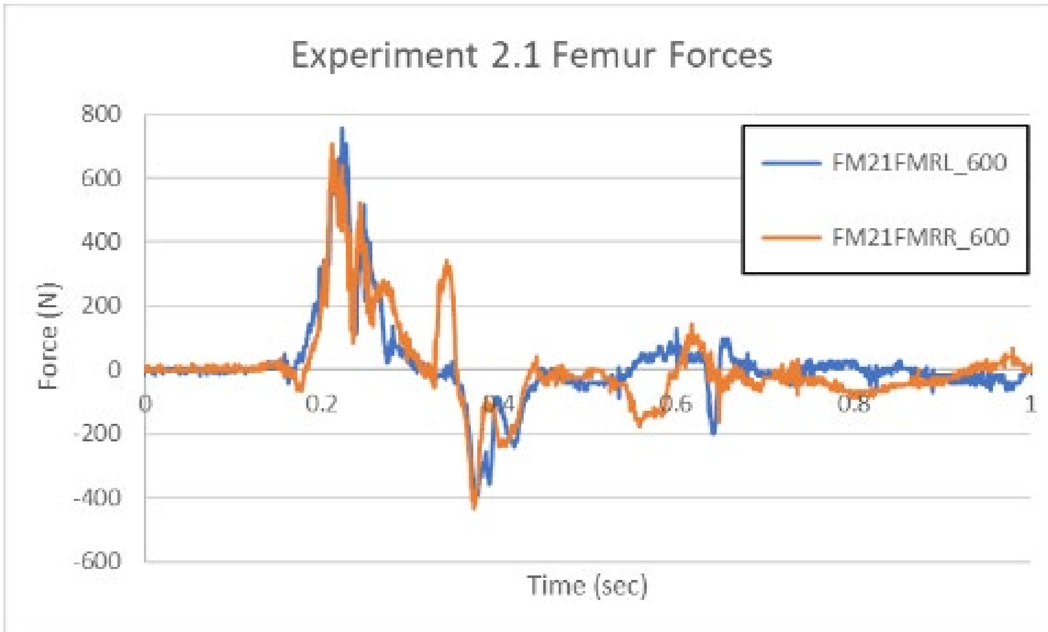

Figure 84. Occupant Protection Experiment 2.1 Femur Force Data

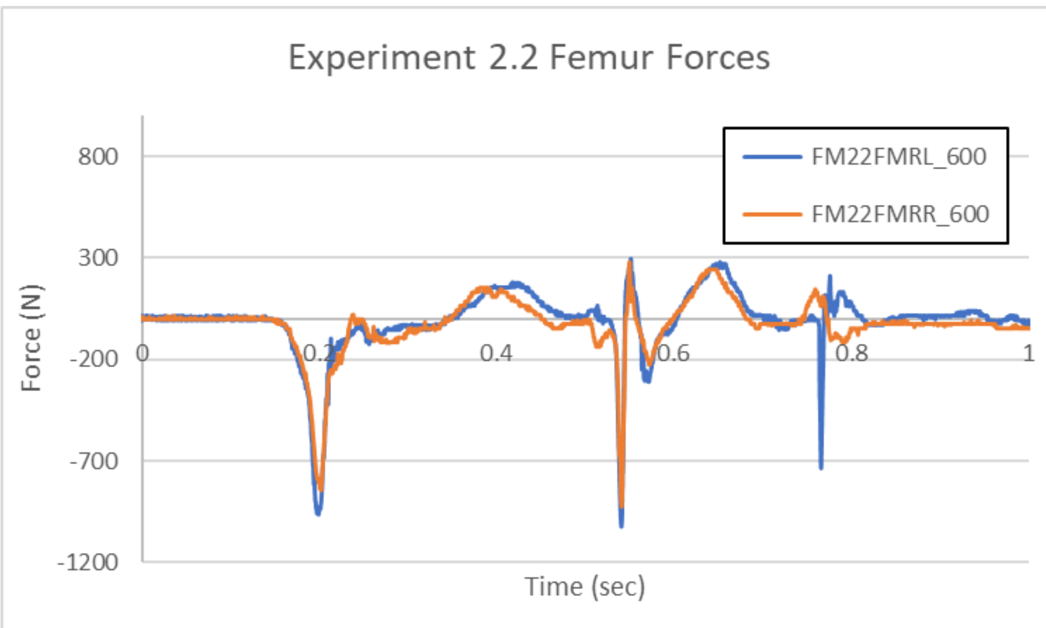

Figure 85. Occupant Protection Experiment 2.2 Femur Force Data

3.3.9 Upper Neck Force

Longitudinal and vertical upper neck force data was collected for the ATDs during the impact test. Figure 87 through Figure 89 display the upper neck force data. The data used a frequency class filter of 1000 Hz. The raw and filtered data are displayed in Appendix B.

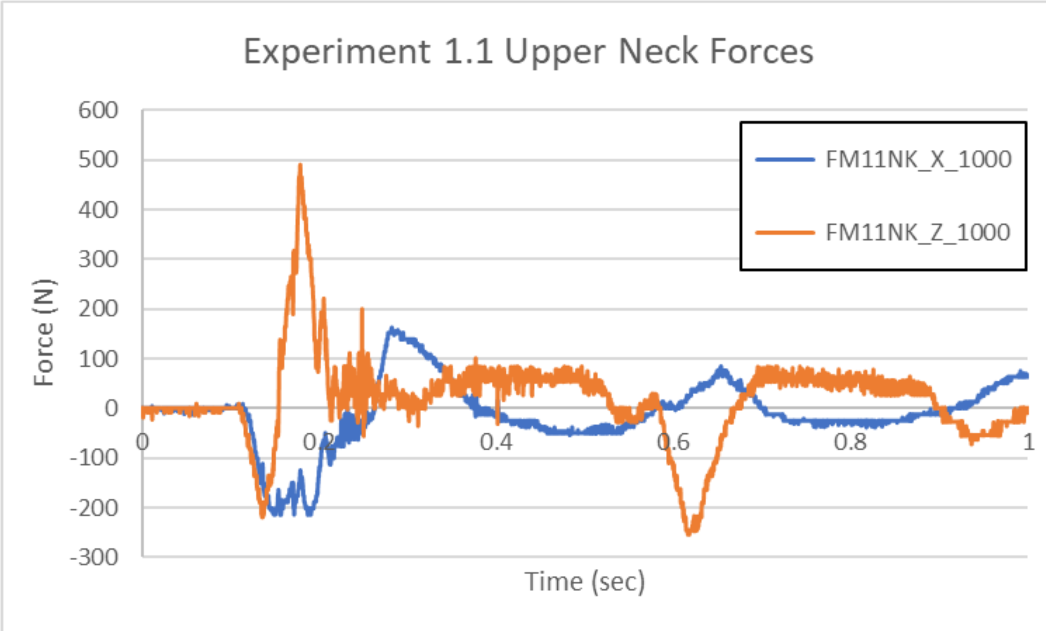

Figure 86. Occupant Protection Experiment 1.1 Upper Neck Force Data

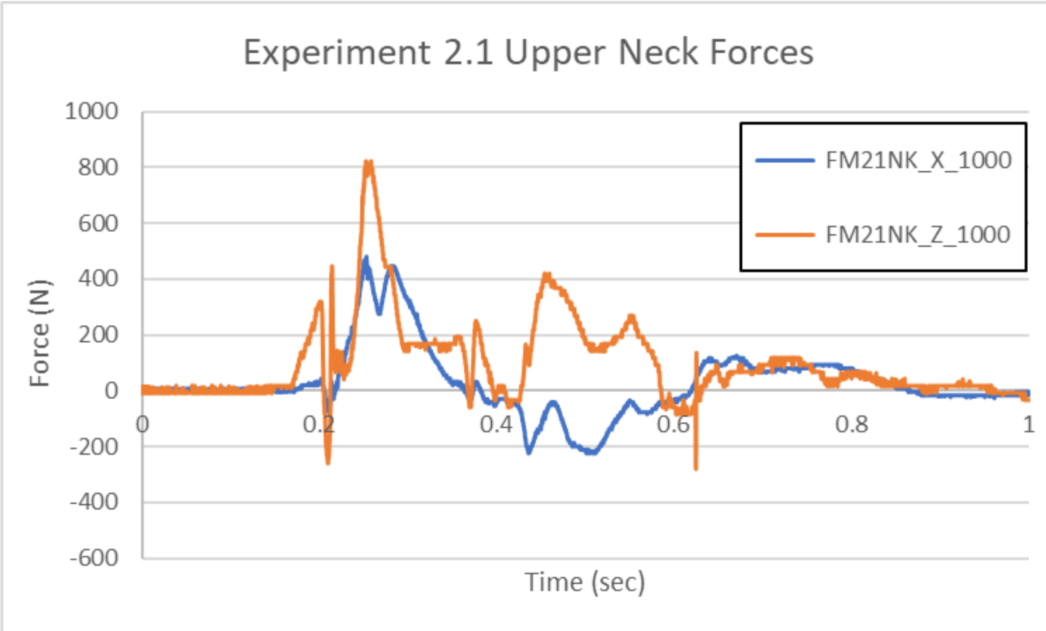

Figure 87. Occupant Protection Experiment 2.1 Upper Neck Force Data

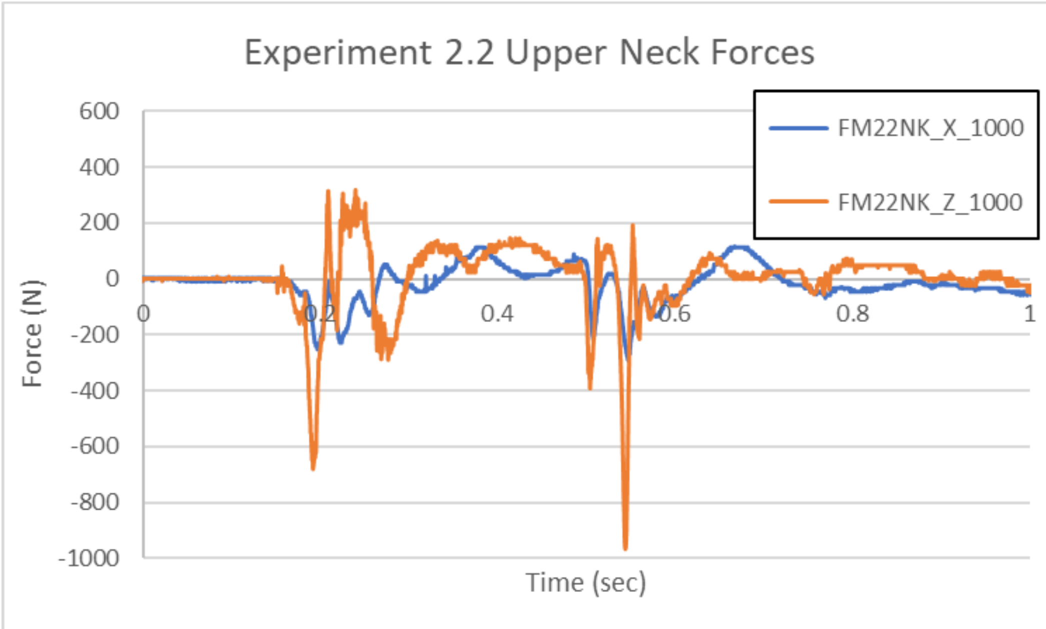

Figure 88. Occupant Protection Experiment 2.2 Upper Neck Force Data

3.3.10 Upper Neck Moment

Upper neck moment data was collected for the ATDs during the impact test. Figure 90 through Figure 92 display the moment data. The data used a frequency class filter of 600 Hz. The raw and filtered data are displayed in Appendix B.

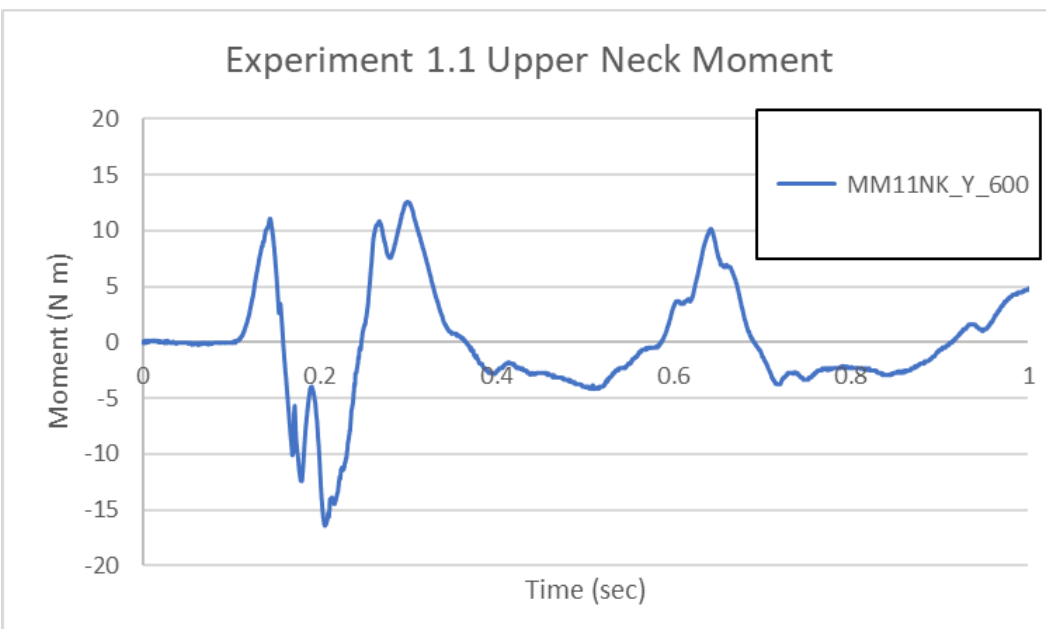

Figure 89. Occupant Protection Experiment 1.1 Upper Neck Moment Data

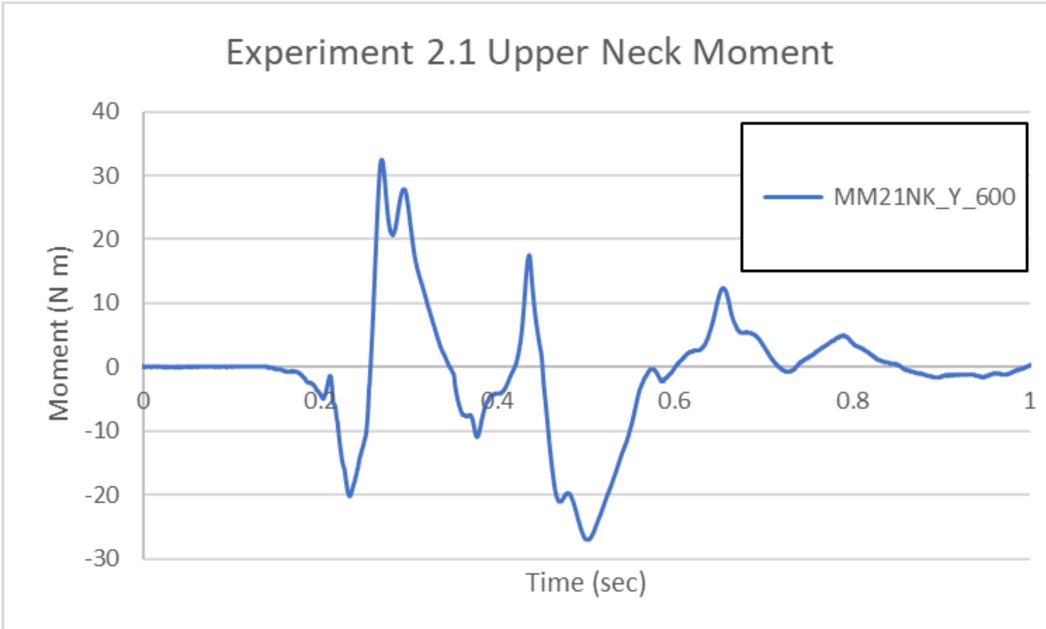

Figure 90. Occupant Protection Experiment 2.1 Upper Neck Moment Data

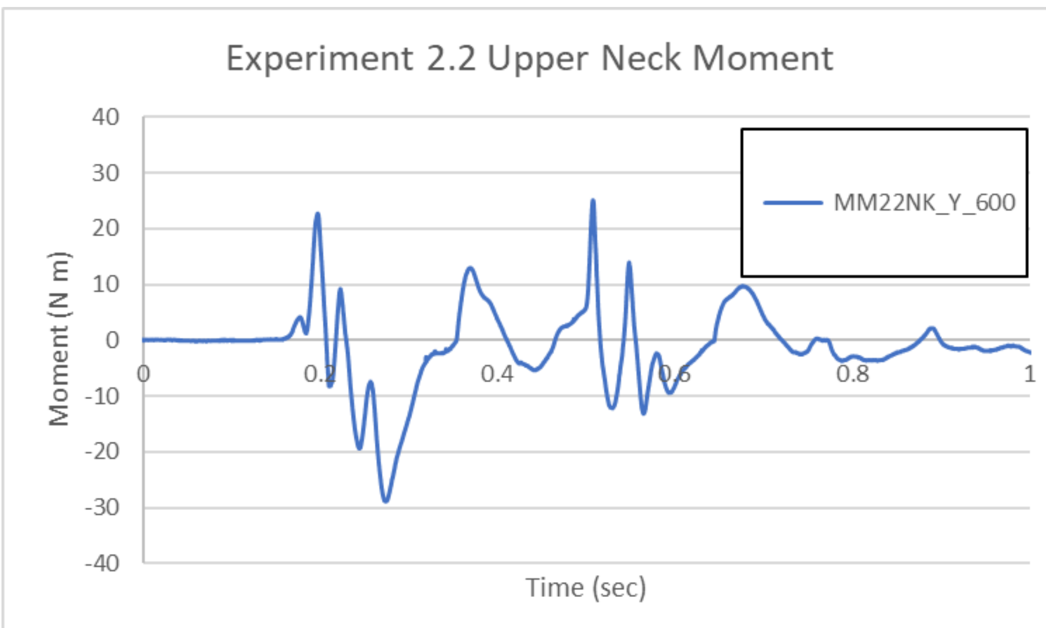

Figure 91. Occupant Protection Experiment 2.2 Upper Neck Moment Data

3.3.11 Chest Displacement

Longitudinal chest displacement data was collected for the ATDs during the impact test. Figure 93 through Figure 95 display the chest displacement data. The data used a frequency class filter of 600 Hz. The raw and filtered data are displayed in Appendix B.

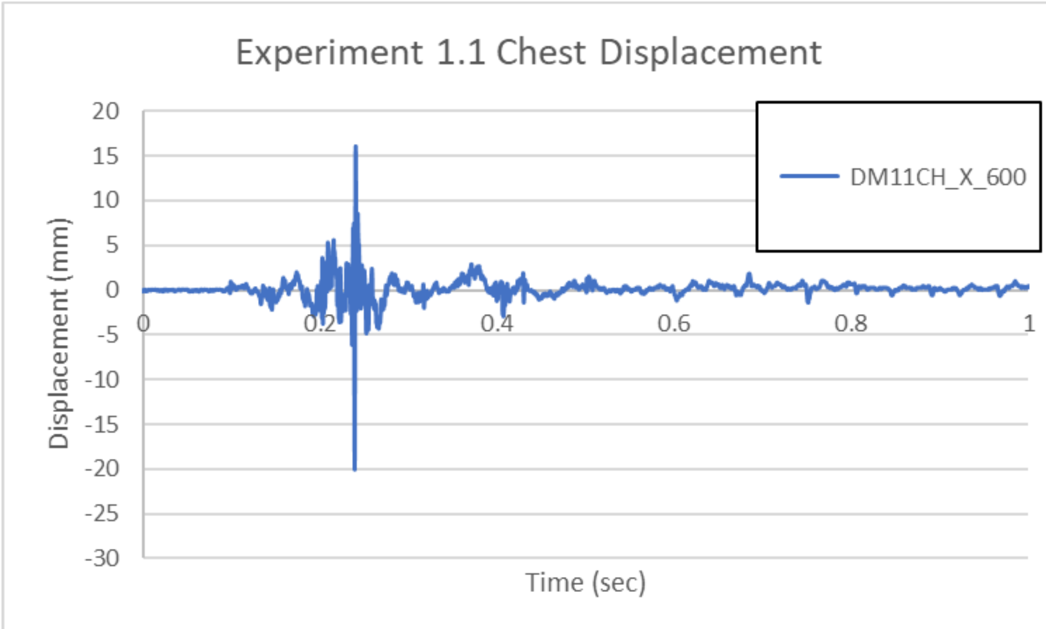

Figure 92. Occupant Protection Experiment 1.1 Chest Displacement Data

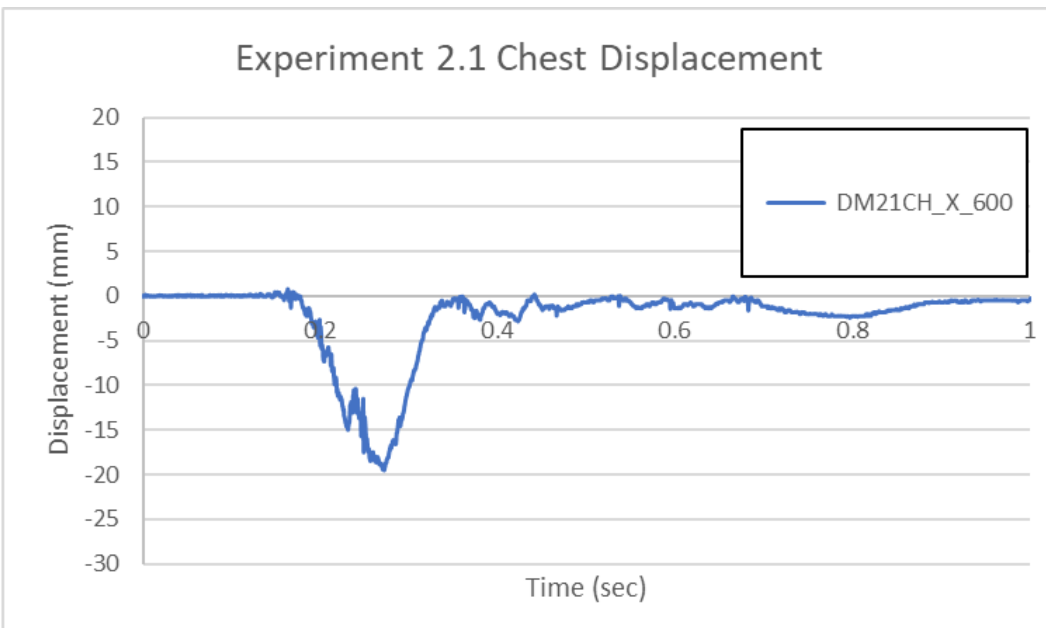

Figure 93. Occupant Protection Experiment 2.1 Chest Displacement Data

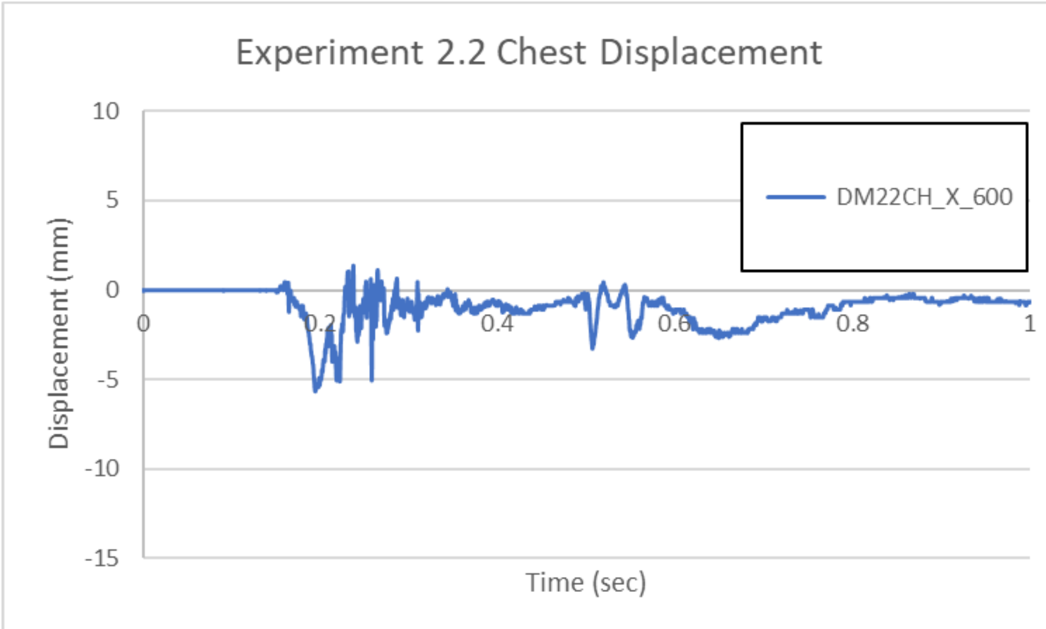

Figure 94. Occupant Protection Experiment 2.2 Chest Displacement Data

3.3.12 Calculated ATD Injury Criteria

The ATD measurements were used to calculate injury criteria for the head, chest, neck, and femurs. The resulting injury criteria are provided below in Table 25, along with the respective limits specified in the American Public Transportation Association (APTA) safety standard, Passenger Seats in Passenger Rail Cars APTA PR-CS-S-016-99 (APTA, 2021). All injury criteria for each ATD were below the injury limits.

Table 25. Summary of ATD Injury Criteria

Injury Criteria	Injury Limit	Occupant Experiment		
		1.1	2.1	2.2
HIC15	700	21	32	17
Axial Neck Tension (kN)	4.17	0.49	0.82	0.32
Axial Neck Compression (kN)	4	0.25	0.28	0.97
Nij	1	0.15	0.26	0.26
Chest Acceleration 3ms (g)	60	11	16	21
Chest Compression (mm)	63	20	20	6
Left Femur Compression (kN)	10	0.40	0.39	1.02
Right Femur Compression (kN)	10	0.59	0.43	0.92

3.4 CEM Activation and Post-Test Damage

All CEM components were activated during the impact. The PBC was activated along its total available stroke, and all the anti-climbers were engaged. Having contacted the nose of the conventional locomotive, the upper DAC was fully deformed. The lower DAC tubes contacted the front plate of the conventional locomotive, but they did not deform along their full length. The impact activated the shear bolts and the sliding lug moved its full length of travel to the back of the draft pocket. The CEM components after the test are shown in Figure 96 through Figure 98.

Figure 95. Crushed Upper DAC and Partially Crushed Lower DAC Tubes

Figure 96. Activated PBC

Figure 97. Sliding Lug after Test

Both the CEM locomotive coupler and conventional locomotive coupler were closed at impact. The force of impact caused the head of the casting on the PBC to split open vertically. The force and damage to the coupler appeared to have allowed the impacting knuckles to bypass each other and end up in a coupled configuration. After both consists stopped, the couplers were locked together and could only be separated using a hydraulic cylinder to force the locomotives apart. The conventional locomotive's coupler showed no outer signs of damage after the impact, but its knuckle did not open correctly. The cracked PBC is shown in Figure 99 and Figure 100. The conventional locomotive's coupler is shown in Figure 101.

Figure 98. Crack Along the Bottom of the PBC Coupler Head

Figure 99. Crack Along the Front and Top of the PBC Coupler Head

Figure 100. Conventional Locomotive Coupler Head – After Impact

The nose of the CEM locomotive showed significant deformation upon impact (Figure 102). The CEM locomotive's front plate also deformed, bending toward the rear of the vehicle at the outboard edges (Figure 103). There appeared to be cracks along the welds between the CEM locomotive front plate and the reinforced DAC plates on both the left and right side of the locomotive, as shown in Figure 104 and Figure 105. The interior floor of the locomotive behind the nose was deformed as well as the bottom of the interior side structures. Figure 106 and Figure 107 show the deformation of the floor and interior side structures, respectively.

Figure 101. CEM Locomotive – Deformed Nose

Figure 102. CEM Locomotive – Bent Front Plate

Figure 103. Left Side of the Cracked Front Plate (Highlight in Red)

Figure 104. Right Side of the Cracked Front Plate

Figure 105. Locomotive Interior Floor behind Nose

Figure 106. CEM Locomotive Left and Right Interior Side Structures

There appeared to be some deformation in either the CEM locomotive's front draft pocket, the center sill, or both. The lower flange of the center sill near the draft pocket had a slight curve after the impact, as shown in Figure 108. In addition, the top of the draft pocket had lowered enough to contact the top of the sliding lug. This caused the sliding lug to bind against the top of the draft pocket, preventing it from moving freely. The top of the draft pocket that contacted the sliding lug is shown in Figure 109.

Figure 107. Curved Center Sill in Front End of CEM Locomotive

Figure 108. Contact between the Top of the Sliding Lug and the Top of the Draft Pocket

The nose of the conventional locomotive also experienced significant deformation upon impact (Figure 110). The upper DAC contacted the conventional locomotive at the floor structure of its front compartment, causing buckling in both the floor and its support structure attached to the locomotive's front plate. The conventional locomotive's front plate was also deformed in the area where the lower DAC tubes made contact. The front plate deformation and buckled floor structure is shown in Figure 111 and Figure 112. The anti-climber structures, the plow, and the decoupling bar all experienced deformation from the impact. There was also deformation in the conventional locomotive's center sill. Much like the CEM locomotive, the center sill appeared to have a curved lower flange near the front draft pocket (Figure 113). There did not appear to be any damage on the rear of the conventional locomotive or on the two hopper cars in the stationary consist.

Figure 109. Damaged Front of the Conventional Locomotive

Figure 110. Buckled Floor Structure and Deformed Front Plate, Right Side

Figure 111. Buckled Floor Structure and Deformed Front Plate, Left Side

Figure 112. Downward Curve in Conventional Locomotive Center Sill Flange

The first M1 car in the mobile consist (i.e., 8332) showed significant damage to its front draft gear. During impact, the plate that held the yoke inside the draft pocket was ejected from the car. The plate ejection allowed the yoke to hang under the draft pocket and forced the front coupler to rest at a sharp upward angle. The upward angle of the coupler also caused a small amount of deformation in the front plate of 8332, just above the draft pocket opening. The yoke and front coupler shank from 8332 are shown in Figure 114 and Figure 115.

Figure 113. Yoke from the Front Coupler on Car 8332

Figure 114. Shank from Front Coupler on 8332 at Upward Angle

Both M1 cars 8332 and 8221 experienced wrinkling in their stainless-steel skin from the impact. The team also observed small amounts of deformation in the car's side sills, especially near the traction rod connections to the trucks. However, no significant structural damage was observed on either the exterior or interior of the M1 cars. Several traction rods were bent on both 8332 and 8221. The left side traction rod on car 8221's cab end was ejected from its mounts during the impact, damaging the mounting connections on both the carbody and the truck. Figure 116 shows an example of side sill deformation on car 8332. One of the bent traction rods is shown in Figure 117. The truck on car 8221 with the ejected traction rod is shown in Figure 118.

Figure 115. Side Sill Deformation on the Right Side of 8332

Figure 116. Bent Traction rod at Cab End of 8332

Figure 117. Broken Traction Rod Mountings on Cab End of 8221

In the onboard occupant protection experiments, researchers observed no damage on either the Q'straint One system (Figure 119) or the Quantum backboard (Figure 120). However, some damage was observed on the fully operational Quantum system. The backboard in the full Quantum system had holes in either side where the surrogate wheelchair's handles contacted the backboard during the impact. This backboard damage is shown in Figure 121. In addition, the surrogate wheelchair in the full Quantum system had a weighted plate that was in contact with the Quantum chassis, as shown in Figure 122. During the impact, this plate provided a point load to the chassis and damaged the cover plate. The damaged chassis covering is shown in Figure 123. Despite the damage noted here, the full Quantum system was still operational after the test.

Figure 118. Post Impact Unrestrained Quantum Backboard

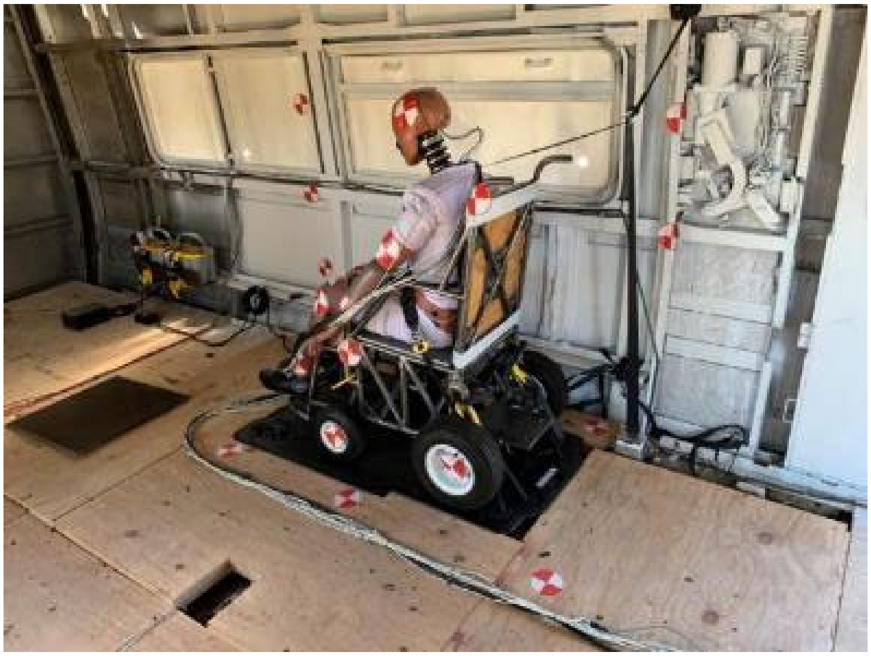

Figure 119. Post Impact Q'Straint One

Figure 120. Holes in the Left and Right Side of the Full Quantum System Backboard

Figure 121. Plate at Base of Surrogate Wheelchair in Contact with Quantum Chassis

Figure 122. Damaged Cover Plate on the Quantum Chassis

4. Conclusion

On August 11, 2022, FRA sponsored MxV Rail to conduct an impact test between a moving three-car consist and a stationary three-car consist at TTC near Pueblo, Colorado. The moving consist included an EMD F40 passenger locomotive equipped with crash energy management components backed by two M1 series passenger cars. The M1 passenger cars were also equipped with three occupant protection experiments that included the use of ATDs seated in wheelchairs. The stationary consist included a conventional F40 locomotive backed by two empty freight cars. This testing was intended to evaluate the combined performance of the CEM components, including the PBC, the DAC, and the shear bolts and sliding lug. The team designed occupant experiments to evaluate the effectiveness of restraint devices and study the effects of the residual energy imparted to passengers after the CEM components on the impacting locomotive were activated.

The conventional locomotive and the two hopper cars were impacted by the 389,800 lb moving consist at 24.3 mph. Although the couplers were closed at impact, the CEM locomotive and the conventional locomotive experienced enough deformation at the couplers and front faces to become intertwined. A hydraulic cylinder was required to separate the two locomotives after the test.

The CEM locomotive impacted the conventional locomotive predominantly at the coupler interface and the upper DAC. The upper DAC deformed to its full extent. The lower DAC tubes made slight contact with the conventional locomotive and only experienced approximately 1 inch of deformation. The PBC was activated and exhausted its available stroke. The impact also activated the shear bolts, causing the sliding lug to move all the way into the draft pocket. The impact caused enough deformation in the draft pocket of the CEM locomotive to prevent the sliding lug from moving freely after the test. The PBC coupler head cracked from the impact and damage occurred in the M1 passenger cars, including bent traction rods and ejection of the plate that holds the yoke in the draft pocket on the first M1 passenger car. The total impact energy was approximately 7.7 million lbf.

The test confirmed that the PBC, the DAC, and the shear bolts in the sliding lug were activated, prevented overclimb, and absorbed the impact energy as intended. In addition, the test demonstrated the feasibility of using wheeled mobility device restraint systems in rail cars and the potential to limit the movement of that equipment and the passengers seated in them in a crash scenario.

Researchers will use the data collected during this test to validate the computer models and prepare for future crashworthiness and occupant protection testing.

5. References

1. SAE International (2014). SAE J211-1 (1995): Instrumentation for Impact Test, Part 1, Electronic Instrumentation. 49 CFR 571.202a.

2. American Public Transportation Association (March 2021). Passenger Seats in Passenger Rail Cars. APTA PR-CS-S-016-99, Rev. 3.

Appendix A. Target Positions

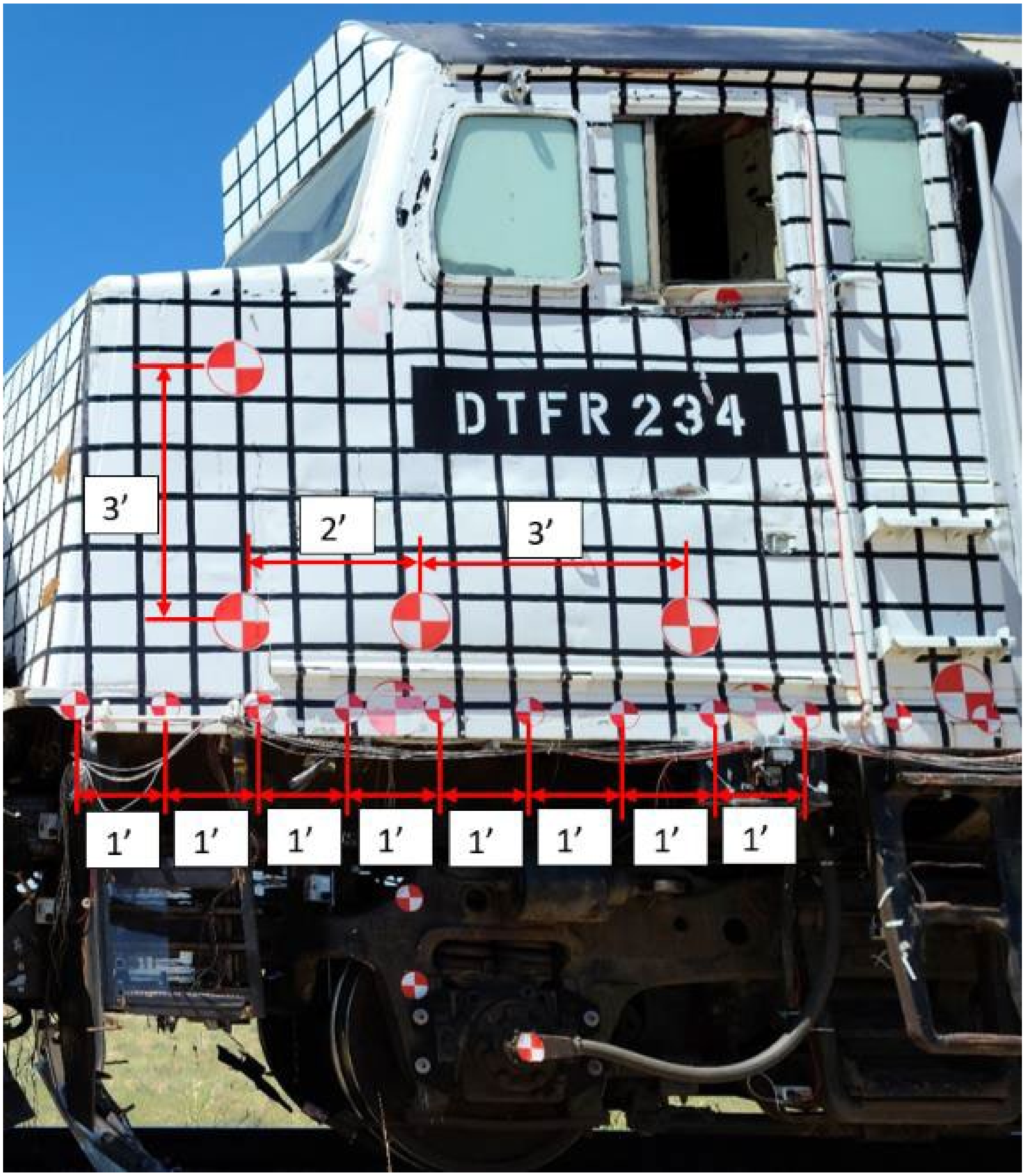

Figure A1. Target Spacing for CEM Locomotive

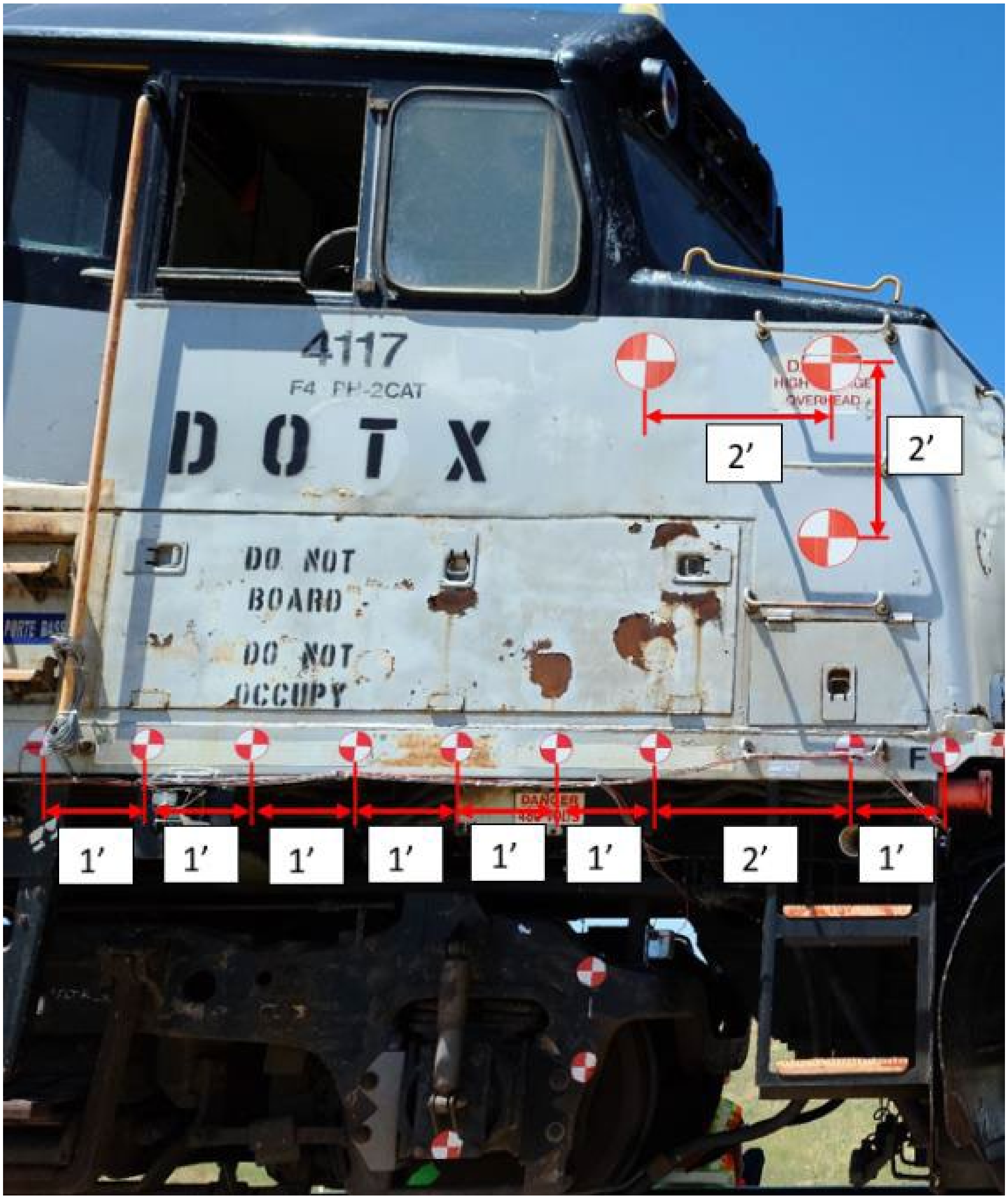

Figure A2. Target Spacing for Conventional Locomotive

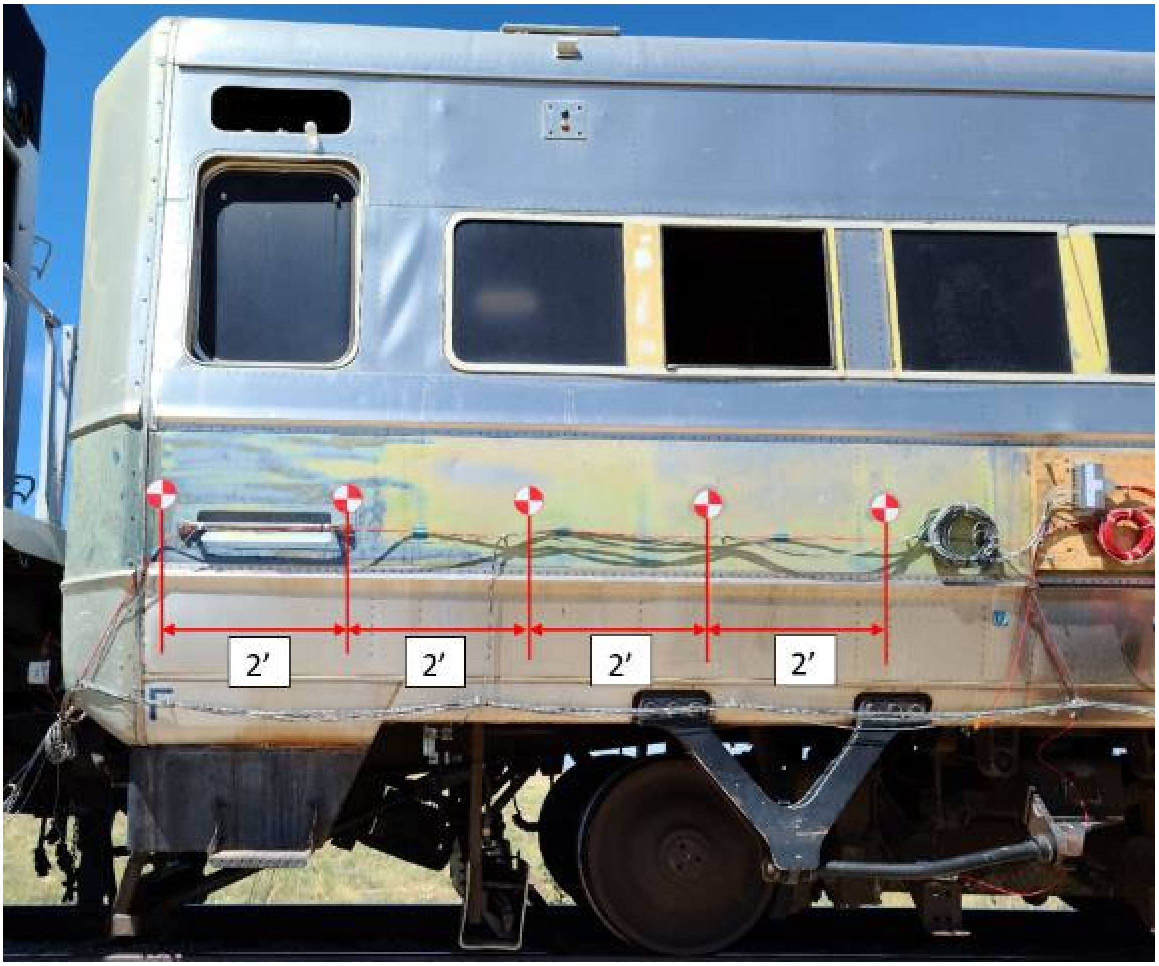

Figure A3. Target Spacing for 8332 M1 Car

Appendix B. Test Data

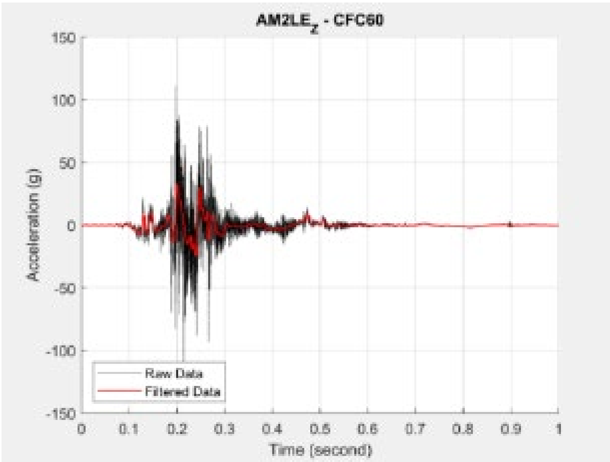

Figure B1. AM2LE_Z Accelerometer Data

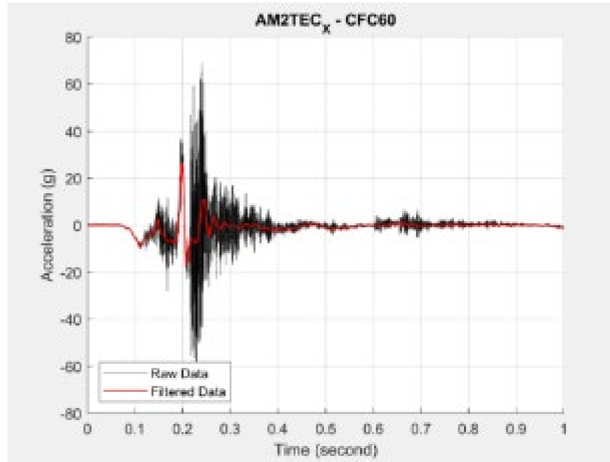

Figure B2. AM2TEC_X Accelerometer Data

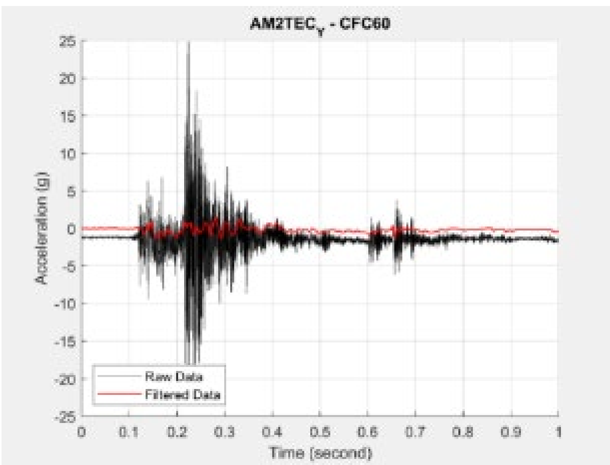

Figure B3. AM2TEC_Y Accelerometer Data

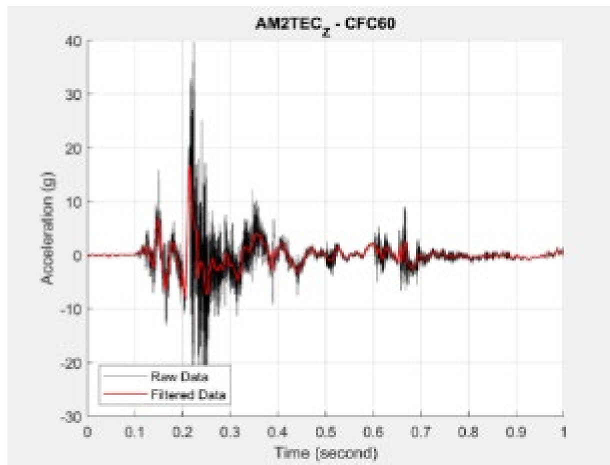

Figure B4. AM2TEC_Z Accelerometer Data

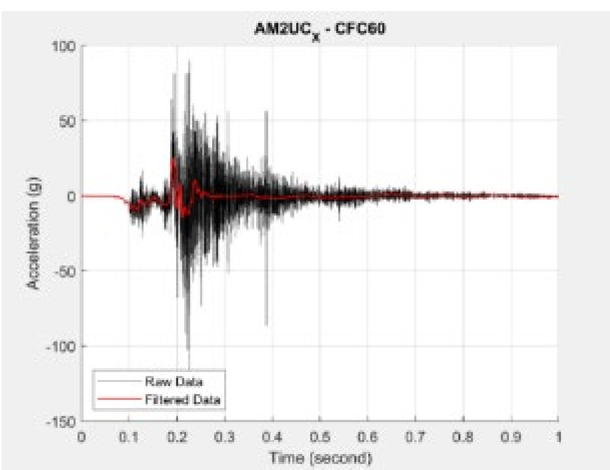

Figure B5. AM2UC_X Accelerometer Data

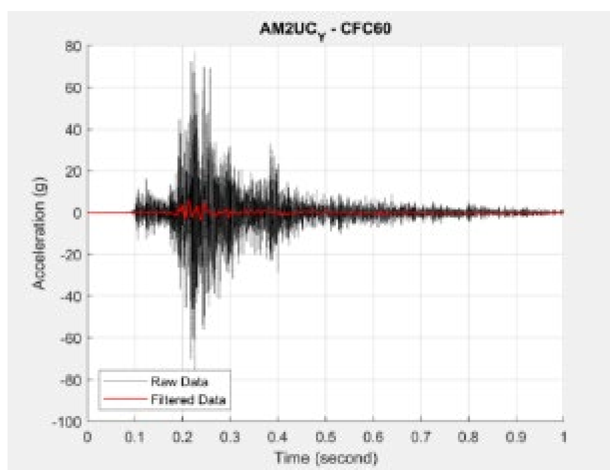

Figure B6. AM2UC_Y Accelerometer Data

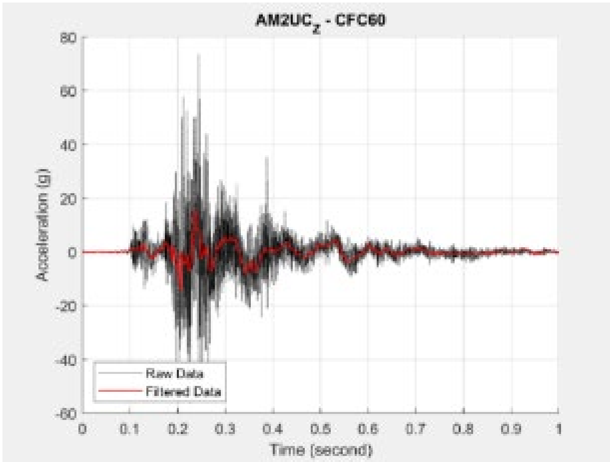

Figure B7. AM2UC_Z Accelerometer Data

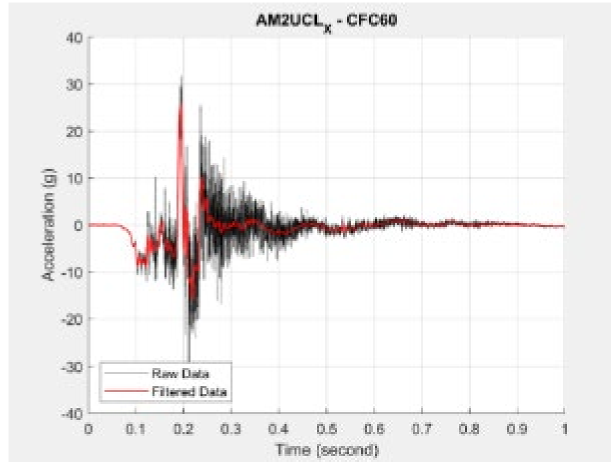

Figure B8. AM2UCL_X Accelerometer Data

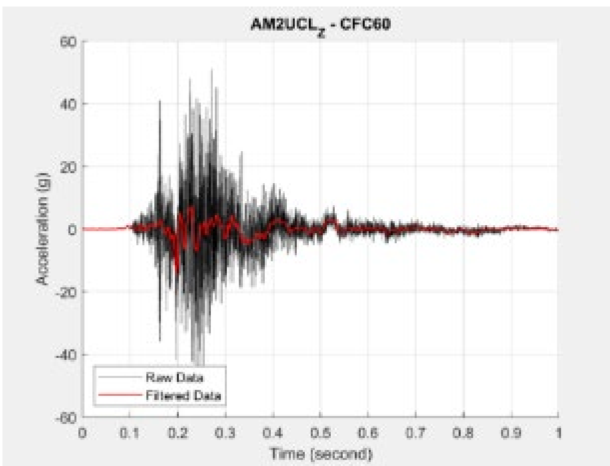

Figure B9. AM2UCL_Z Accelerometer Data

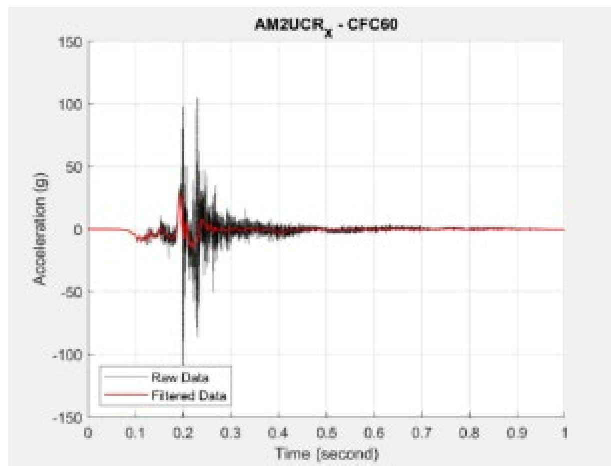

Figure B10. AM2UCR_X Accelerometer Data

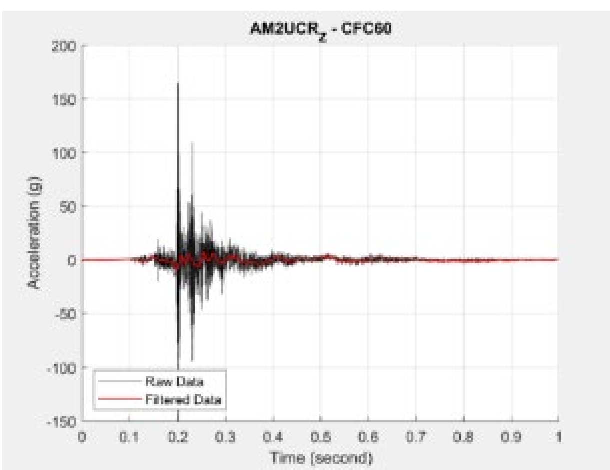

Figure B11. AM2UCR_X Accelerometer Data

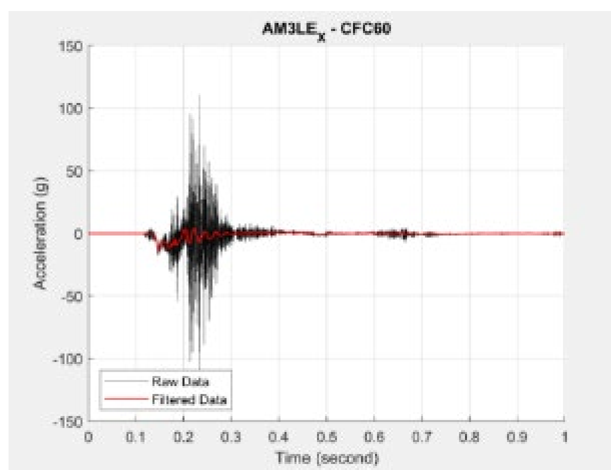

Figure B12. AM3LE_X Accelerometer Data

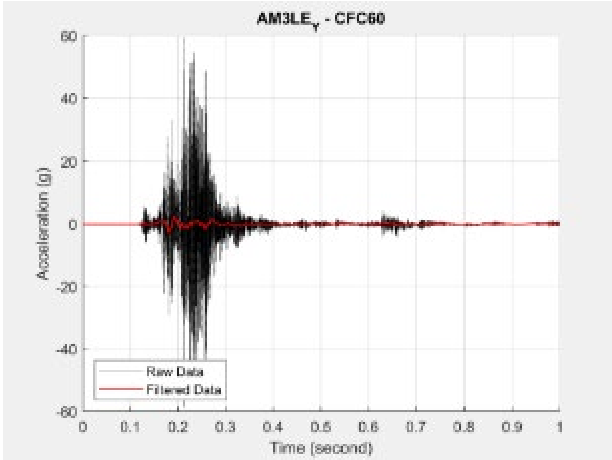

Figure B13. AM3LE_Y Accelerometer Data

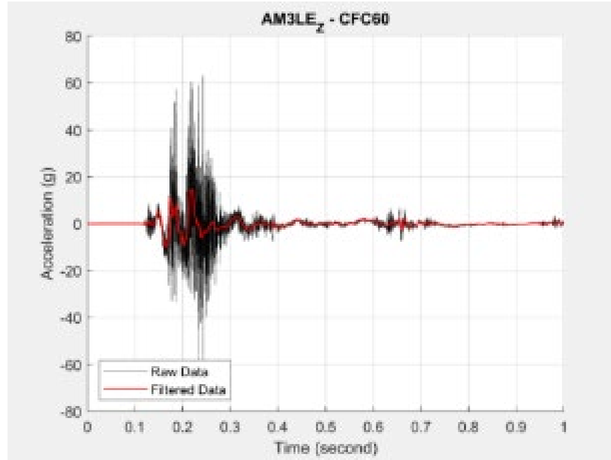

Figure B14. AM3LE_Z Accelerometer Data

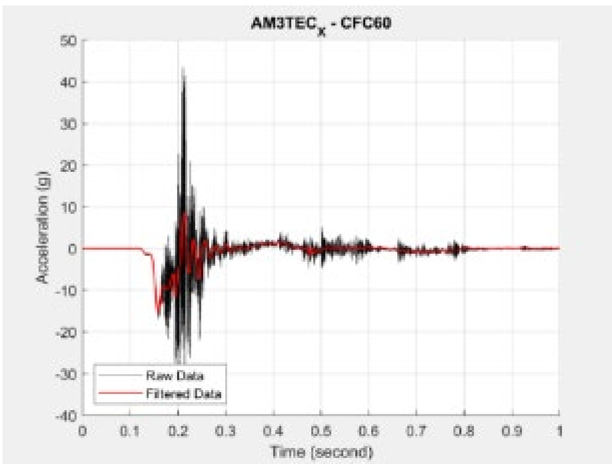

Figure B15. AM3TEC_X Accelerometer Data

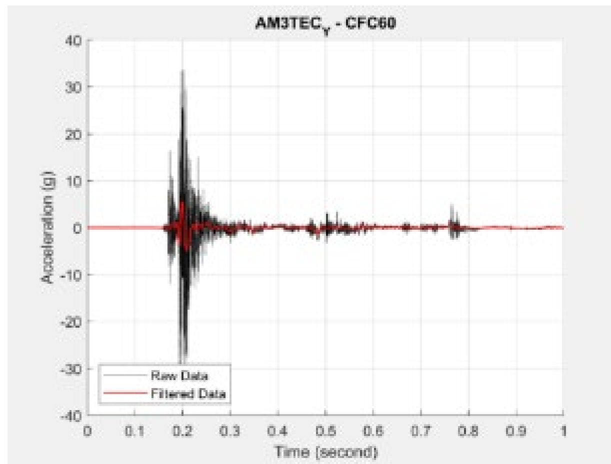

Figure B16. AM3TEC_Y Accelerometer Data

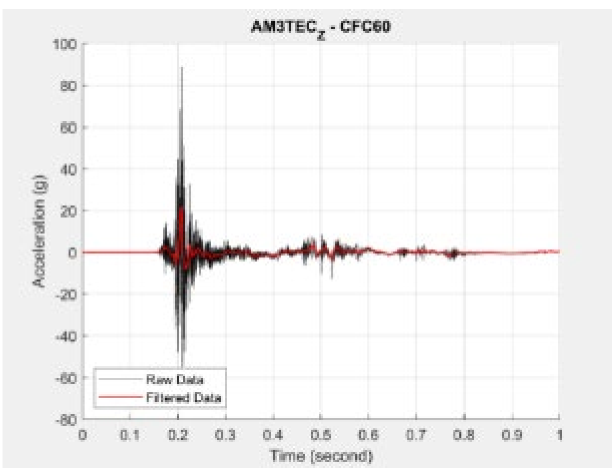

Figure B17. AM3TEC_Z Accelerometer Data

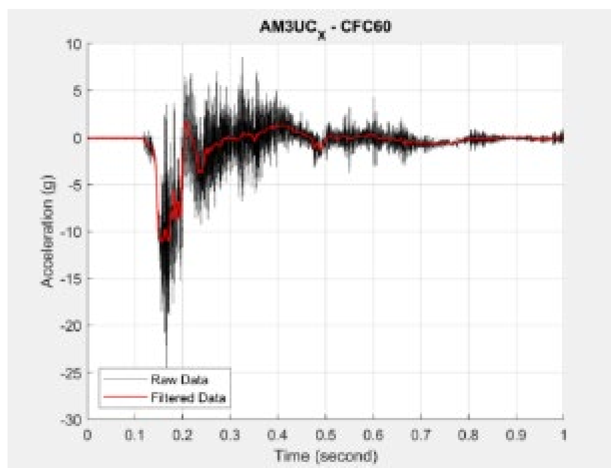

Figure B18. AM3UC_X Accelerometer Data

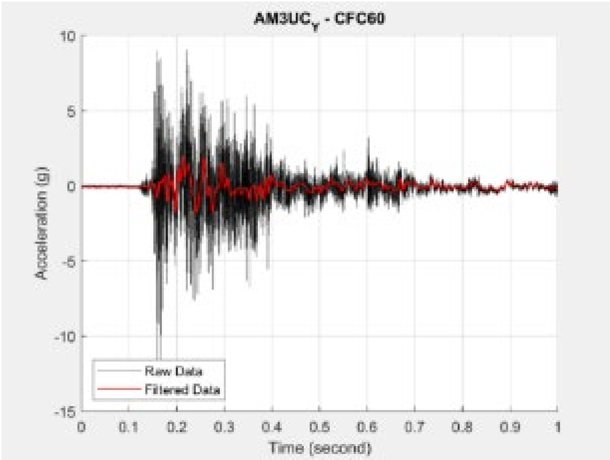

Figure B19. AM3UC_Y Accelerometer Data

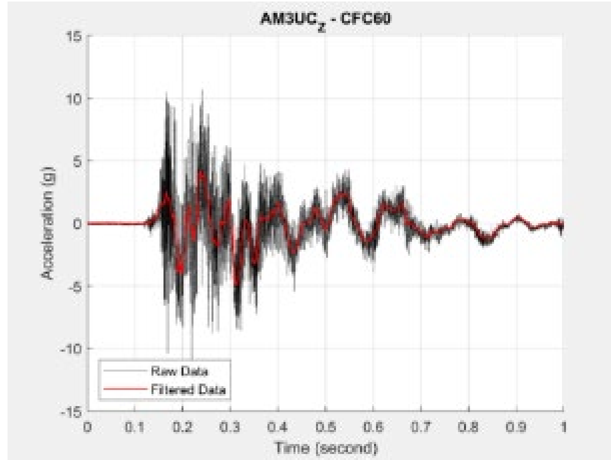

Figure B20. AM3UC_Z Accelerometer Data

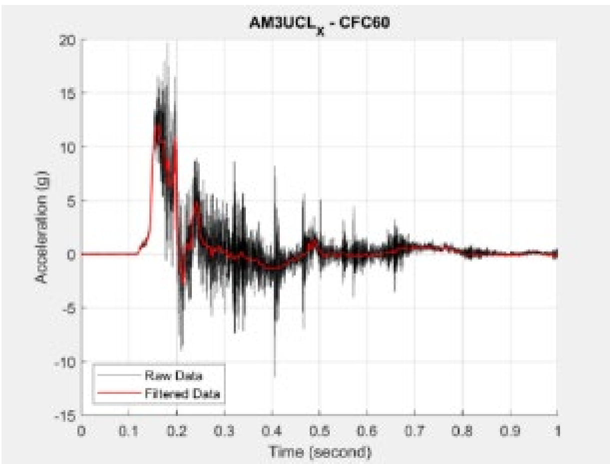

Figure B21. AM3UCL_X Accelerometer Data[1]

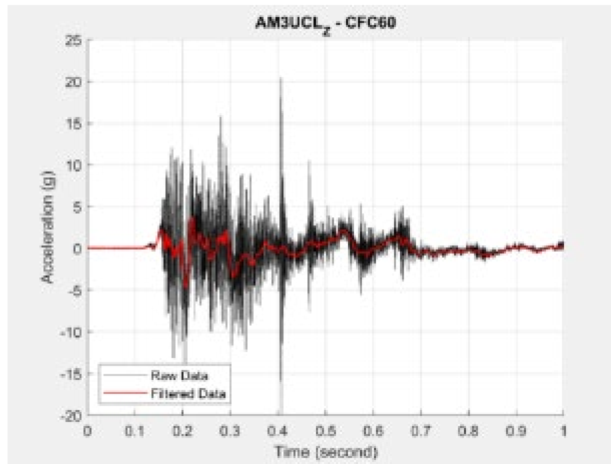

Figure B22. AM3UCL_Z Accelerometer Data

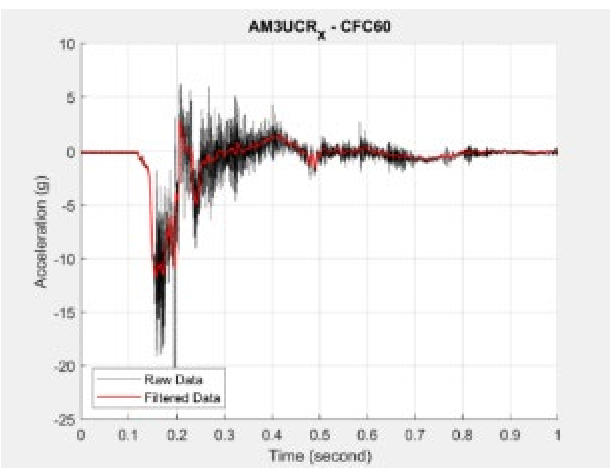

Figure B23. AM3UCR_X Accelerometer Data

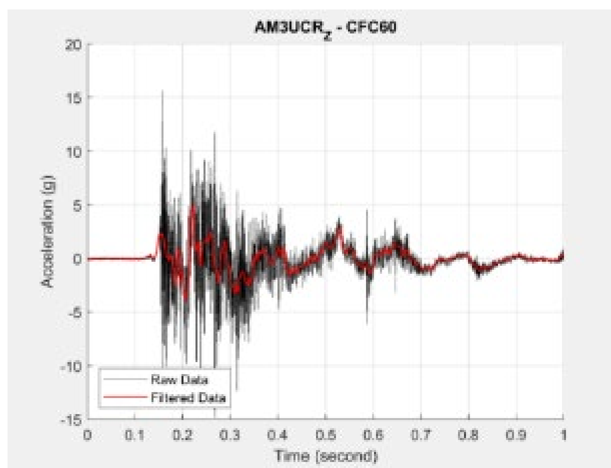

Figure B24. AM3UCR_Z Accelerometer Data

[1] The polarity of AM3UCL_X was mistakenly flipped.

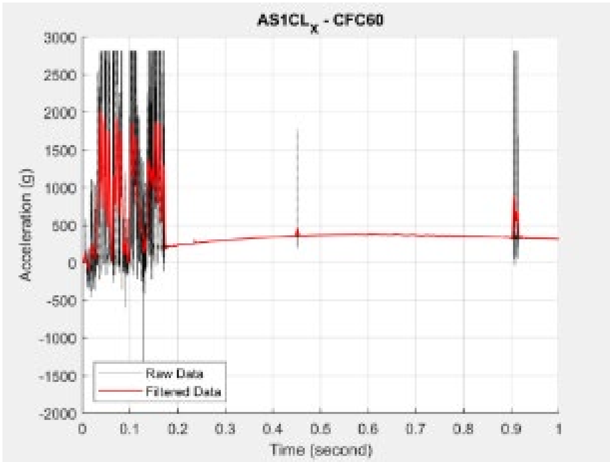

Figure B25. AS1CL_X Accelerometer Data

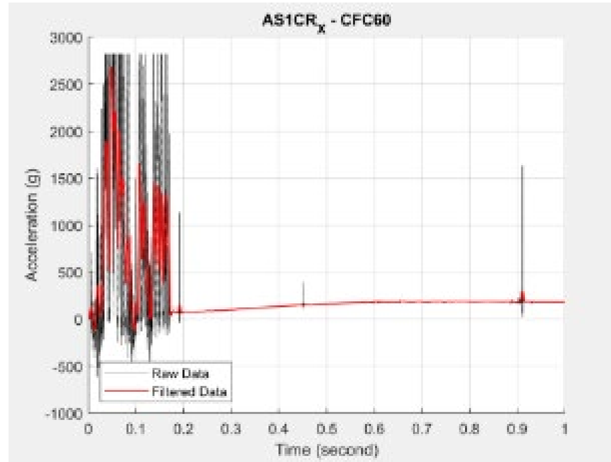

Figure B26. AS1CR_X Accelerometer Data

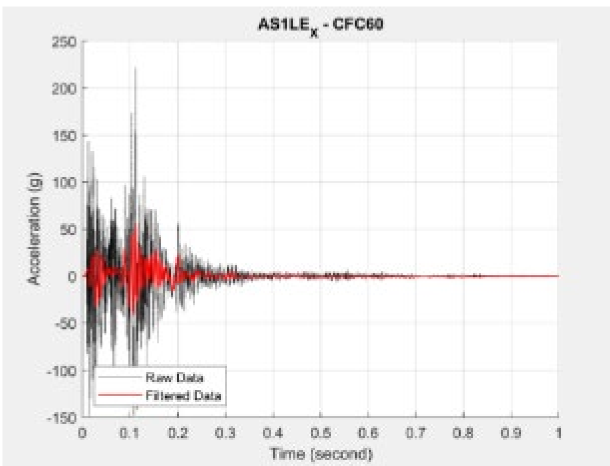

Figure B27. AS1LE_X Accelerometer Data

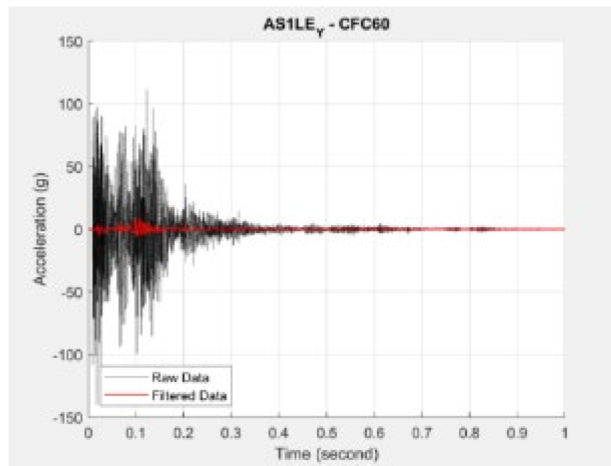

Figure B28. AS1LE_Y Accelerometer Data

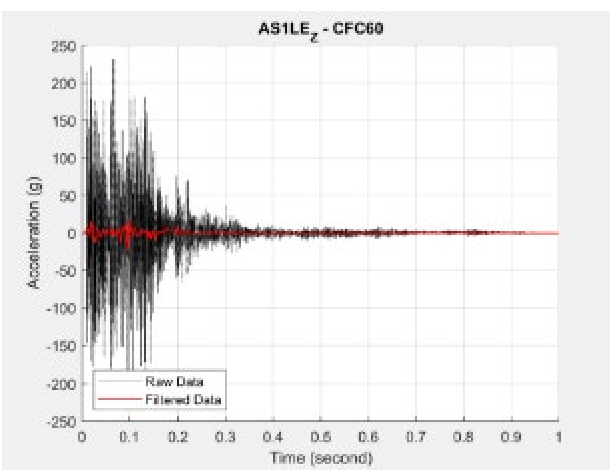

Figure B29. AS1LE_Z Accelerometer Data

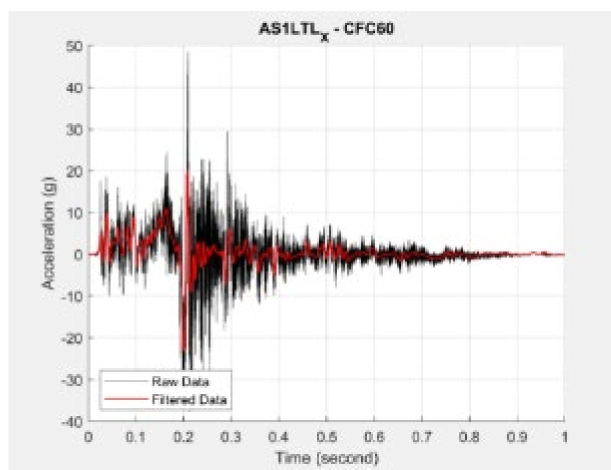

Figure B30. AS1LTL_X Accelerometer Data

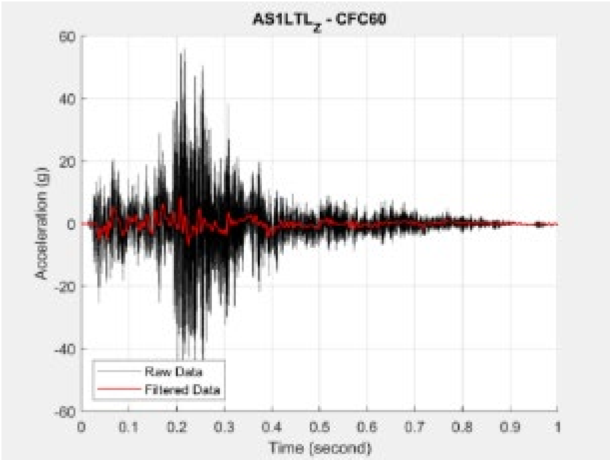

Figure B31. AS1LTL_Z Accelerometer Data

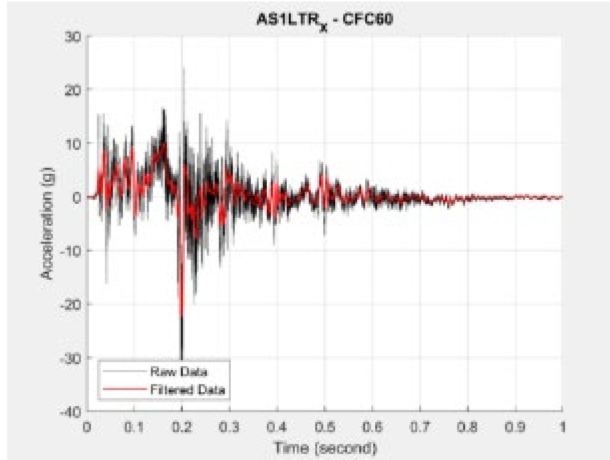

Figure B32. AS1LTR_X Accelerometer Data

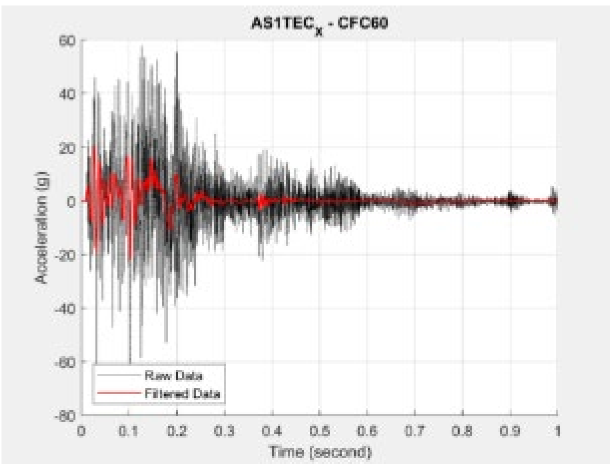

Figure B33. AS1TEC_X Accelerometer Data

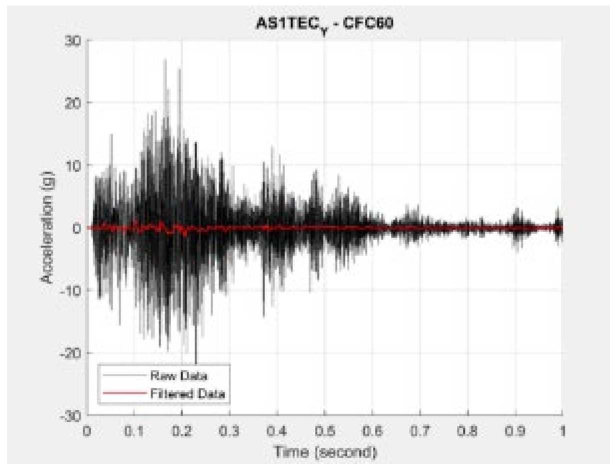

Figure B34. AS1TEC_Y Accelerometer Data

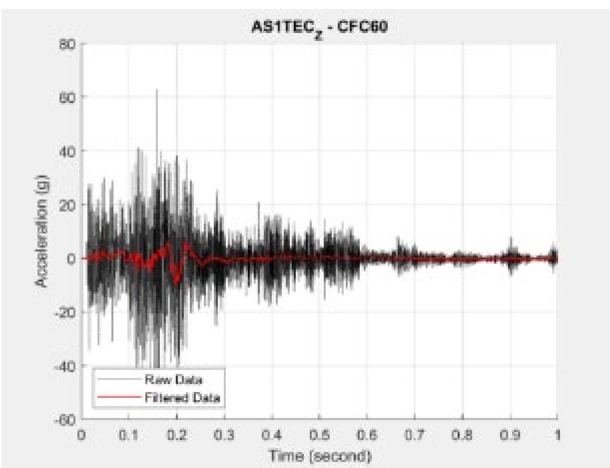

Figure B35. AS1TEC_Z Accelerometer Data

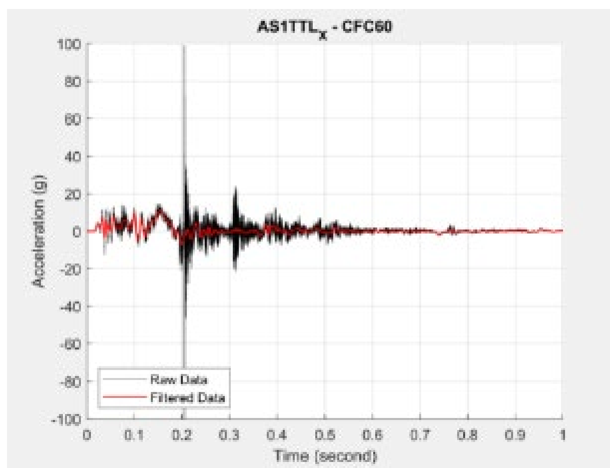

Figure B36. AS1TTL_X Accelerometer Data

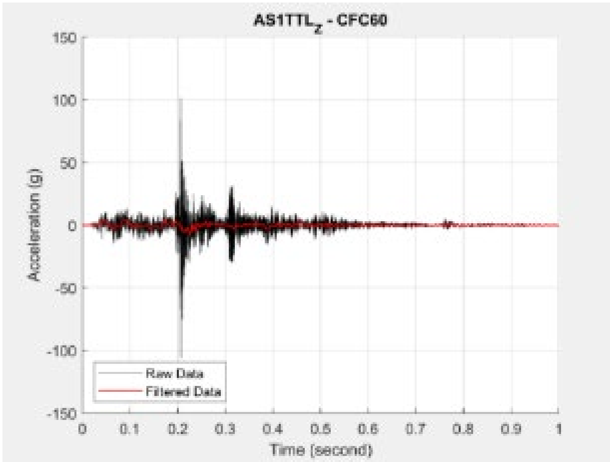

Figure B37. AS1TTL_Z Accelerometer Data

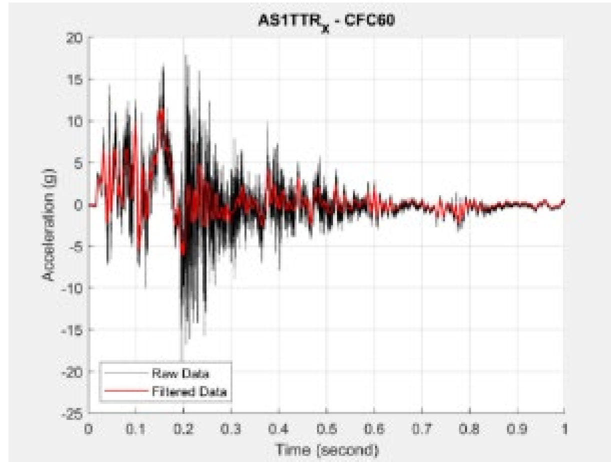

Figure B38. AS1TTR_X Accelerometer Data

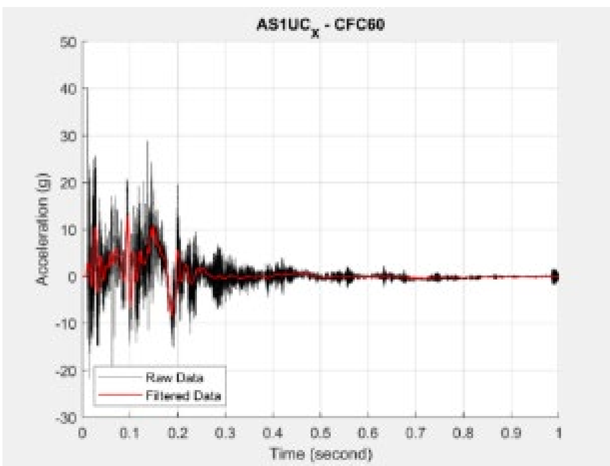

Figure B39. AS1UC_X Accelerometer Data

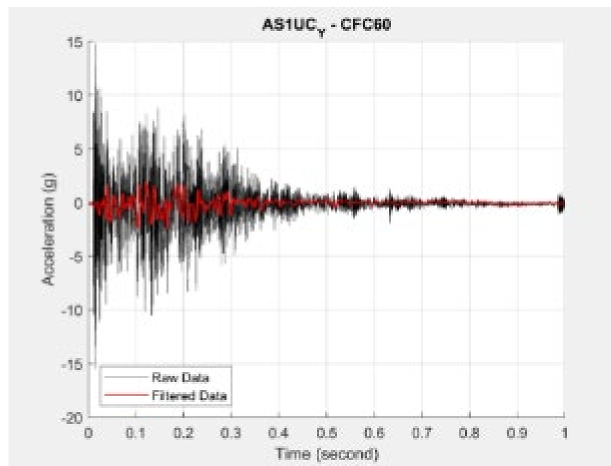

Figure B40. AS1UC_Y Accelerometer Data

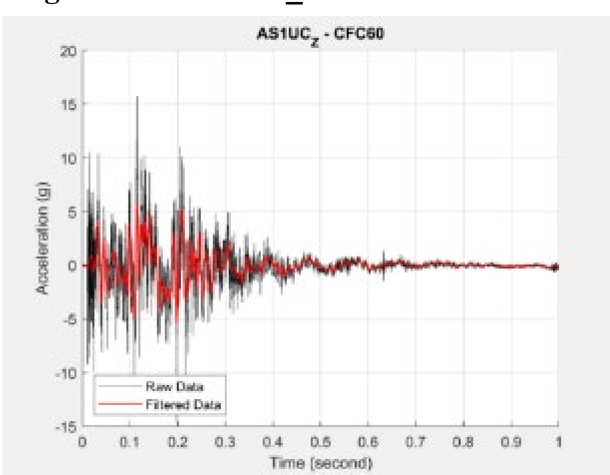

Figure B41. AS1UC_Z Accelerometer Data

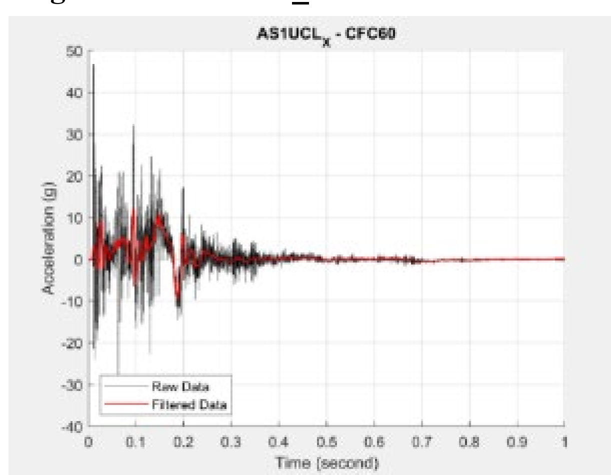

Figure B42. AS1UCL_X Accelerometer Data

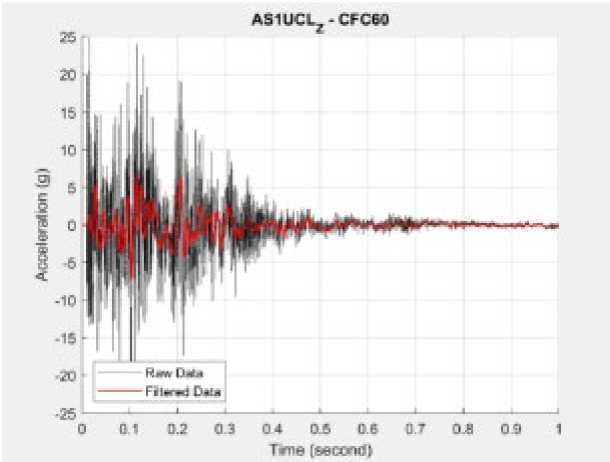

Figure B43. AS1UCL_Z Accelerometer Data

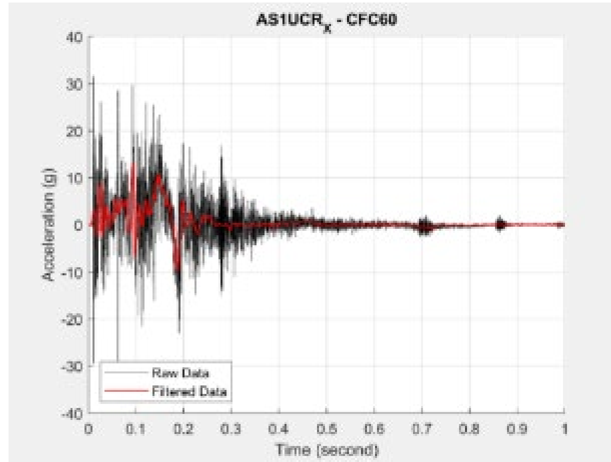

Figure B44. AS1UCR_X Accelerometer Data

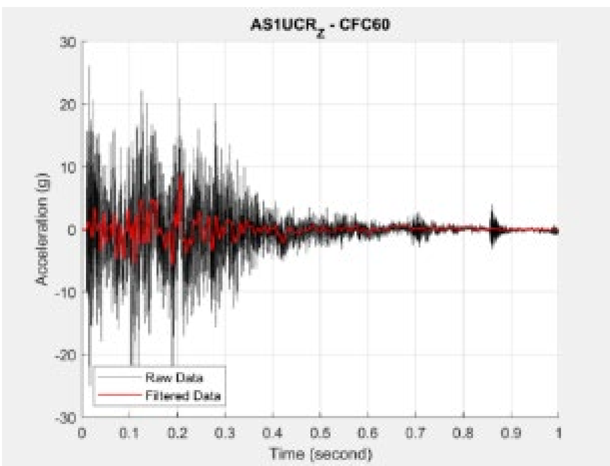

Figure B45. AS1UCR_Z Accelerometer Data

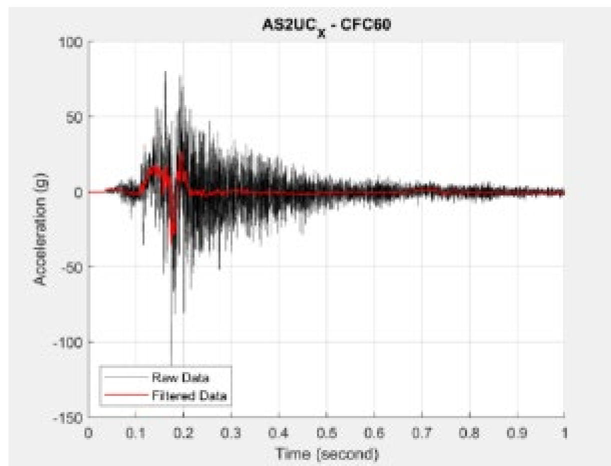

Figure B46. AS2UC_X Accelerometer Data

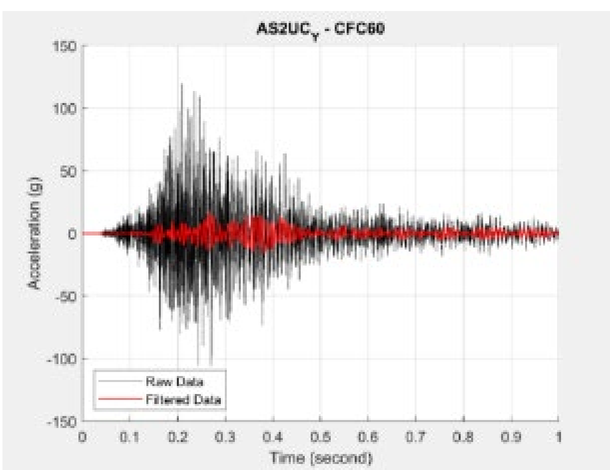

Figure B47. AS2UC_Y Accelerometer Data

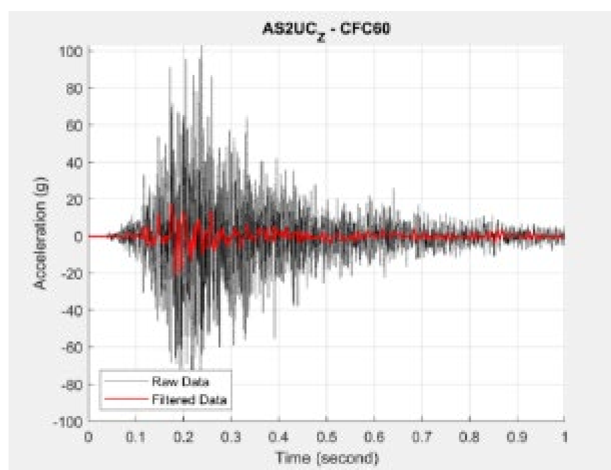

Figure B48. AS2UC_Z Accelerometer Data

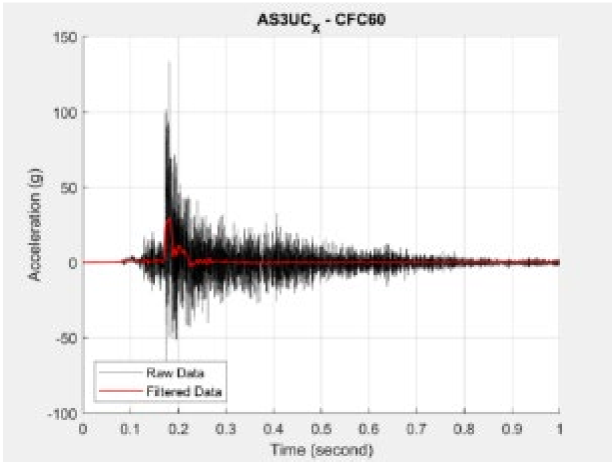

Figure B49. AS3UC_X Accelerometer Data

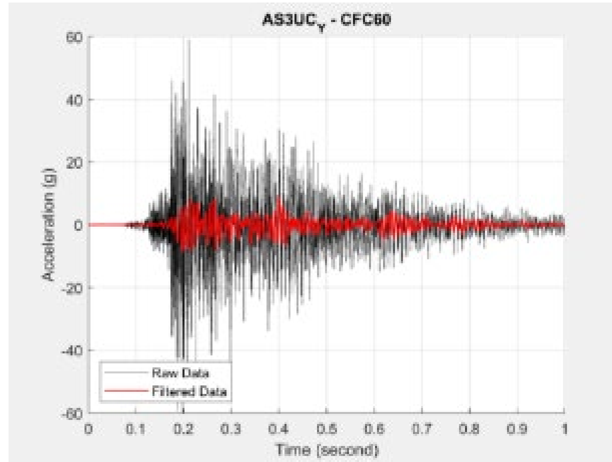

Figure B50. AS3UC_Y Accelerometer Data

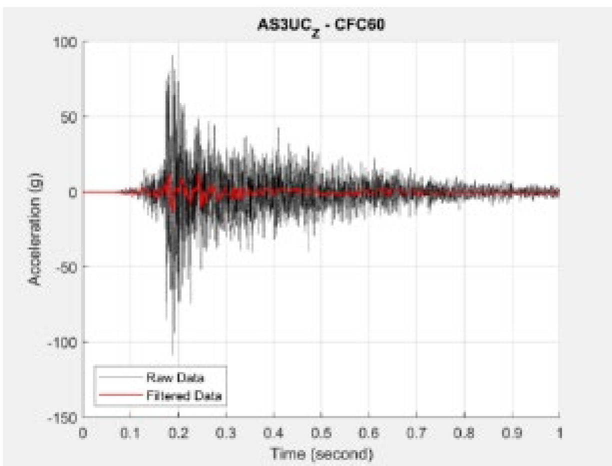

Figure B51. AS3UC_Z Accelerometer Data

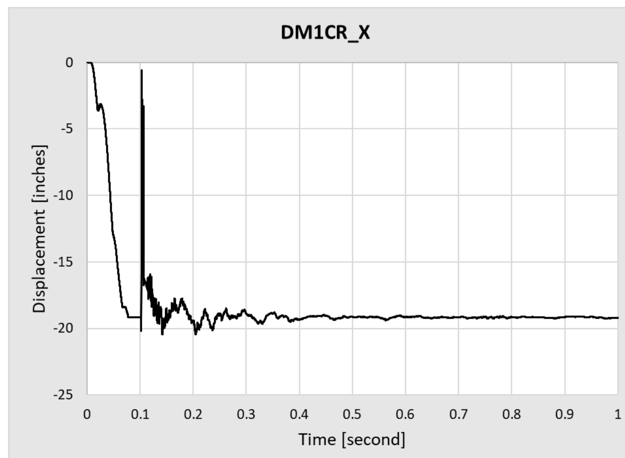

Figure B52. DM1CR_X Displacement Data

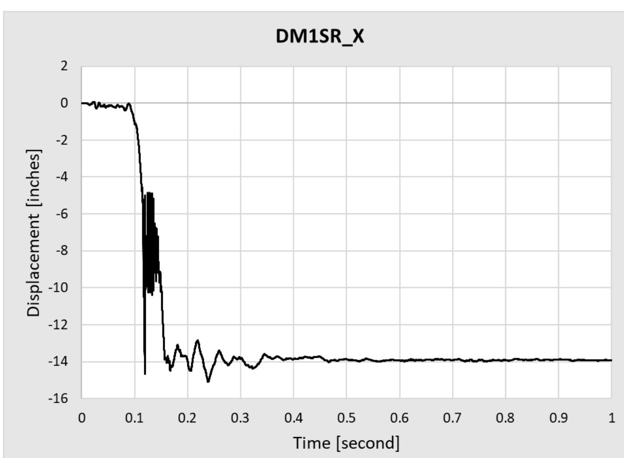

Figure B53. DM1SR_X Displacement Data

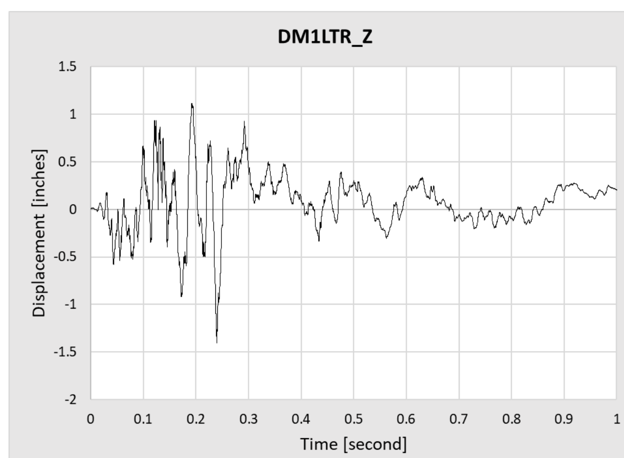

Figure B54. DM1LTR_Z Displacement Data

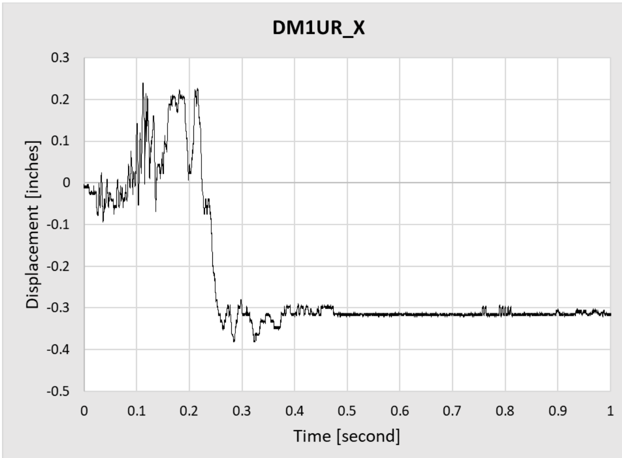

Figure B55. DM1UR_X Displacement Data

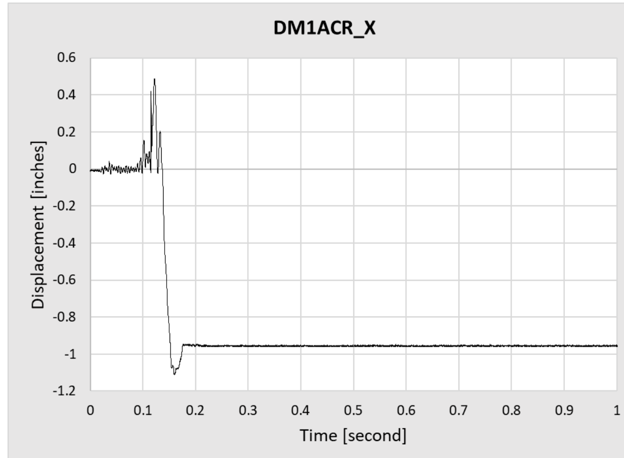

Figure B56. DM1ACR_X Displacement Data

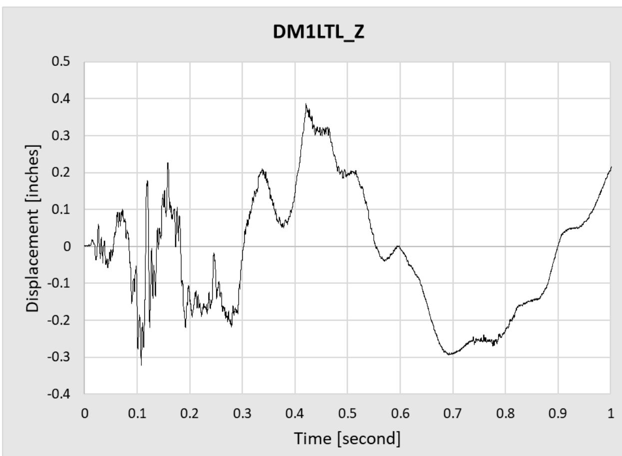

Figure B57. DM1LTL_Z Displacement Data

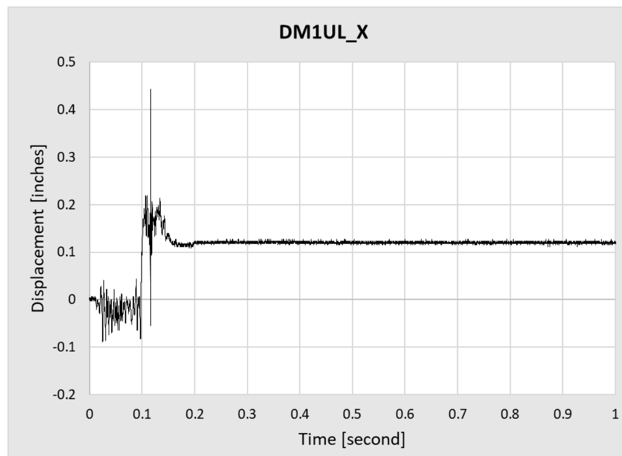

Figure B58. DM1UL_X Displacement Data

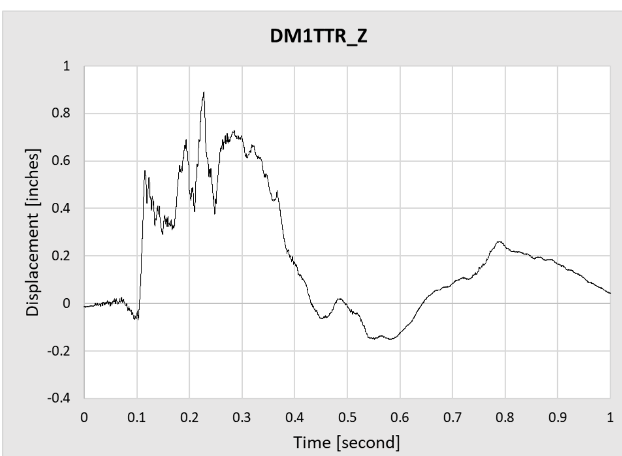

Figure B59. DM1TTR_Z Displacement Data

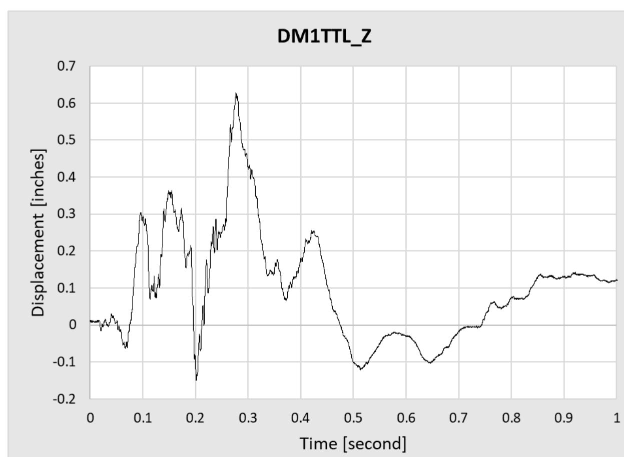

Figure B60. DM1TTL_Z Displacement Data

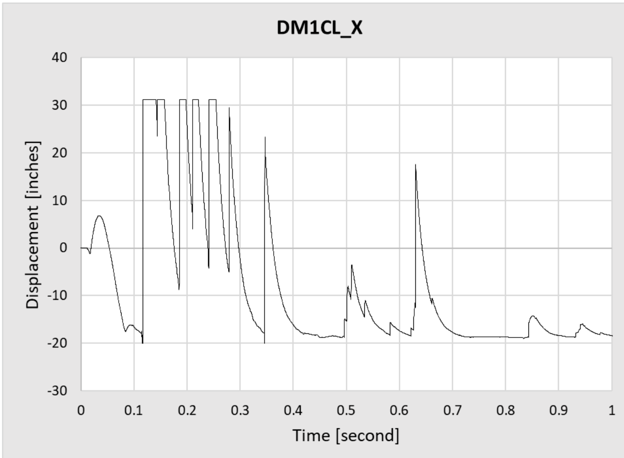

Figure B61. DMCL_X Displacement Data

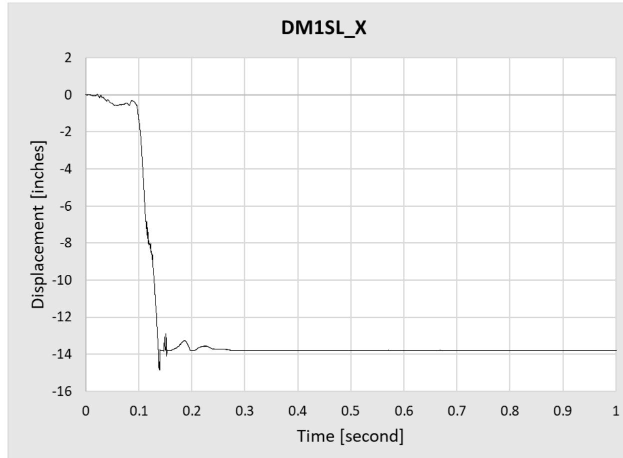

Figure B62. DM1SL_X Displacement Data

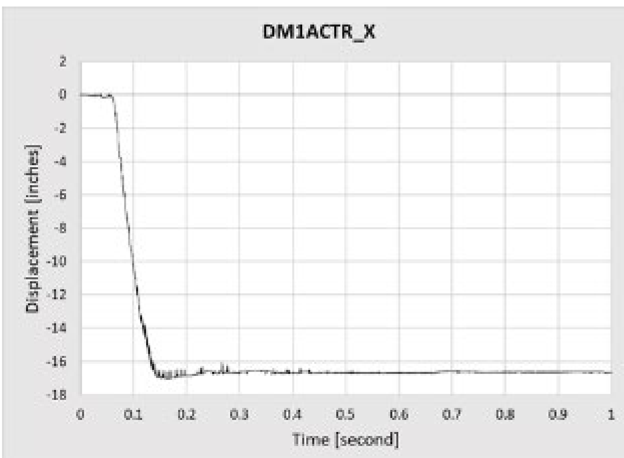

Figure B63. DM1ACTR_X Displacement Data

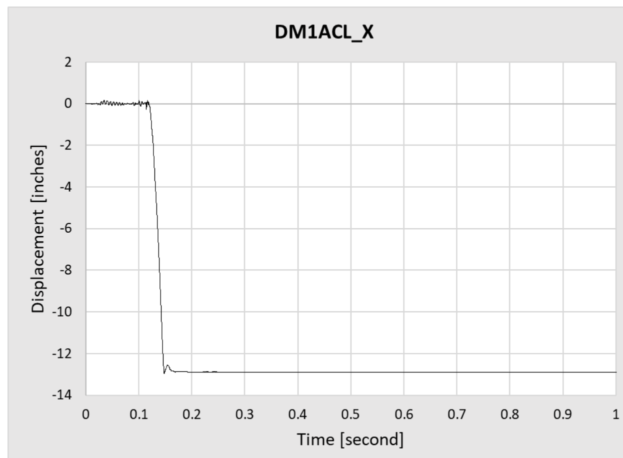

Figure B64. DM1ACL_X Displacement Data

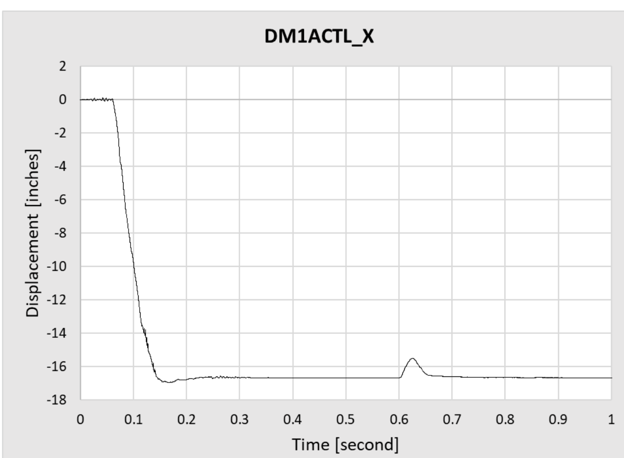

Figure B65. DM1ACTL_X Displacement Data

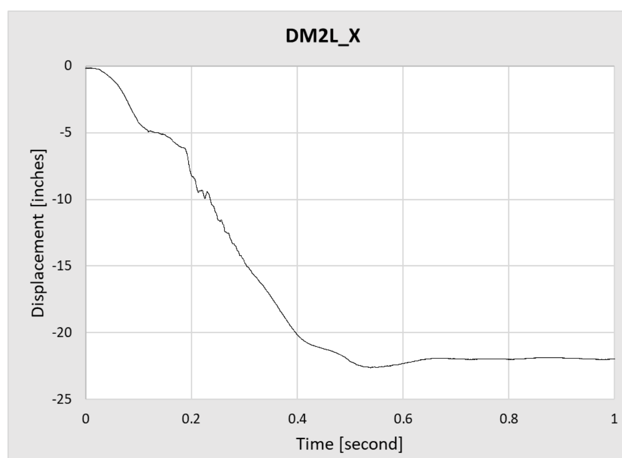

Figure B66. DM2L_X Displacement Data

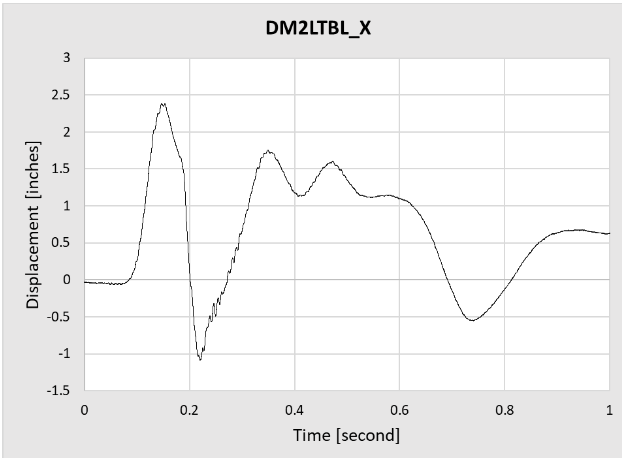

Figure B67. DM2LTBL_X Displacement Data

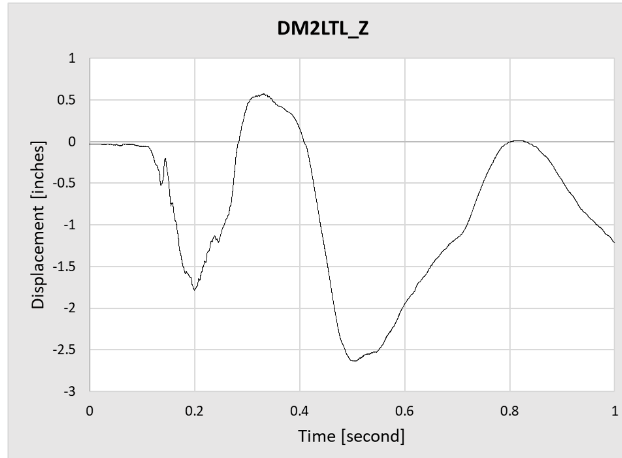

Figure B68. DM2LTL_Z Displacement Data

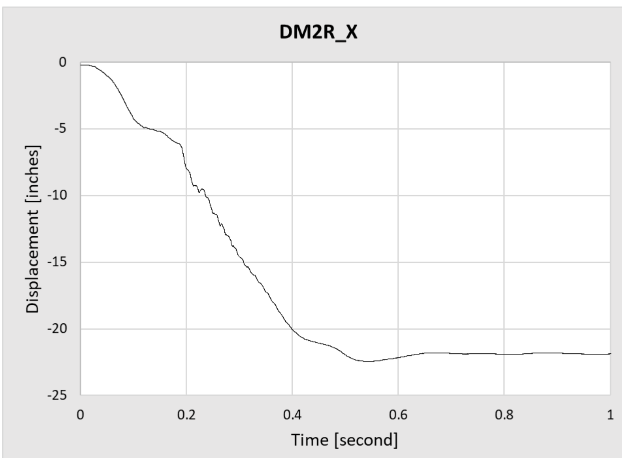

Figure B69. DM2R_X Displacement Data

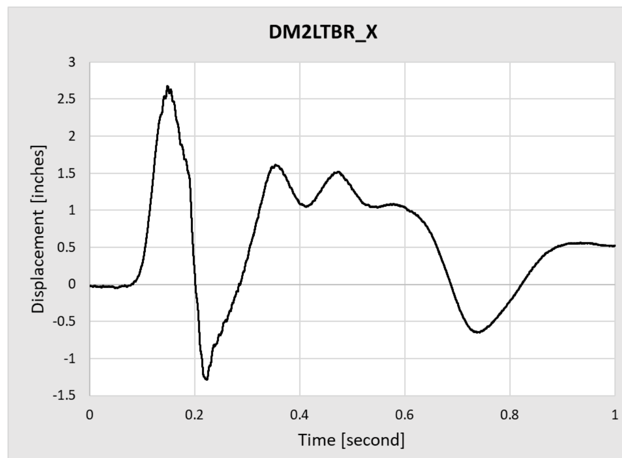

Figure B70. DM2LTBR_X Displacement Data

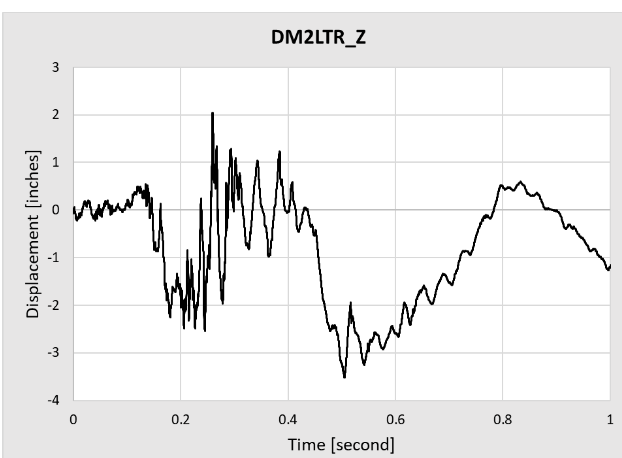

Figure B71. DM2LTR_Z Displacement Data

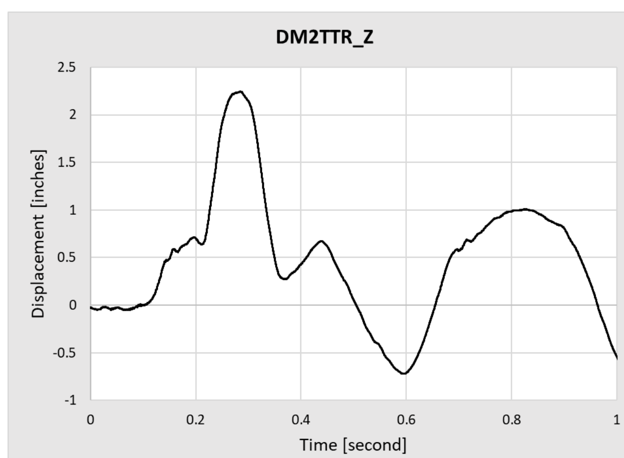

Figure B72. DM2TTR_Z Displacement Data

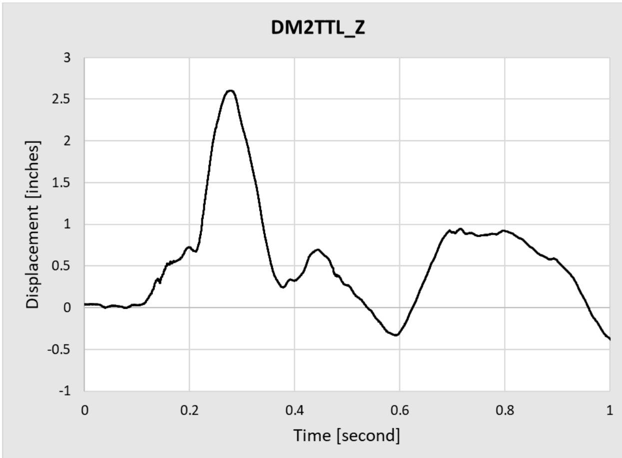

Figure B73. DM2TTL_Z Displacement Data

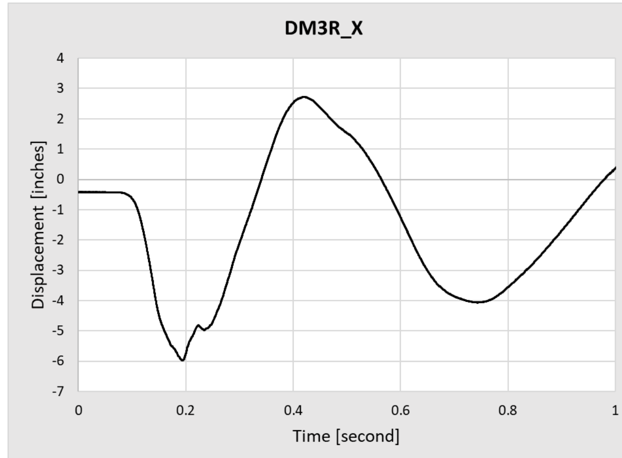

Figure B74. DM3R_X Displacement Data

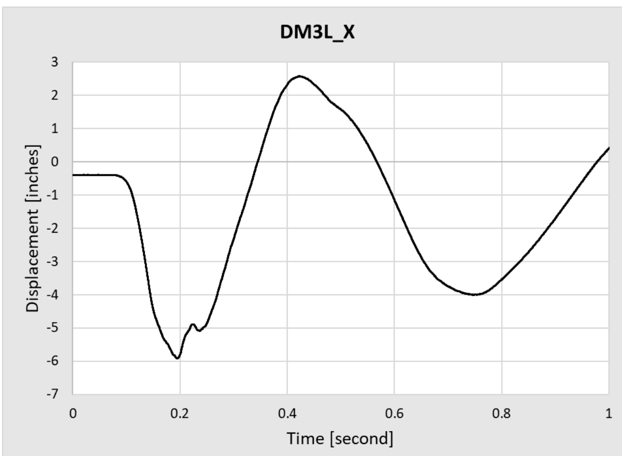

Figure B75. DM3L_X Displacement Data

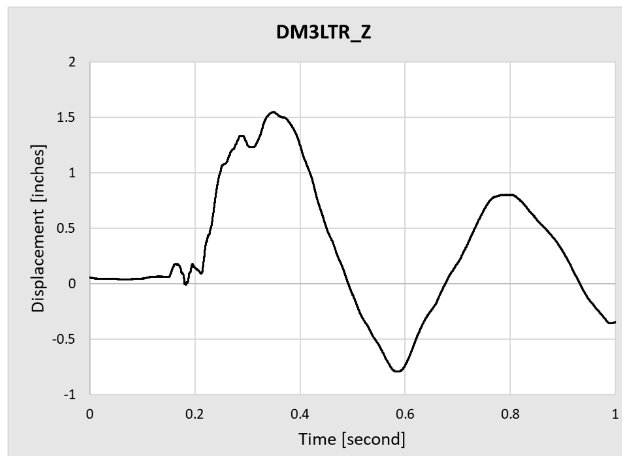

Figure B76. DM3LTR_Z Displacement Data

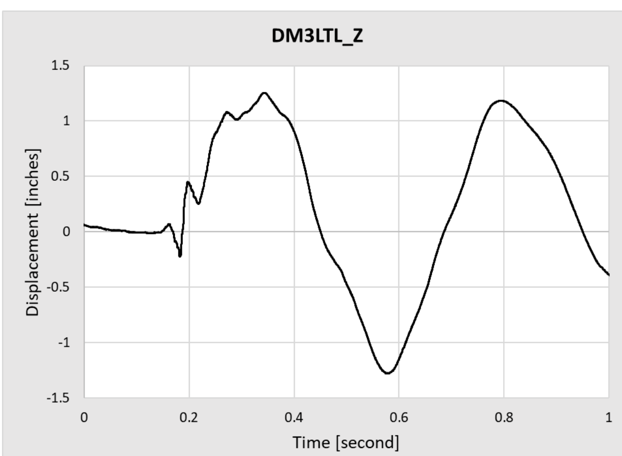

Figure B77. DM3LTL_Z Displacement Data

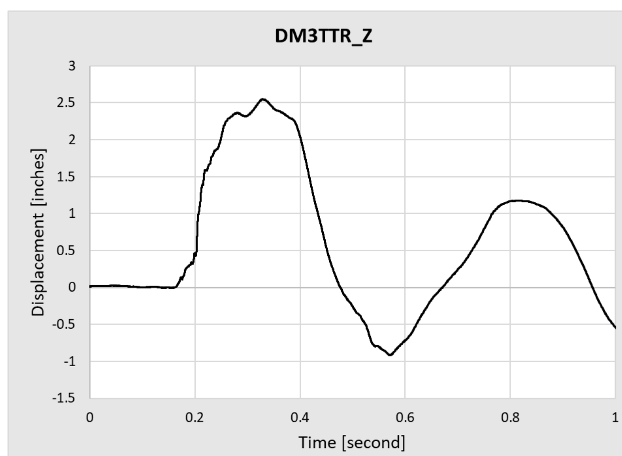

Figure B78. DM3TTR_Z Displacement Data

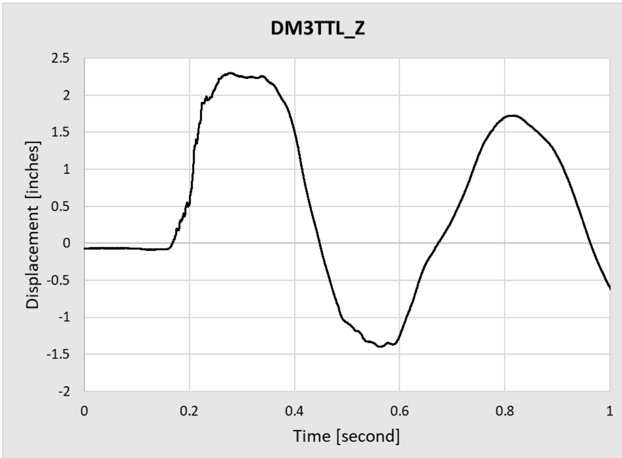

Figure B79. DM3TTL_Z Displacement Data

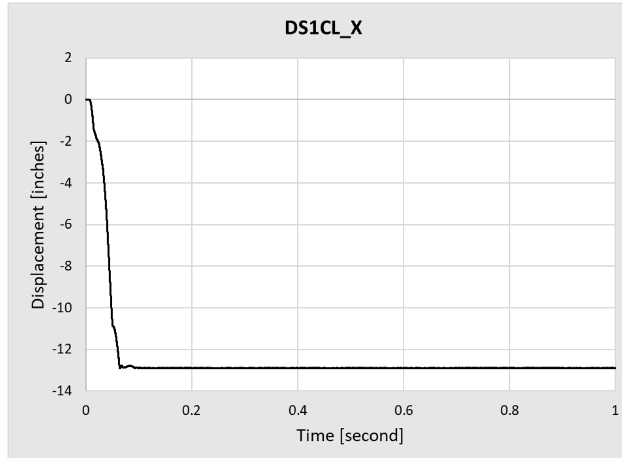

Figure B80. DS1CL_X Displacement Data

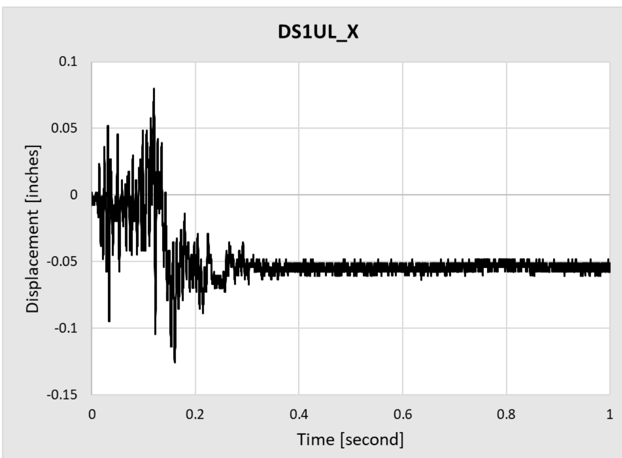

Figure B81. DS1UL_X Displacement Data

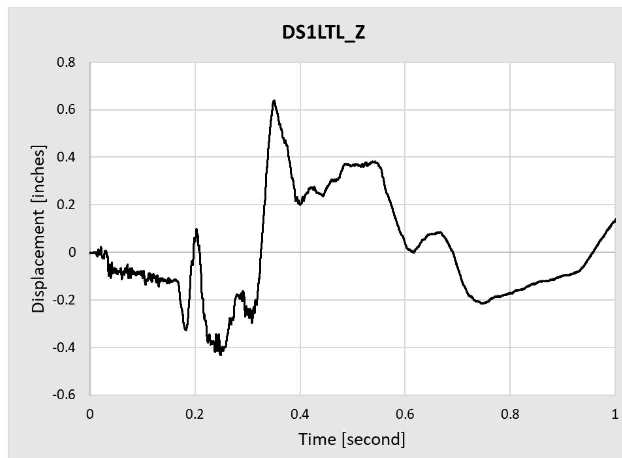

Figure B82. DS1LTL_Z Displacement Data

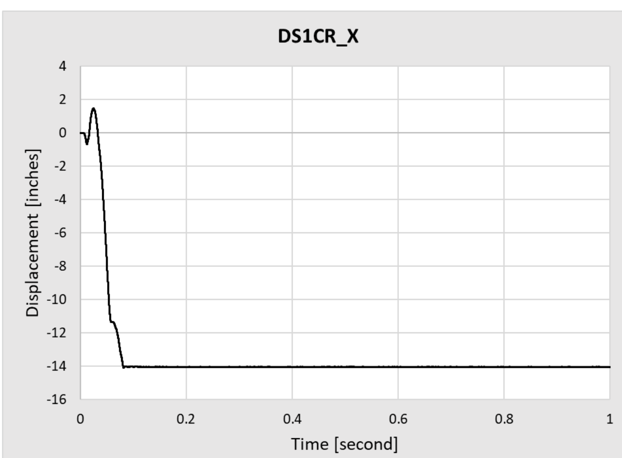

Figure B83. DS1CR_X Displacement Data

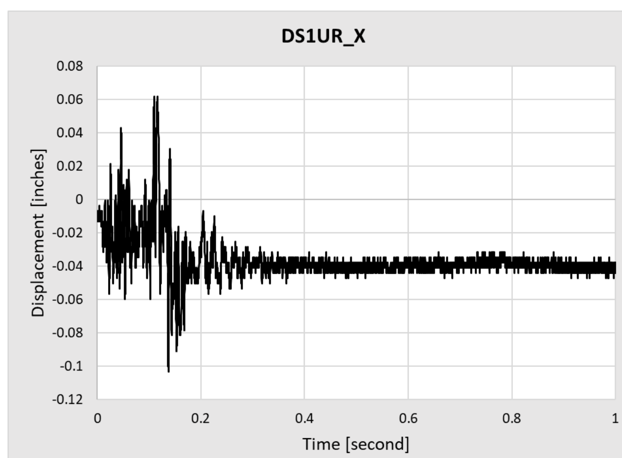

Figure B84. DS1UR_X Displacement Data

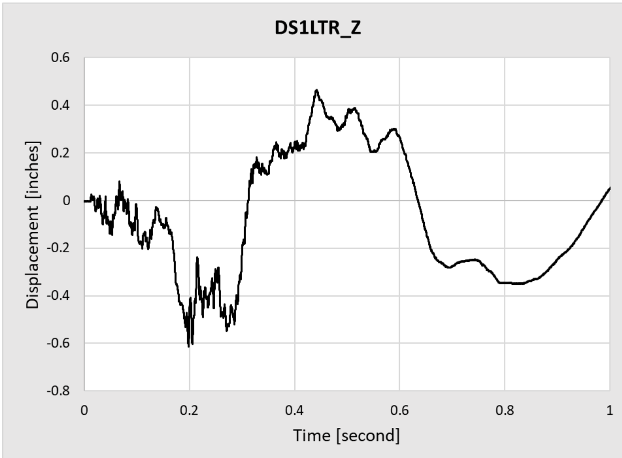

Figure B85. DS1LTR_Z Displacement Data

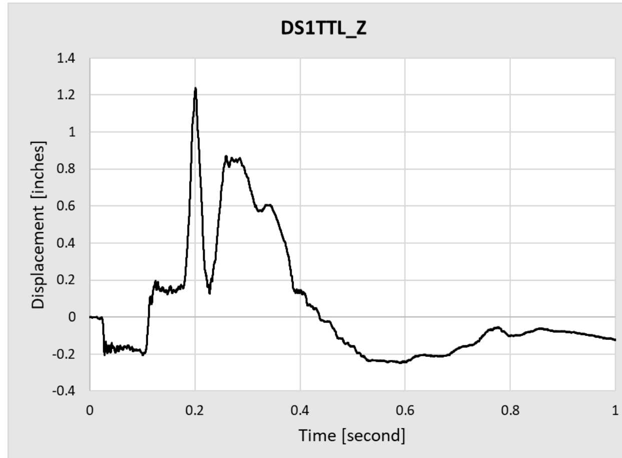

Figure B86. DS1TTL_Z Displacement Data

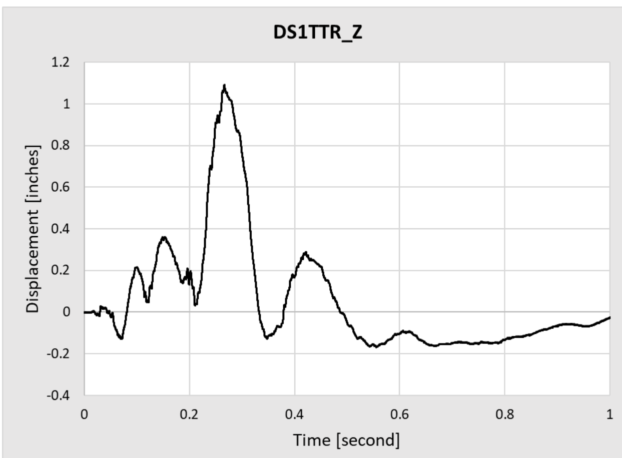

Figure B87. DS1TTR_Z Displacement Data

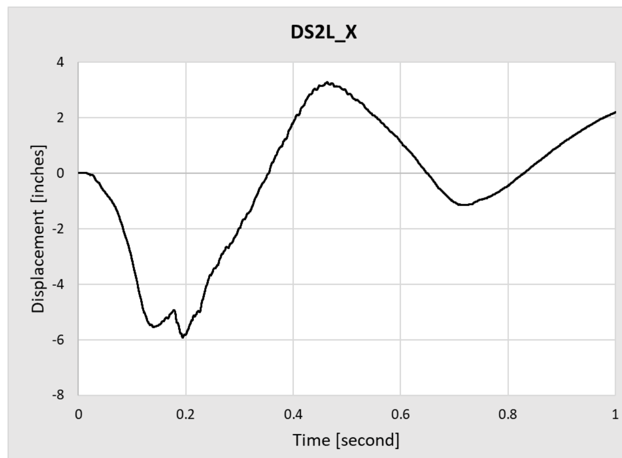

Figure B88. DS2L_X Displacement Data

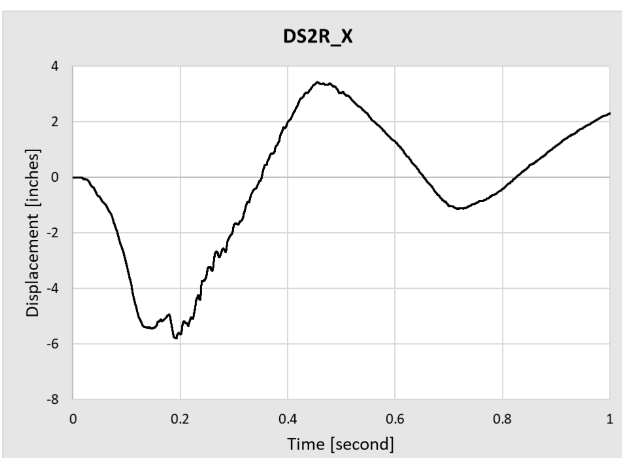

Figure B89. DS2R_X Displacement Data

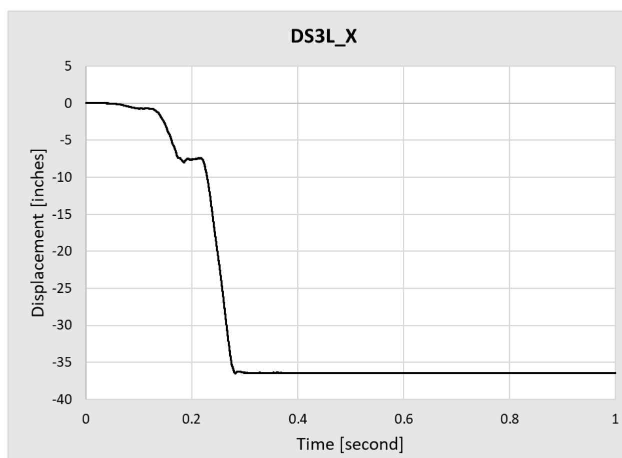

Figure B90. DS3L_X Displacement Data

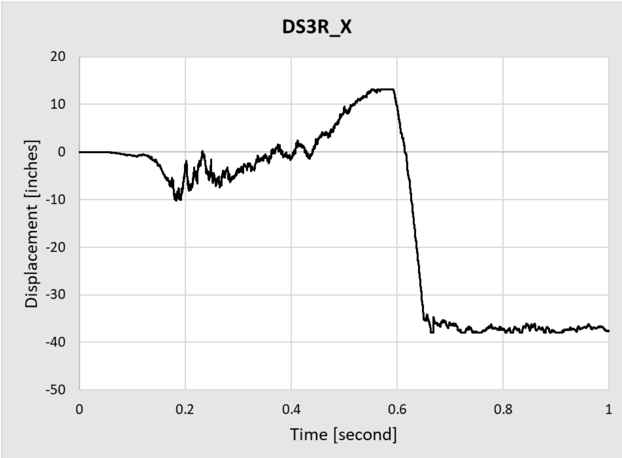

Figure B91. DS3R_X Displacement Data

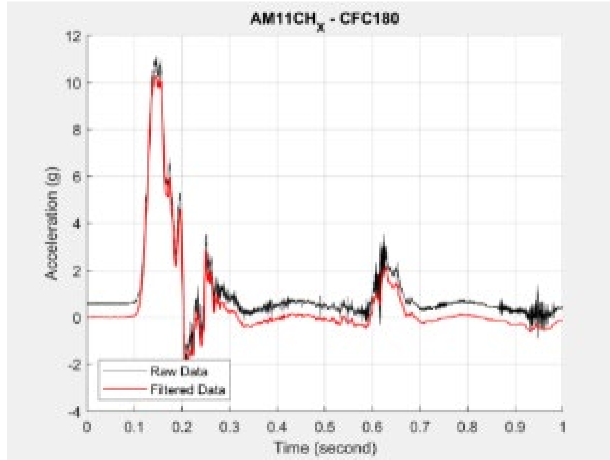

Figure B92. AM11CH_X-CFC180 Accelerometer Data

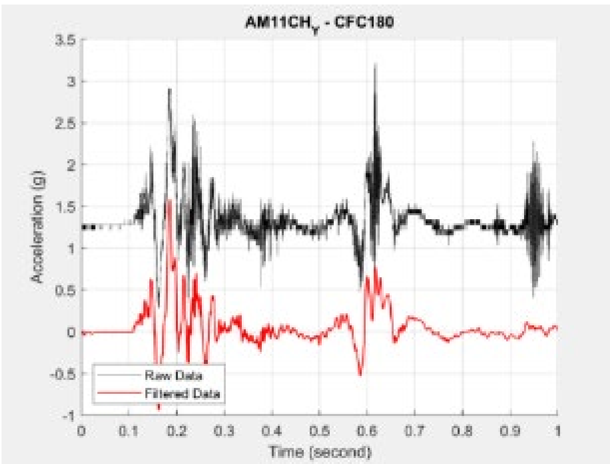

Figure B93. AM11CH_Y-CFC180 Accelerometer Data

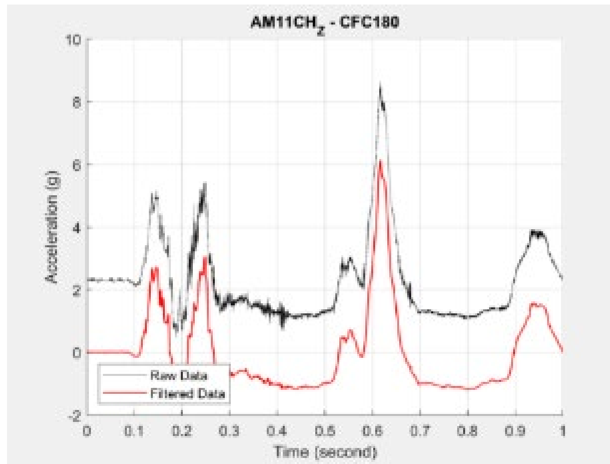

Figure B94. AM11CH_Z-CFC180 Accelerometer Data

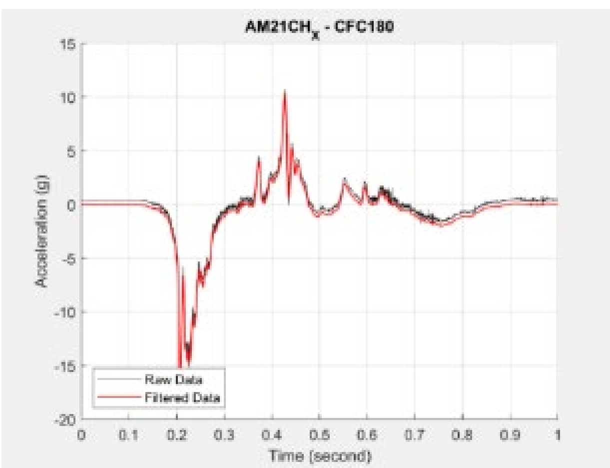

Figure B95. AM21CH_X-CFC180 Accelerometer Data

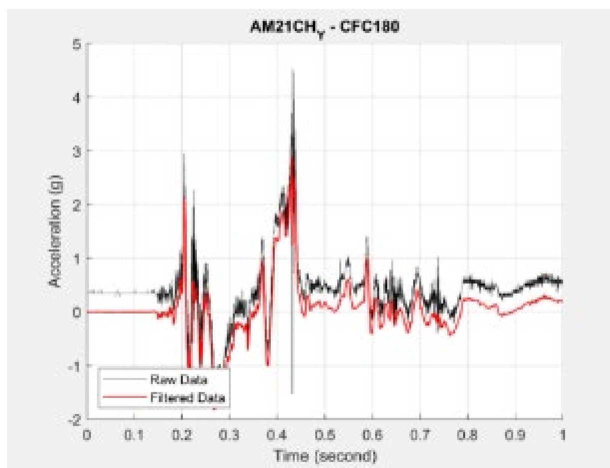

Figure B96. AM21CH_Y-CFC180 Accelerometer Data

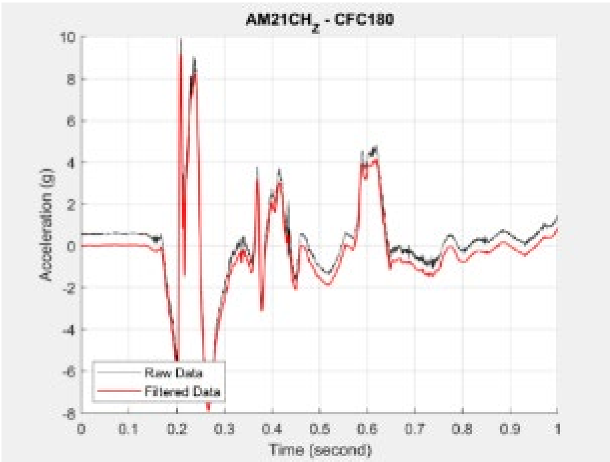

Figure B97. AM21CH_Z-CFC180 Accelerometer Data

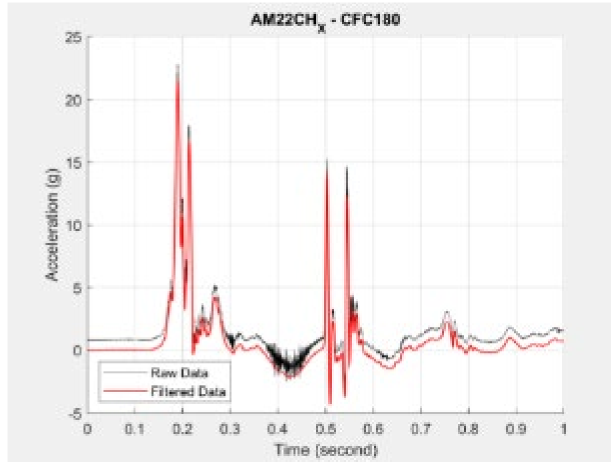

Figure B98. AM22CH_X-CFC180 Accelerometer Data

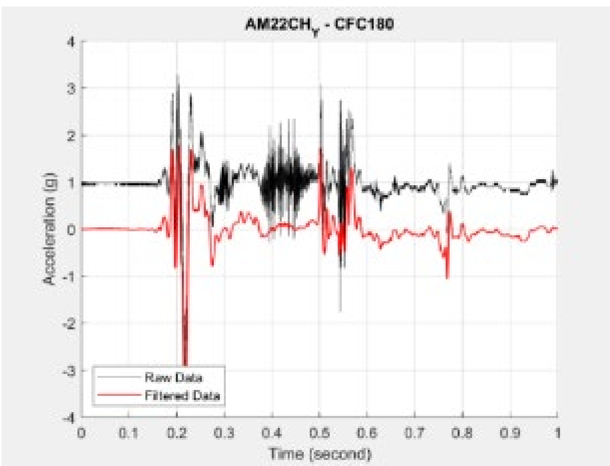

Figure B99. AM22CH_Y-CFC180 Accelerometer Data

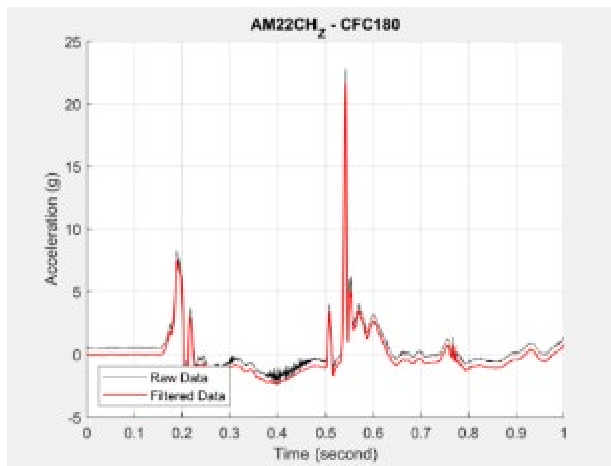

Figure B100. AM22CH_Z-CFC180 Accelerometer Data

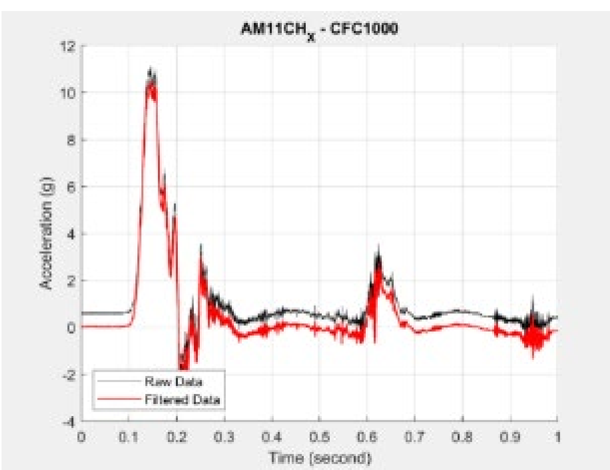

Figure B101. AM11CH_X-CFC1000 Accelerometer Data

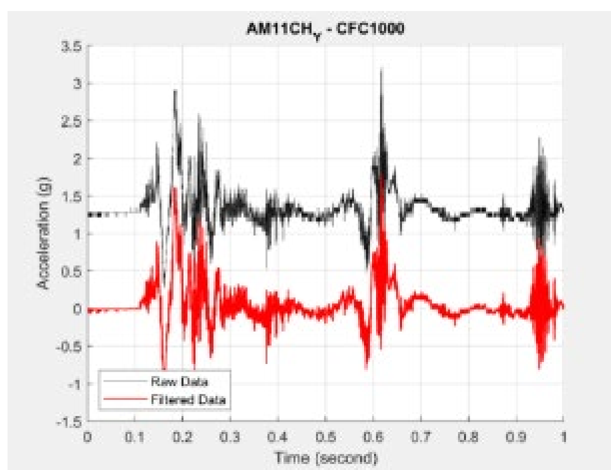

Figure B102. AM11CH_Y-CFC1000 Accelerometer Data

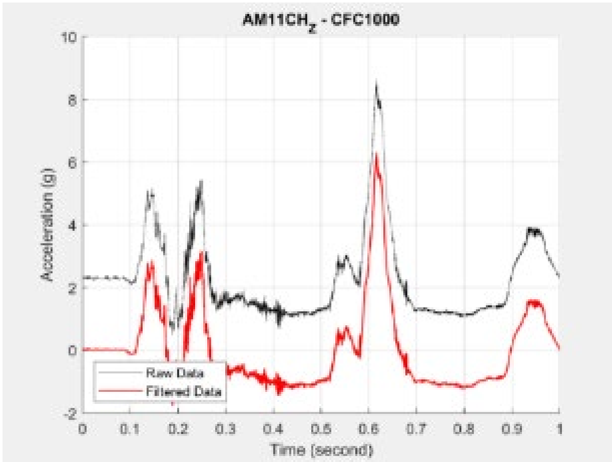

Figure B103. AM11CH_Z-CFC1000 Accelerometer Data

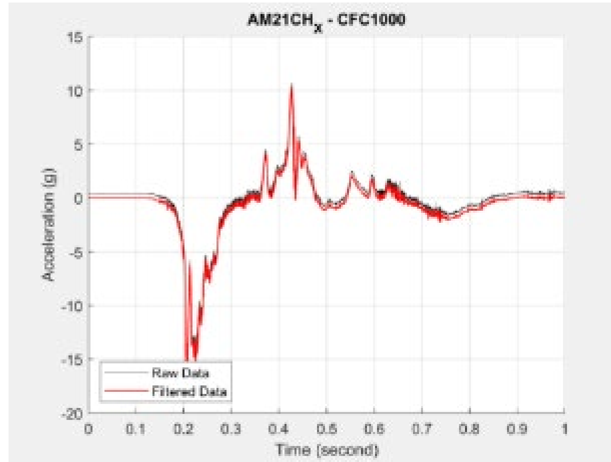

Figure B104. AM21CH_X-CFC1000 Accelerometer Data

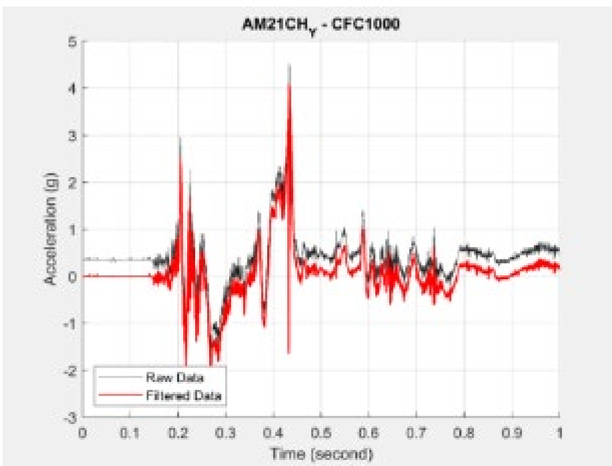

Figure B105. AM21CH_Y-CFC1000 Accelerometer Data

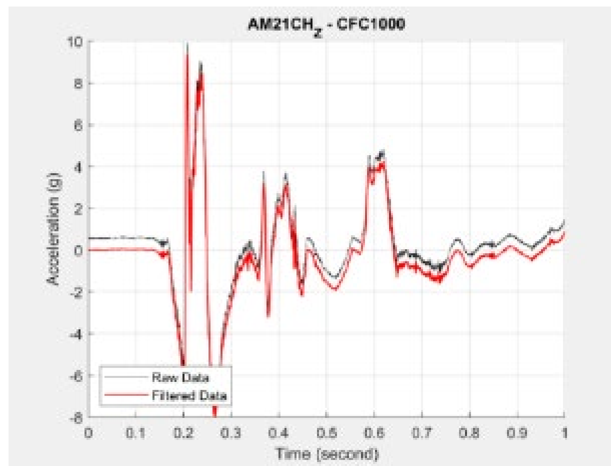

Figure B106. AM21CH_Z-CFC1000 Accelerometer Data

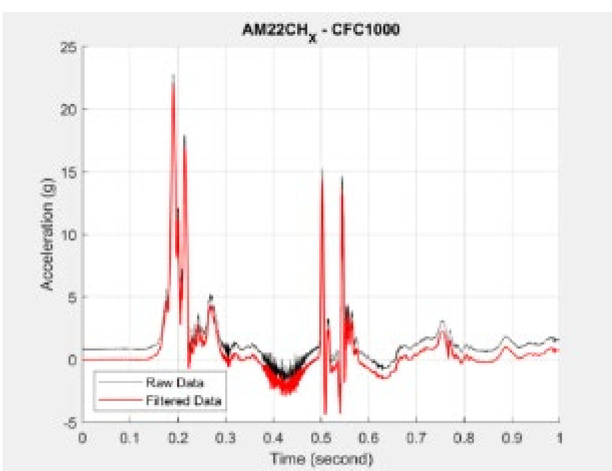

Figure B107. AM22CH_X-CFC1000 Accelerometer Data

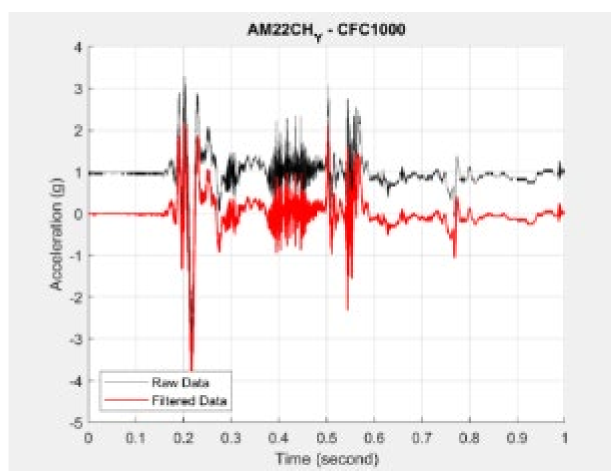

Figure B108. AM22CH_Y-CFC1000 Accelerometer Data

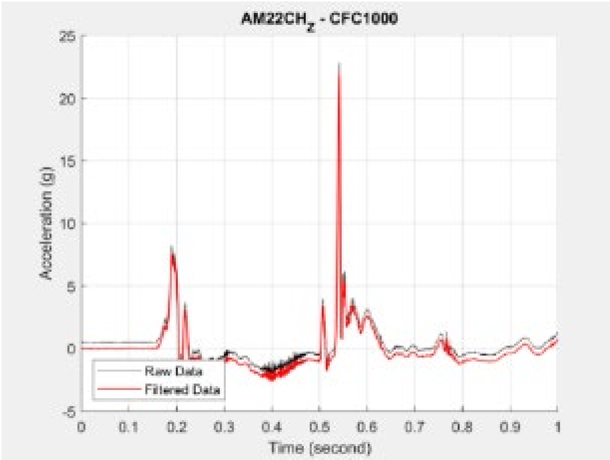

Figure B109. AM22CH_Z-CFC1000 Accelerometer Data

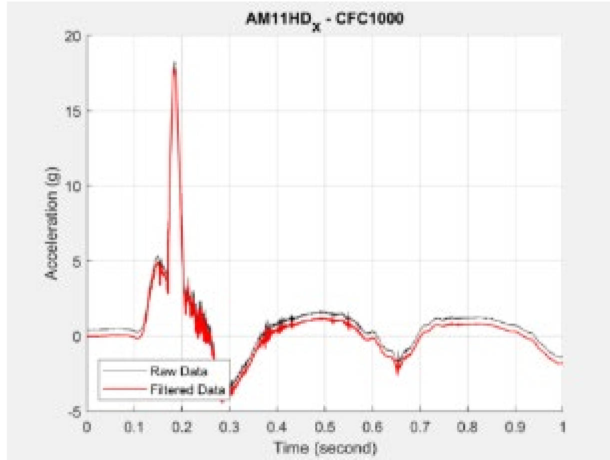

Figure B110. AM11HD_X Accelerometer Data

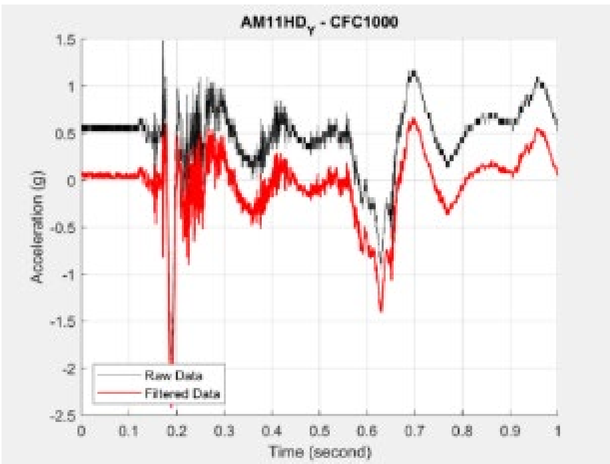

Figure B111. AM11HD_Y Accelerometer Data

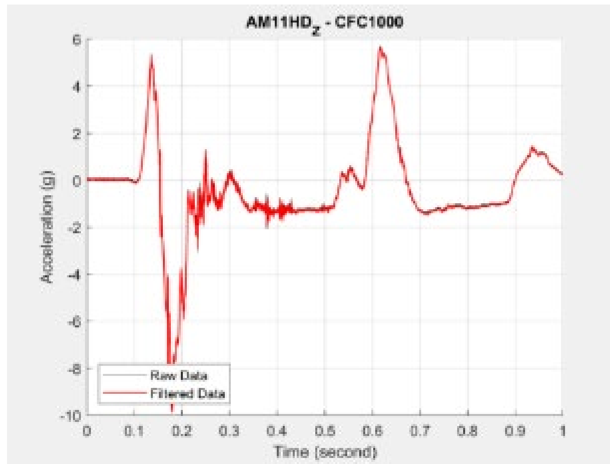

Figure B112. AM11HD_Z Accelerometer Data

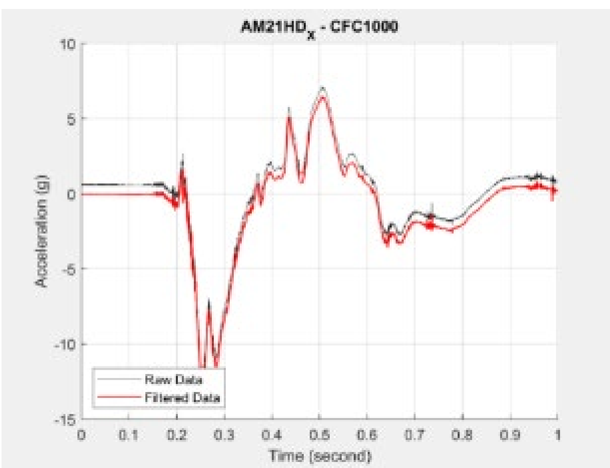

Figure B113. AM21HD_X Accelerometer Data

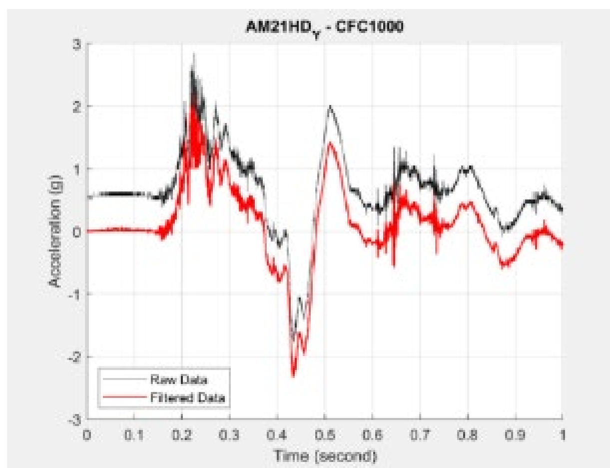

Figure B114. AM21HD_Y Accelerometer Data

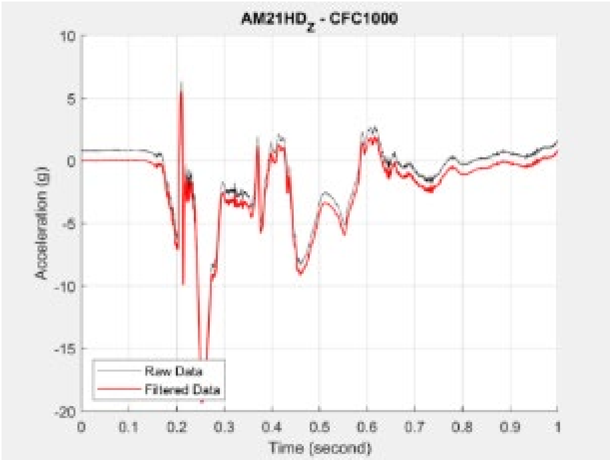

Figure B115. AM21HD_Z Accelerometer Data

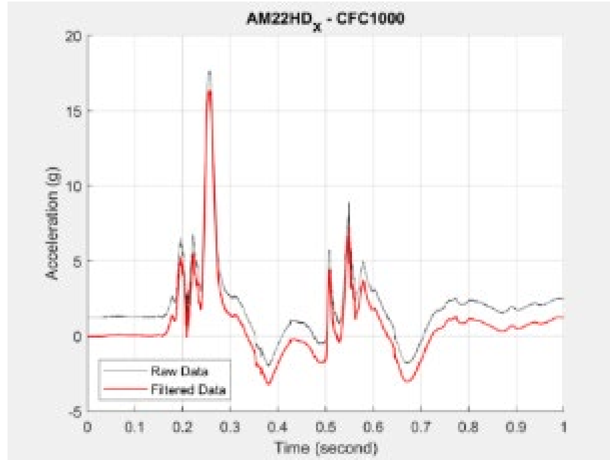

Figure B116. AM22HD_X Accelerometer Data

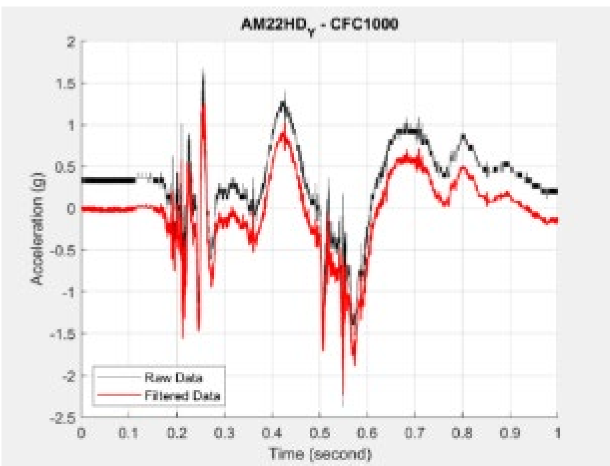

Figure B117. AM22HD_Y Accelerometer Data

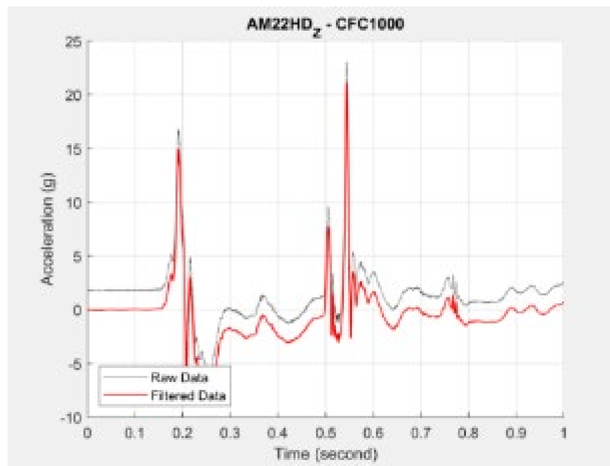

Figure B118. AM22HD_Z Accelerometer Data

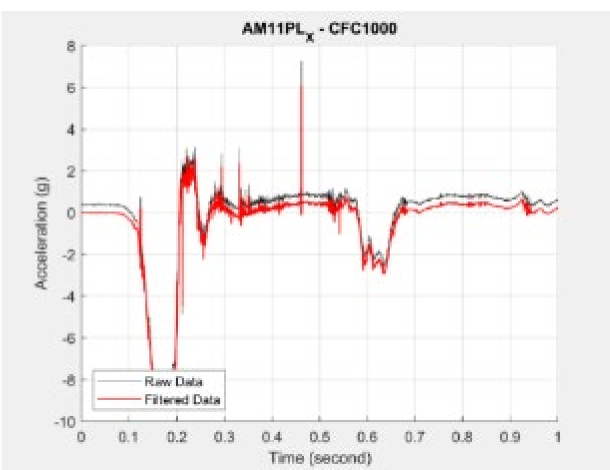

Figure B119. AM11PL_X Accelerometer Data

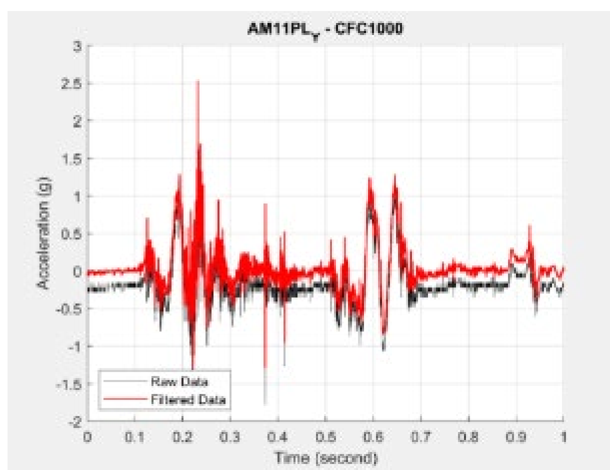

Figure B120. AM11PL_Y Accelerometer Data

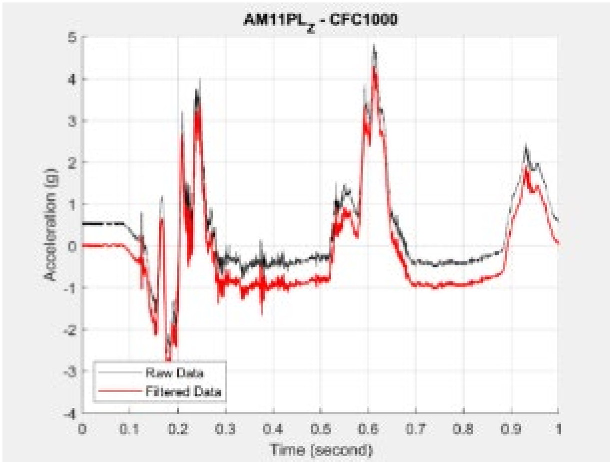

Figure B121. AM11PL_Z Accelerometer Data

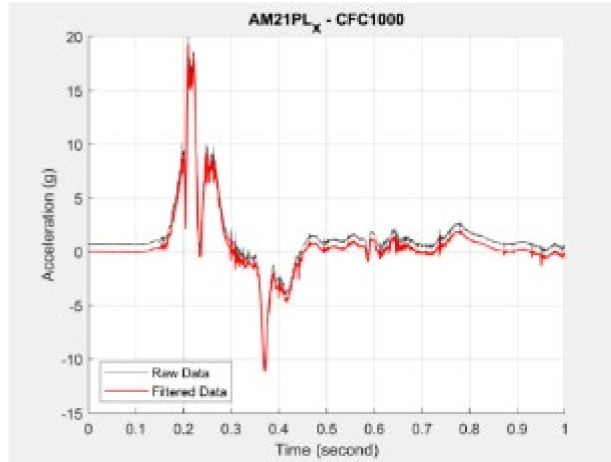

Figure B122. AM21PL_X Accelerometer Data

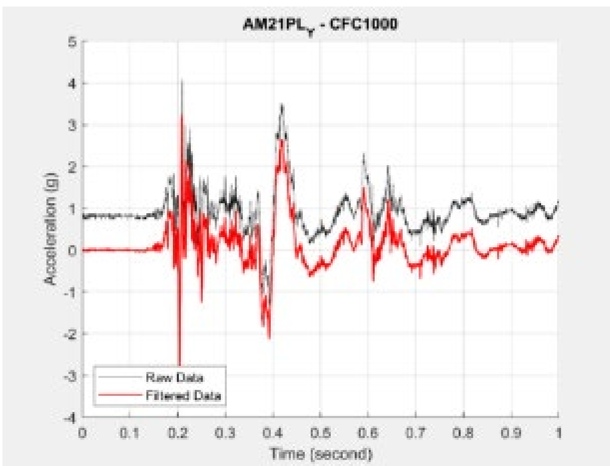

Figure B123. AM21PL_Y Accelerometer Data

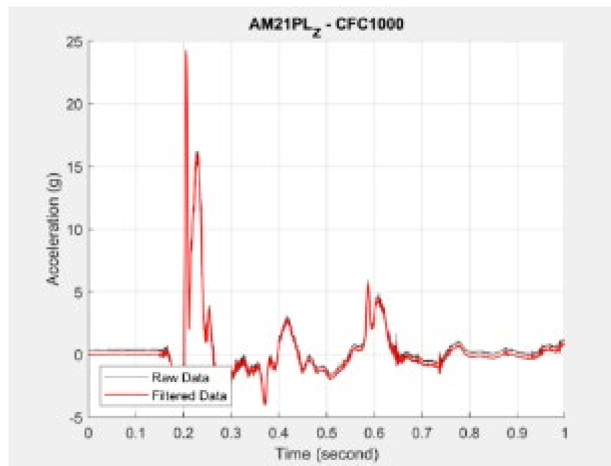

Figure B124. AM21PL_Z Accelerometer Data

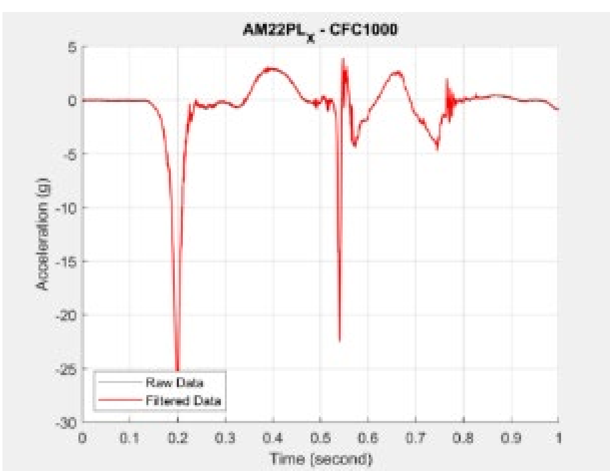

Figure B125. AM22PL_X Accelerometer Data

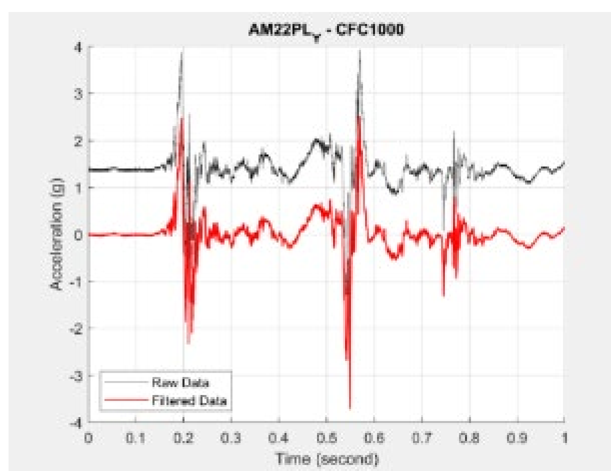

Figure B126. AM22PL_Y Accelerometer Data

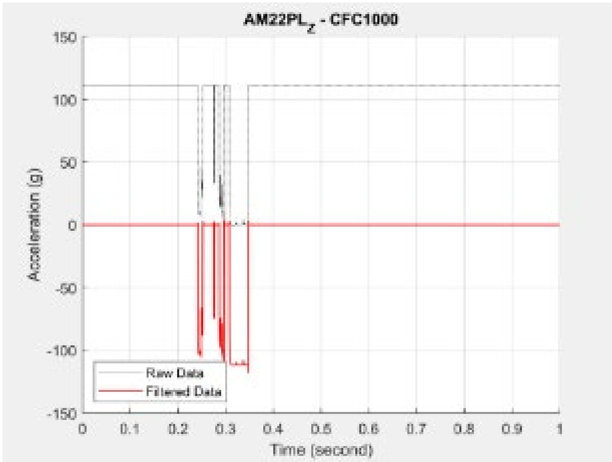

Figure B127. AM22PL_Z Accelerometer Data

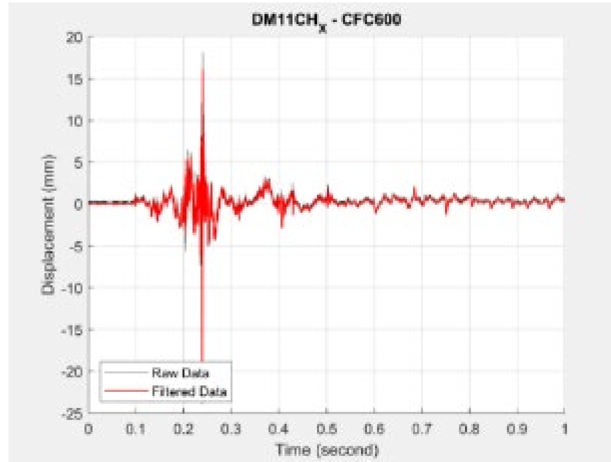

Figure B128. DM11CH_X Displacement Data

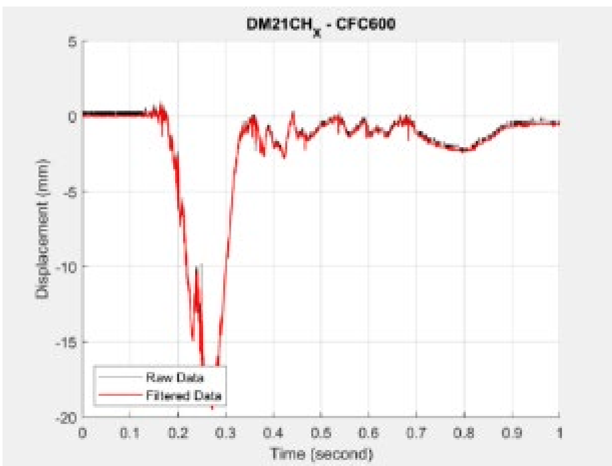

Figure B129. DM21CH_X Displacement Data

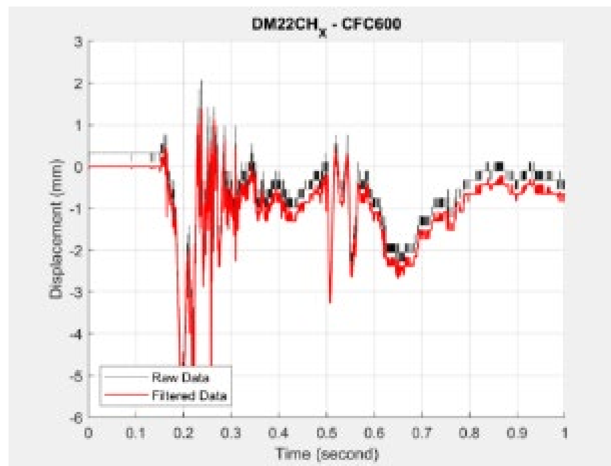

Figure B130. DM22CH_X Displacement Data

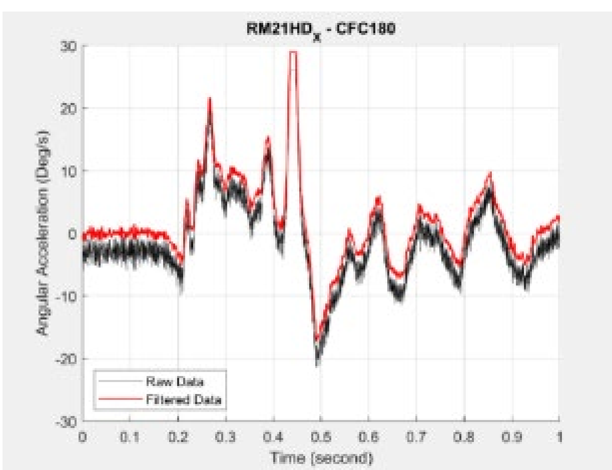

Figure B131. RM21HD_X Rotation Data

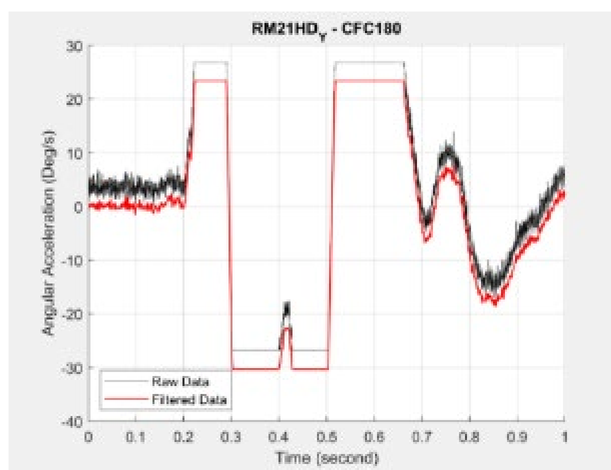

Figure B132. RM21HD_Y Rotation Data

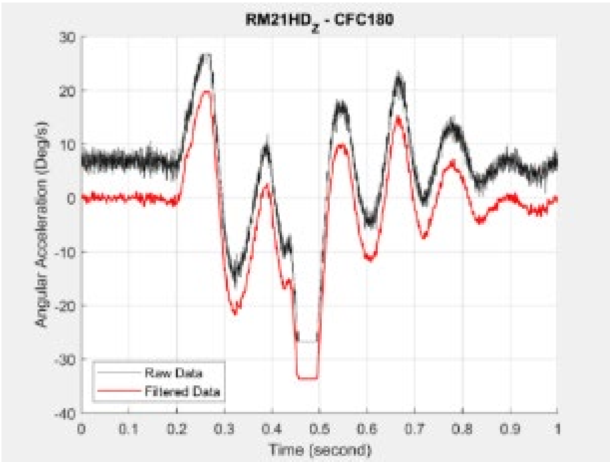

Figure B133. RM21HD_Z Rotation Data

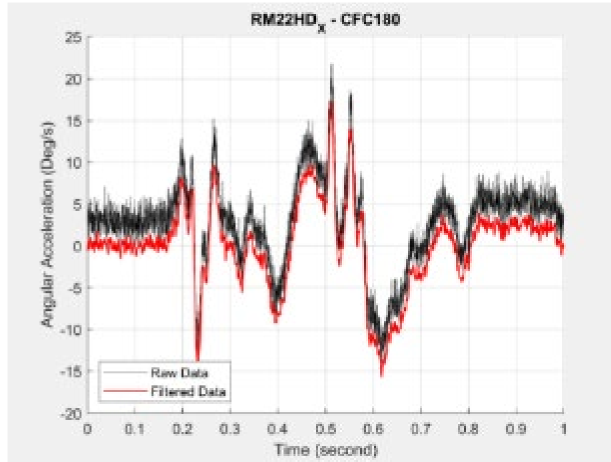

Figure B134. RM22HD_X Rotation Data

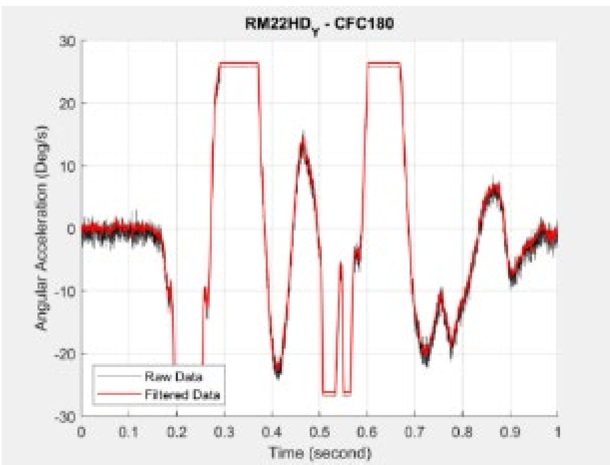

Figure B135. RM22HD_Y Rotation Data

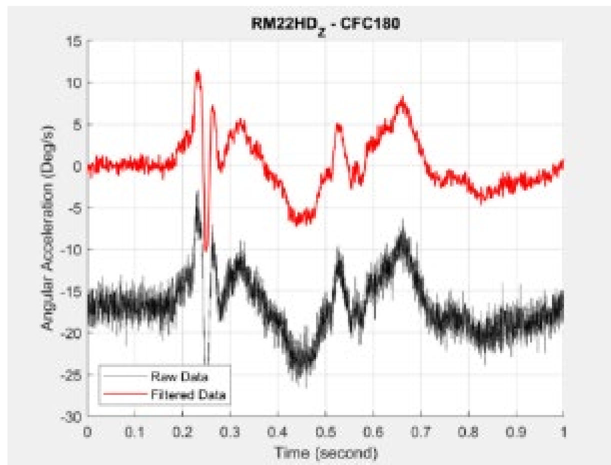

Figure B136. RM22HD_Z Rotation Data

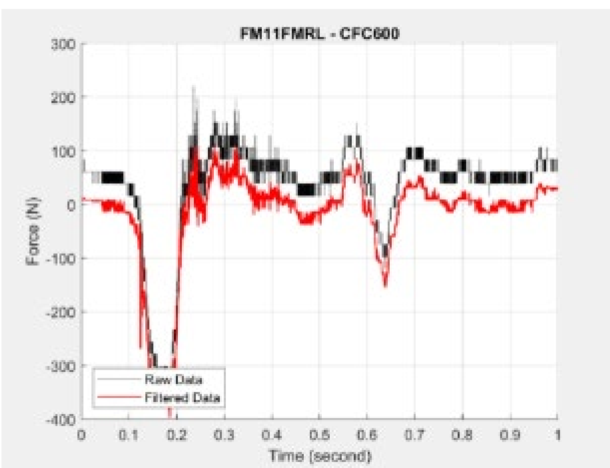

Figure B137. FM11FMRL Force Data

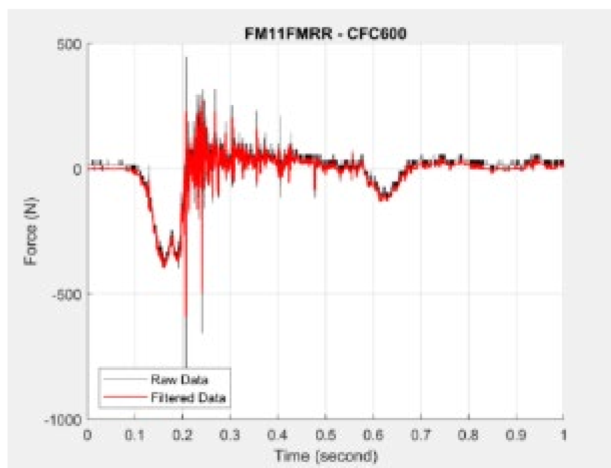

Figure B138. FM11FMRR Force Data

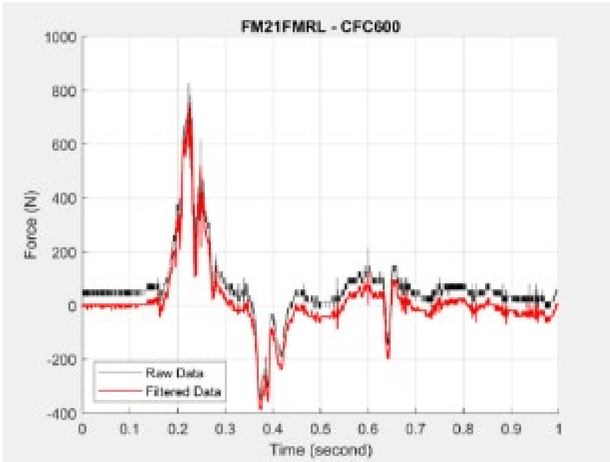

Figure B139. FM21FMRL Force Data

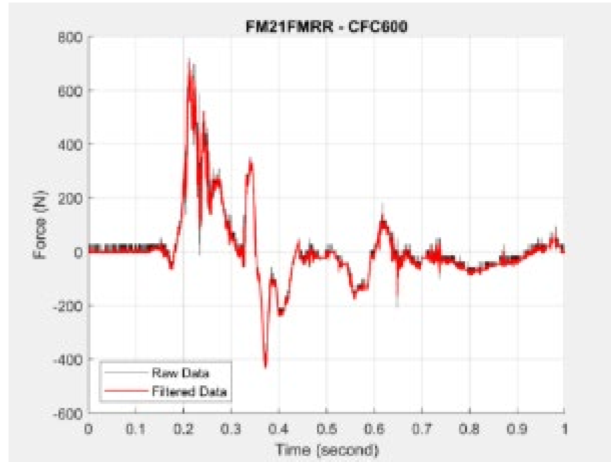

Figure B140. FM21FMRR Force Data

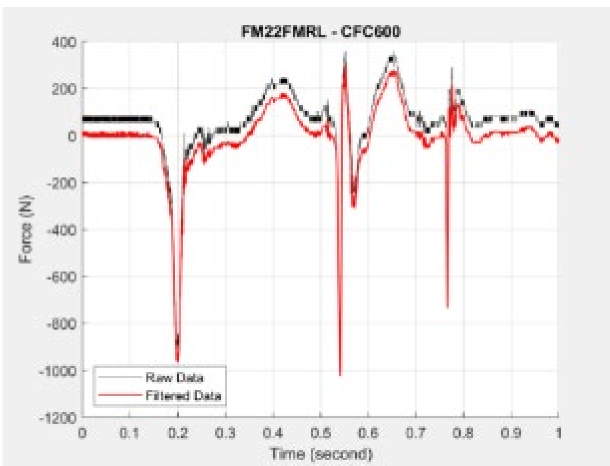

Figure B141. FM22FMRL Force Data

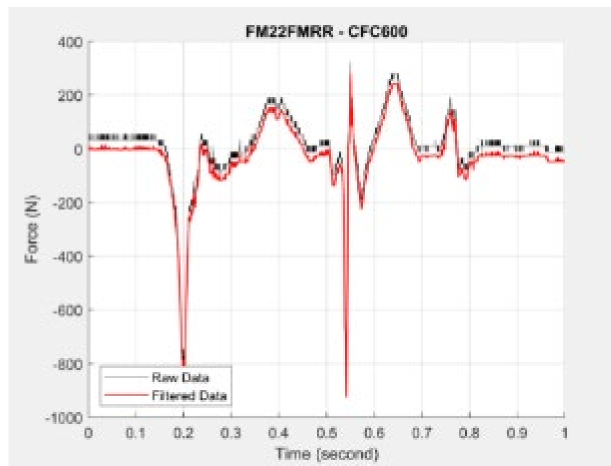

Figure B142. FM22FMRR Force Data

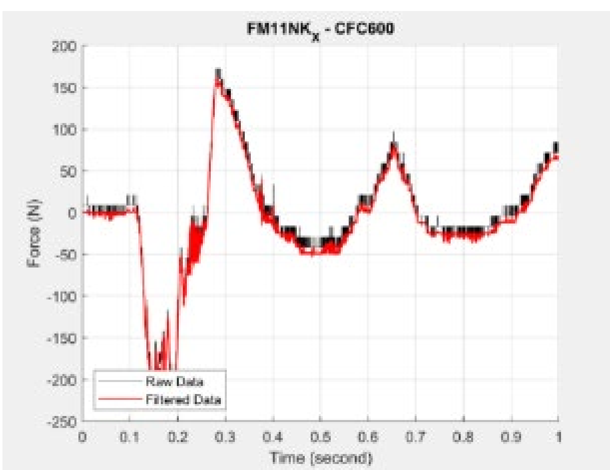

Figure B143. FM11NK_X-CFC600 Force Data

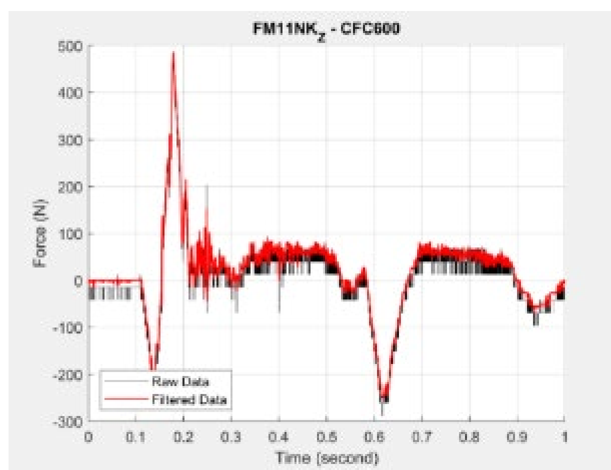

Figure B144. FM11NK_Z-CFC600 Force Data

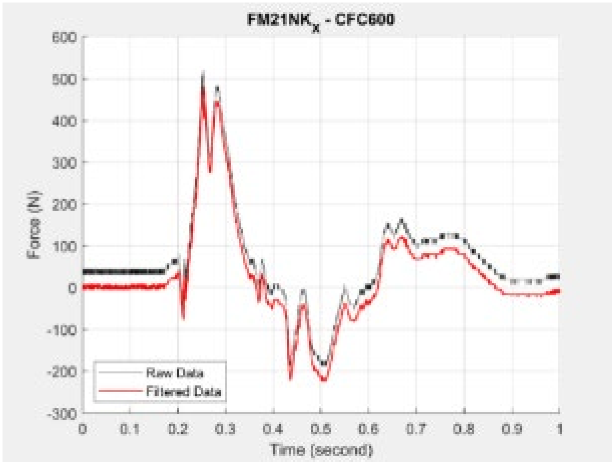

Figure B145. FM21NK_X-CFC600 Force Data

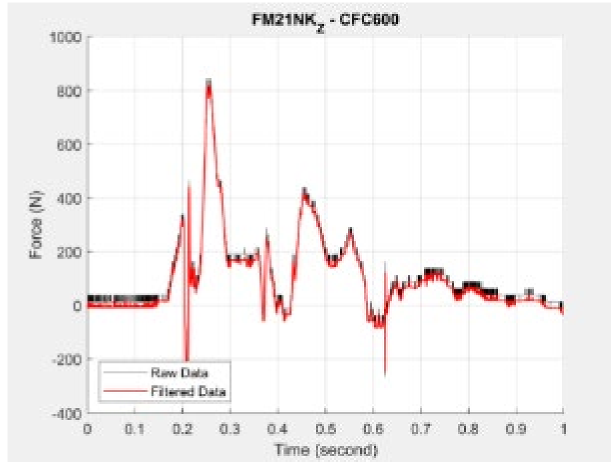

Figure B146. FM21NK_Z-CFC600 Force Data

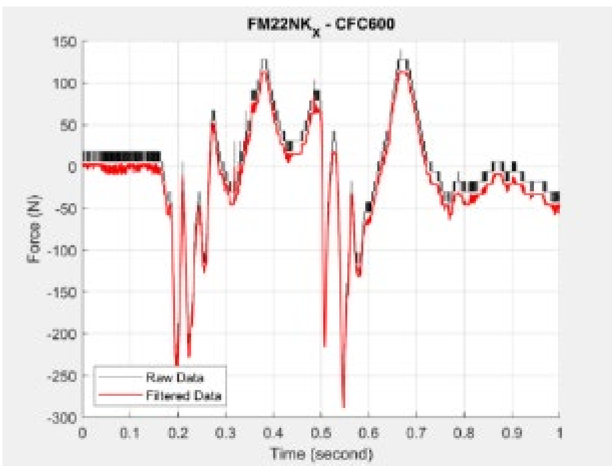

Figure B147. FM22NK_X-CFC600 Force Data

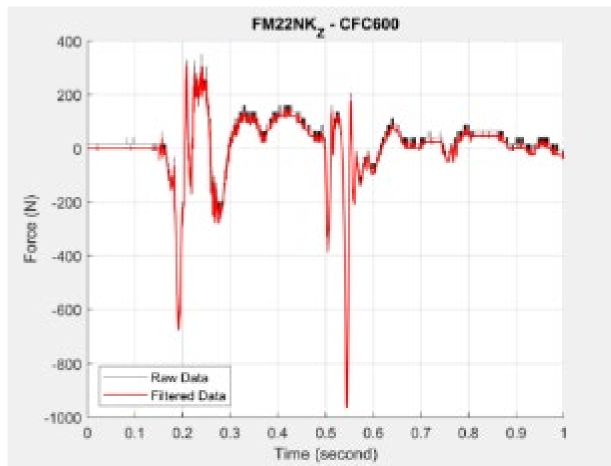

Figure B148. FM22NK_Z-CFC600 Force Data

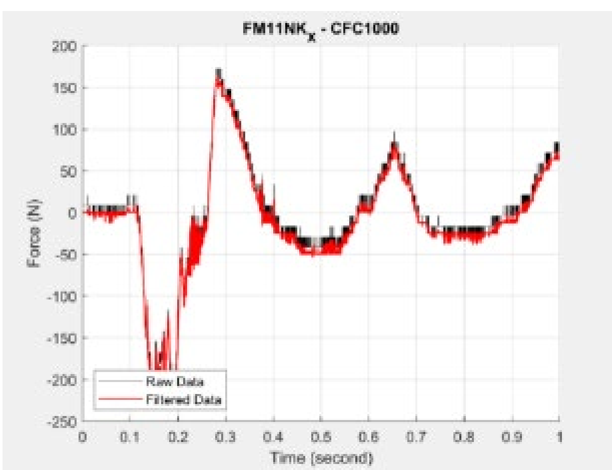

Figure B149. FM11NK_X-CFC1000 Force Data

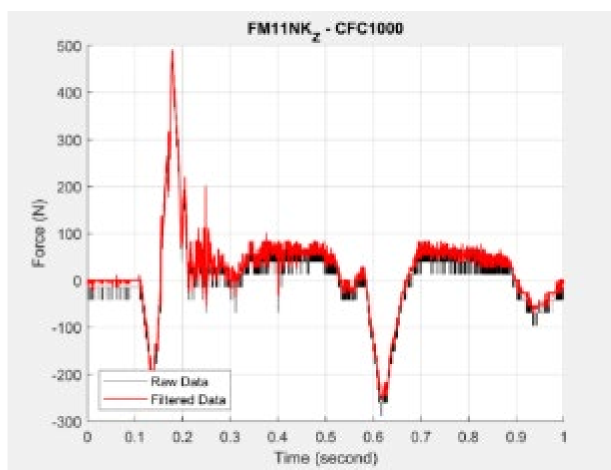

Figure B150. FM11NK_Z-CFC1000 Force Data

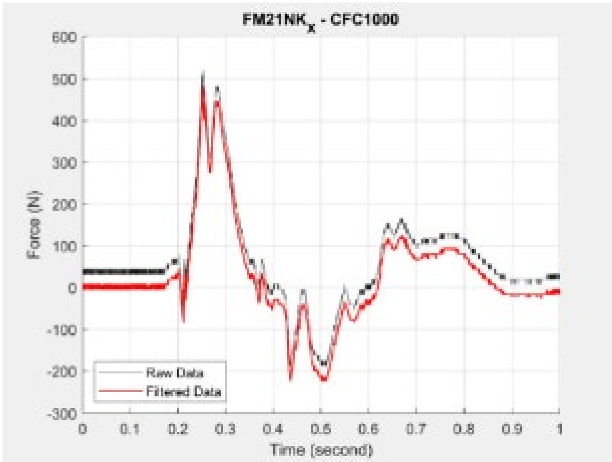

Figure B151. FM21NK_X-CFC1000 Force Data

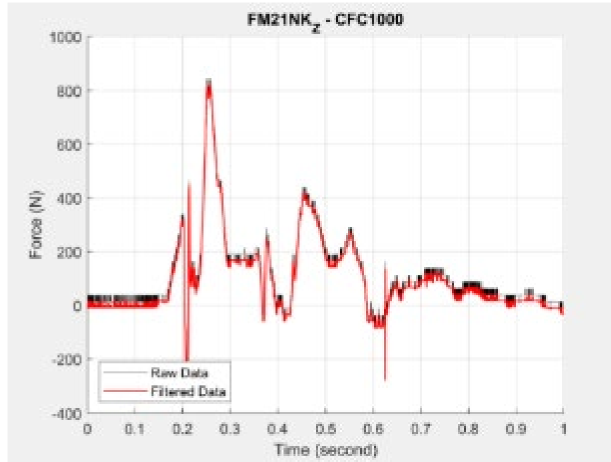

Figure B152. FM21NK_Z-CFC1000 Force Data

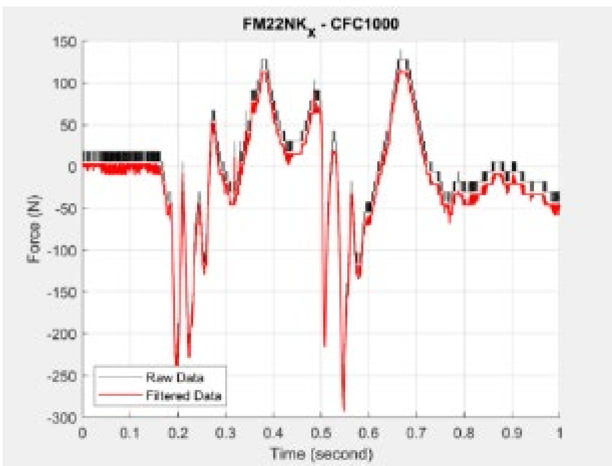

Figure B153. FM22NK_X-CFC1000 Force Data

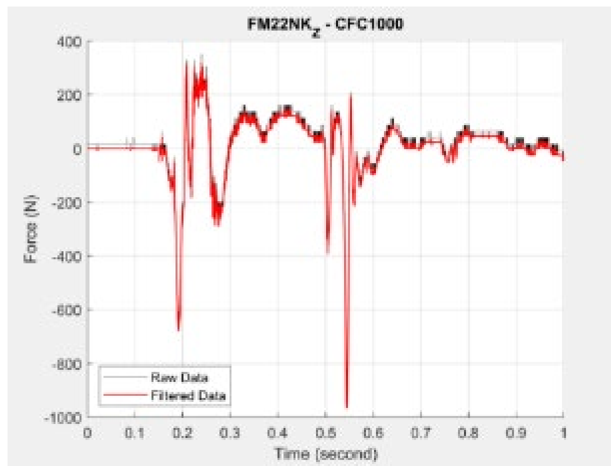

Figure B154. FM22NK_Z-CFC1000 Force Data

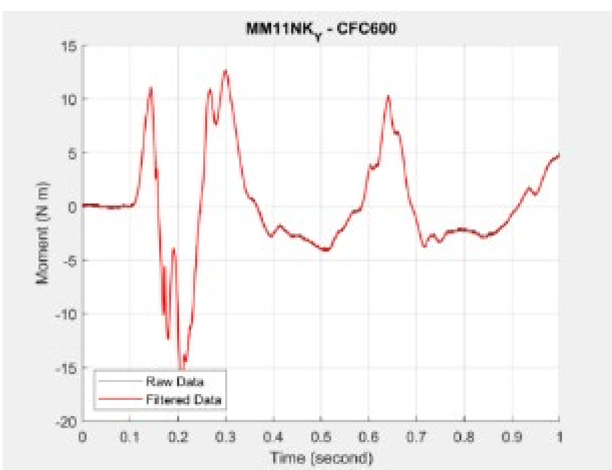

Figure B155. MM11NK_Y Moment Data

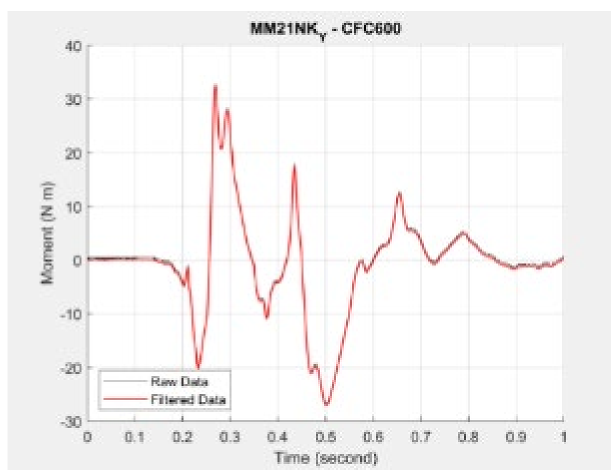

Figure B156. MM21NK_Y Moment Data

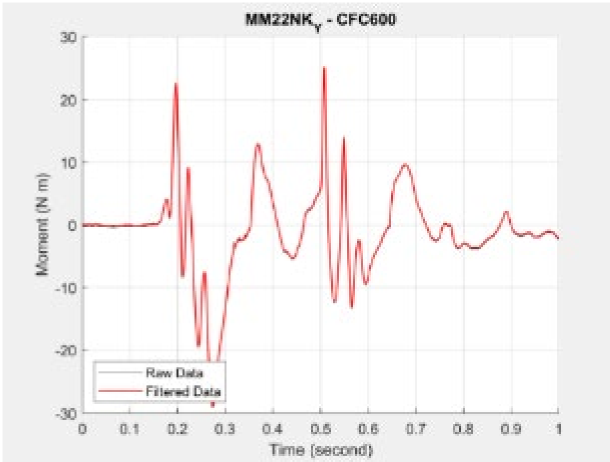

Figure B157. MM22NK_Y Moment Data

Abbreviations and Acronyms

ACRONYM	DEFINITION
APTA	American Public Transportation Association
CEM	Crash Energy Management
DAC	Deformable Anti-Climbers
FRA	Federal Railroad Administration
HD	High Definition
HS	High Speed
lbf	Pound Force
MxV Rail	Formerly Transportation Technology Center, Inc.
PBC	Push-Back Coupler
TTC	Transportation Technology Center
TTCI	Transportation Technology Center, Inc.
Volpe	Volpe National Transportation Systems Center